NIST Technical Note 1848

Sensitivity Analysis of Installation Faults on Heat Pump Performance

Piotr A. Domanski
Hugh I. Henderson
W. Vance Payne

National Institute of
Standards and Technology
U.S. Department of Commerce

NIST Technical Note 1848

Sensitivity Analysis of Installation Faults on Heat Pump Performance

Piotr A. Domanski
Energy and Environment Division
Engineering Laboratory

Hugh I. Henderson
CDH Energy Corporation
Cazenovia, NY

W. Vance Payne
Energy and Environment Division
Engineering Laboratory

September 2014

U.S. Department of Commerce
Penny Pritzker, Secretary

National Institute of Standards and Technology
Willie E. May, Acting Under Secretary of Commerce for Standards and Technology and Acting Director

Sensitivity Analysis of Installation Faults on Heat Pump Performance

Piotr A. Domanski[a], Hugh I. Henderson[b], W. Vance Payne[a]

[a] National Institute of Standards and Technology, Gaithersburg, MD 20899-8631
[b] CDH Energy Corporation, Cazenovia, NY 13035-0641

ABSTRACT

Numerous studies and surveys indicate that typically-installed HVAC equipment operate inefficiently and waste considerable energy due to different installation errors (faults) such as improper refrigerant charge, incorrect airflow, oversized equipment, leaky ducts. This study seeks to develop an understanding of the impact of different faults on heat pump performance installed in a single-family residential house. It combines building effects, equipment effects, and climate effects in a comprehensive evaluation of the impact of installation faults on a heat pump's seasonal energy consumption through simulations of the house/heat pump system.

The study found that duct leakage, refrigerant undercharge, oversized heat pump with nominal ductwork, low indoor airflow due to undersized ductwork, and refrigerant overcharge have the most potential for causing significant performance degradation and increased annual energy consumption. The effect of simultaneous faults was found to be additive (e.g., duct leakage and non-condensable gases), little changed relative to the single fault condition (e.g., low indoor airflow and refrigerant undercharge), or well-beyond additive (duct leakage and refrigerant undercharge). A significant increase in annual energy use can be caused by lowering the thermostat in the cooling mode to improve indoor comfort in cases of excessive indoor humidity levels due to installation faults.

The goal of this study was to assess the impacts that HVAC system installation faults had on equipment electricity consumption. The effect of the installation faults on occupant comfort was not the main focus of the study, and this research did not seek to quantify any impacts on indoor air quality or noise generation (e.g., airflow noise from air moving through restricted ducts). Additionally, the study does not address the effects that installation faults have on equipment reliability/robustness (number of starts/stops, etc.), maintainability (e.g., access issues), or costs of initial installation and ongoing maintenance.

TABLE OF CONTENTS

LIST OF FIGURES

LIST OF TABLES

1. INTRODUCTION

Space cooling is responsible for the largest share (at 21.3 %) of the electrical energy consumption in the U.S. residential sector (DOE, 2011). Space heating, for which a significant portion is provided by heat pumps, accounts for an additional 8.7 % electricity use. Consequently, there are increasing requirements that space-conditioning equipment be highly efficient to improve building energy efficiency as well as address environmental concerns. To this end, state and municipal governments and utility partners have implemented various initiatives that promote sales of high-efficiency air conditioners (ACs) and heat pumps (HPs). However, there is a growing recognition that merely increasing equipment's laboratory-measured efficiency without ensuring that the equipment is installed and operated correctly in the field is ineffective. A key component for maximizing field equipment performance is to ensure that such equipment is sized, selected, and installed following industry recognized procedures. Consistent with this goal, the Air Conditioning Contractors of America (ACCA) released in 2007 a quality installation (QI) standard for heating, ventilating and air-conditioning (HVAC) equipment, which has been updated since then and achieved widespread recognition by various entities in the U.S. concerned with reducing energy consumption by buildings (ACCA, 2010). A companion standard (ACCA, 2011b) defines the verification protocols to ensure that HVAC systems have been installed according to the QI Standard. A related ACCA standard (ACCA, 2013) addresses residential maintenance issues.

Numerous studies and surveys indicate that typically-installed HVAC equipment operate inefficiently and waste considerable energy due to different installation errors (faults) such as improper refrigerant charge, incorrect airflow, oversized equipment, leaky ducts. However, it is unclear whether the effects of such faults are additive, whether small variances within a given fault type are significant, and which faults (in various applications and geographical locations) have a larger impact than others. If this information is known, better attention, resources, and effort can be focused on the most important design, installation, and maintenance parameters.

This project seeks to develop an understanding of the impact of different commissioning parameters on heat pump performance for a single-family residential house application. It combines building effects, equipment effects, and climate effects in a comprehensive evaluation of the impact of installation faults on seasonal energy consumption of a heat pump through simulations of the house/heat pump system. The evaluated commissioning parameters include:

- Building subsystem
  - Duct leakage (unconditioned space)
- Residential split, air-to-air heat pump equipped with a thermostatic expansion valve (TXV)
  - Equipment sizing
  - Indoor coil airflow
  - Refrigerant charge
  - Presence of non-condensable gases
  - Electrical voltage
  - TXV undersizing
- Climates (cooling and heating)
  - Hot and humid
  - Hot and dry
  - Mixed
  - Heating dominated
  - Cold
- Single-family houses (the structures representative for the climate)
  - House on a slab
  - House with a basement.

The goal of this study is to assess the impacts that HVAC system installation faults have on equipment electricity consumption. The effect of the installation faults on occupant comfort is not the main focus of the study, and this research did not seek to quantify any impacts on indoor air quality or noise generation (e.g., airflow noise from air moving through restricted ducts). Additionally, the study does not address the effects that installation faults have on equipment reliability/robustness (number of starts/stops, etc.), maintainability (e.g., access issues), or costs of initial installation and ongoing maintenance.

2. LITERATURE SURVEY

The literature survey is presented in three sections. Section 2.1 presents selected publications related to air conditioner and heat pump installation and maintenance issues, Section 2.2 focuses on heat pump oversizing/undersizing and cycling loses, and Section 2.3 presents relevant studies on heat pump fault detection and diagnostics (FDD).

2.1 Field Surveys, Installation and Maintenance Issues
Numerous field studies have documented degraded performance and increased energy usage for typical air conditioners and heat pumps installed in the United States. Commonly, system efficiency, peak electrical demand, and comfort are compromised. This degraded performance has been linked to several problems, which include:
- improperly designed, insulated, or balanced air distribution systems in the house
- improperly selected heat pump, either by the fact of overall performance characteristics due to mix-matched components or improper capacity (too large or too small) in relation to the building load
- heat pump operating with a fault.

The first two problem categories are a result of negligent or incompetent work prior to the heat pump installation. The third problem category, a heat pump operating with a fault, can be a result of improper installation or improper maintenance. Field study reports describing observations and measurements on new installations are less common than publications on existing installations. For this reason, in this literature review we also include reports on maintenance practices, in particular those covering large numbers of systems.

While discussing heat pump performance measurements taken in the field, we have to recognize that these field measurements offer significant challenges and are burdened by a substantial measurement uncertainty, much greater than the uncertainty of measurements in environmental chambers, which are in the order of 5 % at the 95 % confidence level. Typically, field study reports do not estimate the measurement uncertainty of the reported values; however, the number of installations covered by some of these studies provides an informative picture about the scope and extent of field installation problems. We may also note that most of the articles on field surveys are not published in indexed journals. Consequently, they are not searchable by publication search engines, and many of them are not readily available. In this literature review, we gave a preference to citing publications which can be readily obtained by a reader if desired.

In a study of new installations, Proctor (1997) performed measurements on a sample of 28 air conditioners installed in 22 residential homes in a hot and dry climate (Phoenix, AR, USA). Indoor heat exchanger airflow averaged 14 % below specifications, and only 18 % of the systems had a correct amount of refrigerant. The supply duct leakage averaged 9 % of the air handler airflow, and the return leakage amounted to 5 %. The author cites several prior publications, which reported similar problems.

Davis and Robison (2008) monitored seven new high efficiency residential heat pumps. They diagnosed several installation errors, which included a malfunctioning TXV, non-heat pump thermostat installed, incorrect indoor unit installed, and incorrect control wiring preventing proper system staging. The authors reported that once the problems were repaired, the systems performed at the expected levels.

Parker et al. (1997) investigated the impact of indoor airflow on residential air conditioners in 27 installations in Florida. They measured airflows ranging from 62.8 $m^3 \cdot h^{-1} \cdot kW^{-1}$ to 246.4 $m^3 \cdot h^{-1} \cdot kW^{-1}$ (130 cfm/ton to 510 cfm/ton) while a typical manufacturer's recommendation calls for 193.2 $m^3 \cdot h^{-1} \cdot kW^{-1}$ (400 cfm/ton). Undersized return ducts and grills, improper fan speed settings, and fouled filters were the causes of improper airflow along with duct runs that were long, circuitous, pinched or constricted. Additional flow resistance can result from the homeowner tendency to increase air filtration via higher

efficiency filters during replacement; the measurements showed that substitution of high-efficiency filters typically reduces the airflow by 5 %. Low airflow has system energy-efficiency implications; reduction of airflow by 25 % from 193.2 $m^3 \cdot h^{-1} \cdot kW^{-1}$ to 144.9 $m^3 \cdot h^{-1} \cdot kW^{-1}$ (400 cfm/ton to 300 cfm/ton) can reduce the efficiency of the air conditioner by 4 %. The authors commented that airflows below 169.1 $m^3 \cdot h^{-1} \cdot kW^{-1}$ (350cfm/ton) render invalid most field methods for determining refrigerant charge and can lead to improper charging by a service technician who often does not check the evaporator airflow.

Downey and Proctor (2002) reported on the field survey of 13 000 air conditioners installed on residential and commercial buildings. The measurements were collected during routine installation, repair, and maintenance visits. Of the 8873 residential systems tested, 5776 (65 %) required repairs, and of the 4384 light commercial systems tested, 3100 (71 %) required repairs. Improper refrigerant charge was found in 57 % of all systems. The authors noted that the simple temperature split method for identifying units with low airflow is flawed because it does not account for the system operating condition.

Proctor (2004) presented results from a survey study involving 55000 units. He reported that 60 % of commercial air conditioners and 62 % of residential air conditioners had incorrect refrigerant charge. In all, 95 % of residential units failed the diagnostic test because of duct leakages, poor duct insulation or excessive airflow restriction, improper refrigerant charge, low evaporator airflow, non-condensables in the refrigerant or an improperly sized unit.

Rossi (2004) presented measured performance data and statistics on unitary air conditioners. The data were gathered using commercially available portable data acquisition systems during normal maintenance and service visits. Out of 1468 systems considered in this study, 67 % needed service. Of those 15 % required major repairs (e.g., compressor or expansion device replacement), and 85 % required a tune-up type service (e.g., coil cleaning or refrigerant charge adjustment). Approximately 50 % of all units operated with efficiencies of 80 % or less, and 20 % of all units had efficiencies of 70 % or less of their design efficiency.

Mowris et al. (2004) reported on field measurements of refrigerant charge and airflow, commonly referred to as RCA. Over a three-year period, 4168 new and existing split, package, and heat pumps were tested. The measurements showed that 72 % of the tested units had improper refrigerant charge, and 44 % had improper airflow. Approximately a 20 % efficiency gain was measured after refrigerant charge and airflow were corrected.

Neme et al. (1999) considered four installation issues − equipment sizing, refrigerant charging, adequate airflow, and sealing ducts − and assessed the potential benefits from improved installation practices. The authors relied on an extensive list of publications to determine the range of intensity of the four installation faults and the probable air conditioner efficiency gain resulting from a corrective action. The cited literature indicated the maximum efficiency improvement of 12 % for corrected airflow, 21 % for corrected refrigerant charge, and 26 % for eliminated duct leakage. The authors concluded that improved HVAC installation practices could save an average of 25 % of energy in existing homes and 35 % in new construction. They also pointed out that air conditioner oversizing has the potential of masking a number of other installation problems, particularly improper refrigerant charge and significant duct leakage, while a correctly sized air conditioner makes other installation problems more apparent, particularly at severe operating conditions.

Neal (1998) presented a methodology for calculating a field-adjusted seasonal energy efficiency ratio, which he referred to as SEERFA, with the goal to account for four installation errors and better represent the seasonal performance of the air conditioner installed in the field than the seasonal energy efficiency ratio (SEER) derived from tests in environmental chambers. He used correcting factors of value 1 or smaller, one for each installation fault, which act as multipliers on the SEER. He provided an example

indicating that, on average, a homeowner's cooling cost is approximately 70 % higher than it could be with quality air conditioner installation. It should be noted that the proposed algorithm assumes no interaction between different faults, which seems to be an improper assumption.

While the scope and specific findings presented in the above publications may differ, they uniformly document the prevalence of air conditioner and heat pump faults in the field and a significant performance degradation of this equipment.

2.2 Heat Pump Oversizing, Undersizing and Part-load Losses

It is generally accepted that equipment over-sizing will lead to significant part load losses due to cycling. Unit cycling increases energy use due to efficiency losses (Parken et al., 1985) and also can degrade the moisture removal capacity of the unit which leads to higher space humidity levels (Shirey et al., 2006). For nearly 50 years, proper sizing for residential air conditioners and heat pumps has typically been defined using the ACCA Manual J (ACCA, 2011a).

The energy efficiency of a cycling system is governed by how quickly after startup the capacity and efficiency of the air conditioning unit reaches steady-state conditions. Parken et al. (1977) defined the 'Cyclic Degradation' parameter (C_D) as a simplified metric to predict part load losses. This parameter was integrated into the calculation procedure to determine the seasonal energy efficiency ratio (SEER) for air conditioners and heat pumps. That procedure has been incorporated into federal energy efficiency standards (Federal Register, 1979) and into AHRI Standard 210/240 (AHRI, 2008). The default value for C_D in these calculation procedures is 0.25.

Many researchers have demonstrated the sensible and latent capacity of the air conditioner at startup is a complicated process (Henderson, 1990; O'Neal and Katipamula, 1991). The response includes the delays associated with pumping refrigerant from the low-side to the high-side of the system to establish the steady-state operating pressures as well as the first order delays due to heat exchanger capacitance. Several models have been proposed that represent the overall response as some combination of first order (time-constant) response, delay times, and other non-linear effects. Henderson (1992) compared all these and showed they generally could be represented as an equivalent time constant.

As part of developing a model for latent degradation, Henderson and Rengarajan (1996) showed that the parameter C_D can be directly related to equivalent time constant for capacity at startup while assuming a thermostat cycling rate parameter (Nmax) of 3.1 cycles per hour. O'Neal and Katipamula (1991) and Parken et al. (1977) also indirectly showed a similar relationship. The default value of 0.25 for C_D is equivalent to an overall time constant of 1.27 minutes.

Over the years since the SEER test and rating procedure has been developed, manufacturers have had a strong incentive to improve the cyclic performance of their systems. Dougherty (2003) demonstrated that the typical value of C_D is now in the range 0.05 to 0.10 for most systems. So cyclic degradation and the part load efficiency losses may be of less consequence than was previously thought.

Henderson and Rengarajan (1996) developed a similar part load model to consider the degradation of air conditioner latent or moisture removal capacity at cyclic conditions. This model focused on situations when the fan operated continuously, but the compressor cycled. A more comprehensive study was completed by Shirey et al. (2006) and a more detailed model was developed with physically-based model parameters. The resulting model and the more comprehensive understanding of parametric conditions for a wide variety of systems and conditions allowed them to develop a refined model for latent degradation that could also consider the case when the fan cycles on and off with the compressor (Auto Fan Mode) – the practice most commonly used with residential systems.

Field testing and simulation analysis have been used to assess the impact of over-sizing on energy use and space humidity levels. Sonne et al. (2006) changed out oversized air conditioner units in four Florida houses and replaced them with units sized according to ACCA Manual J (ACCA, 2011a). Detailed performance data was collected both before and after the right-sized unit was installed. Their study found mixed results in terms of seasonal energy use and space humidity levels. In some houses energy use was higher, in some it was lower, and in others the results were inconclusive. Similarly, relative humidity (RH) appears to be either slightly higher and or unchanged after the right-sized unit was installed. They also speculated that duct leakage impacts were greater for the right-sized unit since longer periods of system operation were required to meet the same load. More duct leakage increases the thermal losses to the attic (supply ducts are colder for longer 'on' periods) and brings in more fresh air into the system. Both these effects increase the sensible and latent loads imposed on the system.

A simulation study by Henderson et al., (2007) also confirmed the modest and somewhat unexpected impact of oversizing. They found that, when 20 % duct leakage was factored into the simulations, both energy use and space humidity levels were only slightly affected, even when both latent degradation effects and part load cyclic efficiency losses were considered. For example, oversizing by 30 % in Miami for the HERS Reference house increased energy use by only 2 % and actually resulted in slightly lower space humidity levels.

2.3 Laboratory Studies of Performance Degradation of Heat Pumps Due to Faults
Several studies on degradation of the air conditioner and heat pump performance due to different faults are documented in the literature. While in most cases the main interest of these studies was the fault detection and diagnosis (FDD), some of the findings can be used in the analysis of effects of faulty installation. Reports of major studies on FDD for HVAC systems started to appear in the literature in the nineties, and the number of publications noticeably increased in the last fifteen years.

Table 2.1 lists a few examples of studies published since 2001. The reports by Kim et al. (2006) and Payne et al. (2009) present detailed literature reviews up to the dates these reports were published and include laboratory data for the cooling and heating mode, respectively. These laboratory data are used in our report; however, they had to be extended through tests in environmental chambers to provide complete coverage of the whole range of installation faults of interest in this study (see chapter 3 of this report).

Table 2.1. Selected studies on faults detection and diagnosis

Investigators	System Type	Study Focus
Comstock and Braun (2001)	Centrifugal chiller	Experiment, eight single faults
Kim et al. (2006, 2009)	Split residential heat pump	Experiment for cooling mode, single-faults
Chen and Braun (2001)	Rooftop air conditioner	Simplified rule-based chart method
Navarro-Esbri et al. (2007)	General vapor compression system	Dynamic model based FDD for real-time application
Payne et al. (2009)	Single-speed, split residential heat pump	Experiment for heating model, single-faults
Wang et al. (2010)	HVAC system for new commercial buildings	System-level FDD involving sensor faults
Cho et al. (2005)	Air-handling unit for buildings	Multiple faults
Li and Braun (2007)	Direct expansion vapor compression system	Multiple faults
Du and Jin (2008)	Air handling unit	Multiple faults
Southern California Edison Design and Engineering Services (SCE 2012)	Single-speed, split residential air conditioner	Single faults, dual faults, and triple faults

A large number of laboratory cooling mode tests were performed by Southern California Edison (SCE 2012) to determine the effects of common faults on air conditioner performance. These faults included indoor airflow, outdoor airflow, refrigerant charge, non-condensables, and liquid line restrictions.

SCE single-fault tests at a low refrigerant charge showed similar degradations in cooling capacity and total power as Kim et al. (2006); SCE reported -3 % and 0 % change in cooling capacity and total power, respectively, at 13 % undercharge while Kim et al. (2006) reported -5 % and -2 % change at 10 % refrigerant undercharge. However, at higher fault levels, SCE measured much higher performance degradation than Kim et al.; cooling capacity and total power changed by -54 % and -5 %, respectively, at 27 % undercharge (SCE) compared to -17 % and -3 % at 30 % undercharge (Kim et al., 2006). These large differences in cooling capacity change for a similar fault level exemplify differences in the effect a given fault may have on different systems. In the case of refrigerant undercharge fault, it is possible that different internal volumes were a factor in the different system responses.

SCE also performed several tests with dual and triple faults, which included reduction of the outdoor airflow by imposing different levels of airflow restriction. For the highest level of outdoor airflow blockage, 40 % refrigerant undercharge, and 56 % reduction in indoor airflow, the cooling capacity decreased by almost 70 %. The conducted multiple fault tests show the range of possible performance degradation, however, more tests are required to allow modeling of these faults within annual simulations of the house/heat pump system.

3. HEAT PUMP PERFORMANCE DEGRADATION DUE TO FAULTS

A significant number of laboratory tests were taken by Kim et al. (2006) and Payne et al. (2009) to characterize heat pump performance degradation due to faults. For the purpose of this study, we conducted additional tests using the same heat pump and test apparatus to expand the ranges of previously studied faults and to include faults that were not covered earlier, specifically, improper electric line voltage and improper liquid line subcooling. The goal of this experimental effort was to enable the development of correlations that characterize the heat pump performance operating with these faults. These correlations are presented in a non-dimensional format with performance parameters expressed as a function of operating conditions and fault level.

3.1 Laboratory Measurements
3.1.1 Experimental Apparatus and Test Conditions
The studied system was a single-speed, split heat pump with an 8.8 kW (2.5 ton) rated cooling capacity. The heat pump was equipped with a thermostatic expansion valve (TXV). Figure 3.1 shows a schematic diagram of the experimental setup with the locations of the main measurements. The air-side measurements included indoor dry-bulb and dew-point temperatures, outdoor dry-bulb temperature, barometric pressure, and pressure drop across the air tunnel (not shown on the schematic). Twenty-five node, T-type thermocouple grids and thermopiles measured air temperatures and temperature change, respectively. On the refrigerant side, pressure transducers and T-type thermocouple probes measured the inlet and exit parameters at every component of the system.
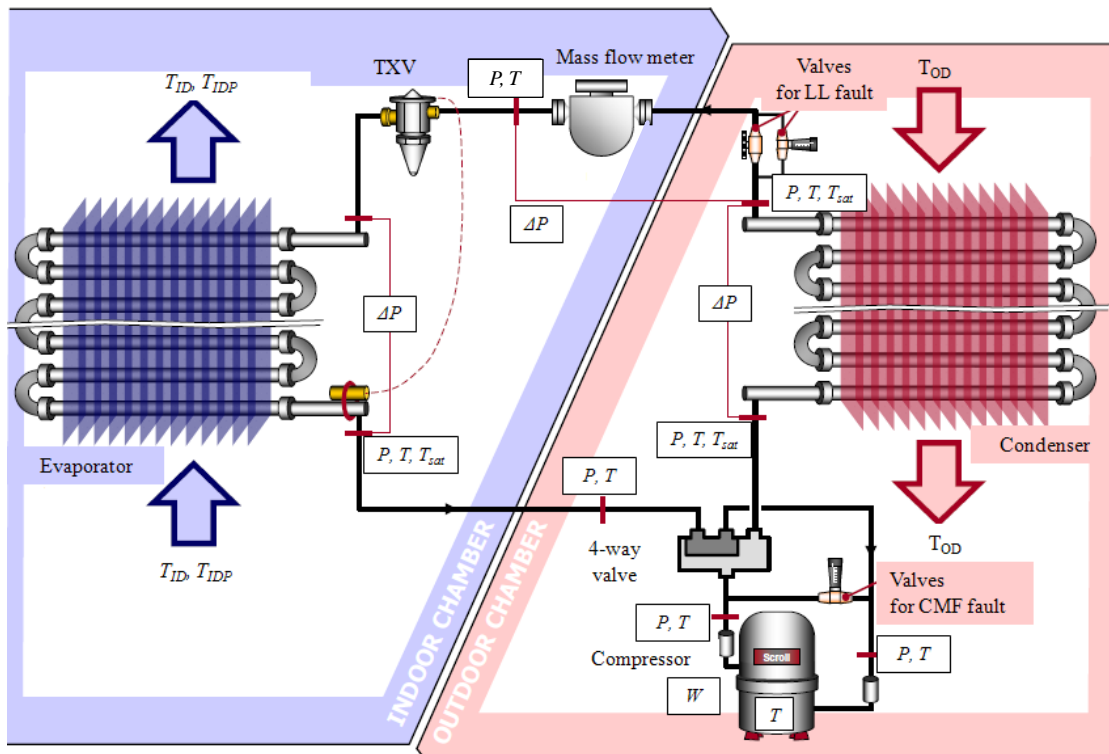
Figure 3.1. Schematic diagram of experimental apparatus (Kim et al. (2006))

Tables 3.1 presents the cooling and heating test conditions (indoor dry bulb, indoor dew point, and outdoor dry bulb temperatures), and Table 3.2 presents the measurement uncertainties. For the uncertainty analysis and detailed description of the experimental setup the reader should refer to Kim et al. (2006).

8

Table 3.1. Cooling and heating test temperatures

Cooling			Heating		
T_{ID} °C (°F)	T_{IDP} °C (°F)	T_{OD} °C (°F)	T_{ID} °C (°F)	T_{IDP} °C (°F)	T_{OD} °C (°F)
21.1 (70)	10.3 (50.5)	27.8 (82)	18.3 (65)	dry	-8.3 (17)
21.1 (70)	10.3 (50.5)	37.8 (100)	21.1 (70)	dry	-8.3 (17)
26.7 (80)	15.8 (60.4)	27.8 (82)	21.1 (70)	dry	1.7 (35)
26.7 (80)	15.8 (60.4)	35.0 (95)	21.1 (70)	dry	8.3 (47)
26.7 (80)	15.8 (60.4)	37.8 (100)			

Note: The dew-point temperature in the cooling mode corresponds to a relative humidity of 50 %

Table 3.2. Measurement uncertainties

Measurement	Measurement Range		Uncertainty at the 95% confidence level
Air dry-bulb temperature	(-9 ~ 38) °C	((15 ~ 100) °F))	±0.4 °C (±0.7 °F)
Air dew-point temperature	(0 ~ 38) °C	(32 ~ 100) °F)	±0.4 °C (±0.7 °F)
Air temperature difference	(0 ~ 28) °C	(0 ~ 50) °F)	±0.3 °C (±0.5 °F)
Air nozzle pressure	(0 ~ 1245) Pa	((0 ~ 5) in H_2O)	±1.0 Pa (0.004 in H_2O)
Refrigerant temperature	(-12 ~ 49) °C	((10 ~ 120) °F)	±0.3 °C (±0.5 °F)
Refrigerant mass flow rate	(0 ~ 272) kg·h⁻¹	((0 ~ 600) lb·h⁻¹)	±1.0 %
Cooling capacity	(3 ~ 11) kW	((3 ~ 11) kW)	±4.0 %
Power	(25 ~ 6000) W	((25 ~ 6000) W)	±2.0 %
COP	2.5 ~ 6.0		±5.5 %

3.1.2 Studied Faults and Their Implementation

Table 3.3 lists seven studied faults, including their definition and range. The first six faults were studied experimentally. The impact of the last listed fault, cooling-mode TXV undersizing, was determined based on a detailed analysis; the inherent variable-opening capability masks the TXV undersizing, and the performance penalty occurs only after the outdoor temperature is below a certain threshold temperature, referred to by us as the 'departure temperature', which is related to the level of this fault. We did not include the TXV mismatched fault in the heating mode because it is very unlikely to occur as the heating TXV is installed in the outdoor section at the factory at time of assembly.

The indoor airflow fault was implemented by lowering the speed of the nozzle chamber booster fan to increase the external static pressure across the indoor air handler. The fault level was calculated as a ratio of the fault-imposed air mass flow rate to the no-fault air mass flow rate, with the -100 % fault level indicating a complete loss of airflow.

The no-fault refrigerant charge was set in the cooling mode at the AHRI 210/240 Standard A-test condition (AHRI, 2008). The refrigerant undercharge and overcharge faults were implemented by adding or removing the refrigerant from a correctly charged system. The fault level was defined as the ratio of the refrigerant mass by which the system was overcharged or undercharged to the no-fault refrigerant charge, with 0 % indicating the correct, no-fault charge, -100 % indicating no refrigerant charge, and 100 % indicating doubled charge.

Table 3.3. Definition and range of studied faults

Fault name	Symbol	Definition of fault level	Fault range (%)
Improper indoor airflow rate	AF	% above or below correct airflow rate	-50 ~ 20
Refrigerant undercharge	UC	% mass below correct (no-fault) charge	-30 ~ 0
Refrigerant overcharge	OC	% mass above correct (no-fault) charge	0 ~ 30
Improper liquid line refrigerant subcooling (indication of improper refrigerant charge)	SC	% above the no-fault subcooling value	0 ~ 200
Presence of non-condensable gases	NC	% of pressure in evacuated indoor section and line set, due to non-condensable gas, with respect to atmospheric pressure	0 ~ 20
Improper electric line voltage	VOL	% above or below 208 V	-8.7 ~ 25
TXV undersizing, cooling	TX	% below the nominal cooling capacity	-60 ~ -20

The amount of refrigerant in a TXV-equipped system can also be estimated by examining the refrigerant subcooling in the liquid line; this method is commonly used by field technicians installing or servicing a heat pump. Therefore, we also characterized the effect of refrigerant overcharge by noting the liquid line subcooling at increased charge levels. The ratio of fault-imposed subcooling to the no-fault subcooling indicated the fault level with the 0 % fault corresponding to the proper subcooling, and the 100 % fault indicating a doubled subcooling level.

The non-condensable gas fault is caused by incomplete evacuation of the system during installation or after a repair that required opening the system to the atmosphere. When a new heat pump is installed, the outdoor unit is typically pre-charged, and the installer needs to evacuate the indoor section and the connecting tubing before charging it with refrigerant. Industry practice (ACCA, 2010) is to evacuate the system to a vacuum of 500 µPa (29.9 in Hg vacuum). The non-condensable gas fault was implemented by adding dry nitrogen to the evacuated system before the charging process. This fault level is defined by the ratio of pressure in the evacuated indoor section due to non-condensable to the atmospheric pressure. The 0 % fault level occurs when the refrigerant charging process starts with a vacuum, and the 100 % fault level would occur when the nitrogen filled refrigerant lines are at atmospheric pressure before the refrigerant is charged.

The electrical line voltage fault was implemented by varying the supply voltage to the system from the nominal, no-fault value of 208 VAC. The fault level was defined by the percentage by which the line voltage was above or below the nominal level, with a positive fault indicating a voltage above 208 VAC.

TXV mismatch results in the TXV being unable to adjust its opening to match the refrigerant mass flow rate pumped by the compressor. This fault level is defined as the ratio of the difference in the nominal system capacity and the TXV capacity with respect to the nominal system capacity. With this definition, it is assumed TXVs are rated at the midpoint of their opening range of ±40 %.

10

3.2 Fault Effects on Cooling Mode Performance
3.2.1 Cooling Mode Normalized Performance Parameters and Correlations
The cooling mode tests considered the effect of faults on six performance parameters: total cooling capacity (Q_{tot}, capacity includes the indoor fan heat), refrigerant-side cooling capacity (Q_R, capacity does not include the indoor fan heat), coefficient of performance (COP), sensible heat ratio (SHR), outdoor unit power (W_{ODU}, includes the compressor, outdoor fan, and controls powers), and total power (W_{tot}, includes W_{ODU} and indoor fan power). These parameters are presented in a dimensionless, normalized format obtained by dividing the values as obtained for the heat pump operating under a selected fault to their value obtained for the heat pump operating fault free. We used Eq. (3.1) to correlate the dimensionless parameters as a function of the indoor dry-bulb temperature (T_{ID}), outdoor dry-bulb temperature (T_{OD}), and fault level (F).

$$Y=\frac{X_{\text{fault}}}{X_{\text{no-fault}}}=1+(a_1+a_2 T_{ID}+a_3 T_{OD}+a_4 F)F \qquad (3.1)$$

where a_1, a_2, a_3, and a_4 are correlation coefficients, X_{fault} and $X_{\text{no-fault}}$ are performance parameters for a faulty and fault-free heat pump, and Y is a dimensionless parameter representing the ratio of the faulty performance from that of the fault-free heat pump.

Table 3.4 shows coefficients for a correlation using three input variables, T_{ID}, T_{OD}, and F. The coefficients were determined by means of a multivariate polynomial regression method using the normalized values of performance parameters determined from heat pump test data. If the heat pump is fault free, values of all normalized parameters equal unity. The fit standard error of the normalized correlation dependent variable, Y, was a maximum of 3 % over the range of operating conditions listed in Table 3.1. Table 3.5 shows an example of propagation of uncertainty for the faulty COP and cooling capacity obtained from calculations using the measurement uncertainties of the corresponding fault-free values and the 3 % uncertainty in the dimensionless parameter Y.

The following is an explanation of the procedure used to calculate the dimensionless capacity and COP due to undersizing of the cooling mode TXV. This fault occurs if the expansion valve's equivalent orifice area is too small to control refrigerant superheat during periods of low ambient temperature conditions at reduced condenser pressures. A properly sized TXV will regulate refrigerant flow rate and maintain proper superheat over a wide range of indoor and outdoor air temperatures. However, if the indoor TXV is undersized for the particular outdoor unit, the system performance is degraded due to a restricted mass flow of refrigerant at certain evaporator and condenser pressure differentials. The rated TXV capacity and nominal system capacity are used to determine the TXV undersizing fault level. For example, if a 7.0 kW (2 ton) TXV is installed in a system with the nominal capacity of 8.8 kW (2.5 ton), the fault level is 20 %. (F = 1-7.0/8.8=0.20).

Since the pressure difference between upstream and downstream becomes smaller with decreasing outdoor temperature, the TXV opens to increase refrigerant mass flow rate at low outdoor temperatures. The outdoor temperature at which the TXV reaches its maximum orifice size, referred to as the 'departure temperature', is determined from calculations and empirical fits to previous data. The resulting departure temperature below which the TXV cannot supply adequate mass flow rate is given by Eq. (3.2).

$$T^{\text{dep}}[°C]=80.326 \cdot F+11.682 \qquad (3.2)$$

Table 3.4. Correlations for non-dimensional performance parameters in the cooling mode

Fault	Performance parameter Y	$Y=1+(a_1+a_2 T_{ID}+a_3 T_{OD}+a_4 F)\cdot F^*$				FSE**
		a_1	a_2	a_3	a_4	
Improper indoor airflow rate (AF)	COP	$Y_{COP}=Y_{Qtot}/Y_{Wtot}$				1.65E-02
	Q_{tot}	1.85E-01	1.77E-03	-6.40E-04	-2.77E-01	1.53E-02
	Q_R	2.95E-01	-1.17E-03	-1.57E-03	6.92E-02	5.39E-03
	SHR***	5.93E-02	5.16E-03	1.81E-03	-2.89E-01	9.82E-03
	W_{ODU}	-1.03E-01	4.12E-03	2.38E-03	2.10E-01	6.91E-03
	W_{tot}	1.35E-02	2.95E-03	-3.66E-04	-5.88E-02	5.68E-03
Refrigerant undercharge (UC))	COP	$Y_{COP}=Y_{Qtot}/Y_{Wtot}$				1.17E-02
	Q_{tot}	-5.45E-01	4.94E-02	-6.98E-03	-1.78E-01	1.02E-02
	Q_R	-9.46E-01	4.93E-02	-1.18E-03	-1.15E+00	1.44E-02
	SHR***	4.19E-01	-2.12E-02	1.26E-03	1.39E-01	8.56E-03
	W_{ODU}	-3.13E-01	1.15E-02	2.66E-03	-1.16E-01	5.14E-03
	W_{tot}	-2.54E-01	1.12E-02	2.06E-03	5.74E-03	5.29E-03
Refrigerant overcharge (OC)	COP	$Y_{COP}=Y_{Qtot}/Y_{Wtot}$				2.00E-02
	Q_{tot}	4.72E-02	-1.41E-02	7.93E-03	3.47E-01	1.96E-02
	Q_R	-1.63E-01	1.14E-02	-2.10E-04	-1.40E-01	5.67E-03
	SHR***	-7.75E-02	7.09E-03	-1.93E-04	-2.76E-01	7.34E-03
	W_{ODU}	2.19E-01	-5.01E-03	9.89E-04	2.84E-01	5.17E-03
	W_{tot}	1.46E-01	-4.56E-03	9.17E-04	3.37E-01	5.43E-03
Improper liquid line refrigerant subcooling (SC)	COP	$Y_{COP}=Y_{Qtot}/Y_{Wtot}$				2.26E-02
	Q_{tot}	6.77E-02	0.00E+00	-1.22E-03	-1.91E-02	2.18E-02
	Q_R	4.16E-02	0.00E+00	-3.51E-04	-1.55E-02	1.39E-03
	SHR***	-9.04E-02	0.00E+00	2.13E-03	1.60E-02	3.06E-02
	W_{ODU}	2.11E-02	0.00E+00	-4.18E-04	4.25E-02	4.34E-03
	W_{tot}	1.06E-02	0.00E+00	-2.93E-04	3.88E-02	4.84E-03
Non-condensable gas (NC)	COP	$Y_{COP}=Y_{Qtot}/Y_{Wtot}$				1.71E-02
	Q_{tot}	2.77E-01	-1.75E-02	1.78E-02	-1.96E+00	1.63E-02
	Q_R	-1.78E+00	4.04E-02	1.78E-02	9.98E-01	9.59E-03
	SHR***	-4.67E-01	1.69E-02	9.89E-04	2.90E-01	5.59E-03
	W_{ODU}	-6.92E-01	2.01E-02	1.20E-02	6.62E-01	6.13E-03
	W_{tot}	-5.37E-01	1.52E-02	1.09E-02	4.36E-01	6.20E-03
Improper line voltage (VOL)	COP	$Y_{COP}=Y_{Qtot}/Y_{Wtot}$				1.98E-02
	Q_{tot}	5.84E-01	-1.21E-02	-8.57E-03	-3.35E-01	1.80E-02
	Q_R	1.03E-01	-6.10E-03	3.64E-03	-1.04E-01	6.41E-03
	SHR***	-6.65E-02	5.21E-03	-2.10E-03	4.23E-02	2.95E-02
	W_{ODU}	7.66E-01	-3.85E-03	-1.83E-02	1.14E+00	4.39E-03
	W_{tot}	9.06E-01	-6.37E-03	-1.75E-02	1.10E+00	7.39E-03
TXV undesizing, cooling (TXV)	Refer to Eqs. (3.6, 3.7) and Table 3.6					

* All temperatures are in Celsius
** FSE (fit standard error) equals the square root of the sum of the squared errors divided by the degrees of freedom
*** The applicable range of SHR for wet coil predictions: 0.7 to 0.85

Table 3.5. Example uncertainty propagation due to normalized correlation (Y) uncertainty of 3 % for faulty COP and cooling capacity at AHRI Standard 210/240 B-test condition (AHRI, 2008)

Fault	Parameter	Parameter Value	Uncertainty (%) (95 % confidence level)
10 % reduced indoor airflow	COP	3.67	± 6.4
	Cooling capacity	9.4 kW	± 5.0

The cooling capacity and the gross COP of the undersized TXV-equipped system can be expressed as functions of outdoor temperature and fault level. To develop equations for the normalized capacity and COP, non-dimensional variables for outdoor temperature, cooling capacity, and gross COP are defined by Eqs. (3.3, 3.4, 3.5), respectively, where T_{OD} has Celsius units.

$$T_r = \frac{T_{OD}}{35\ °C} \tag{3.3}$$

$$Y_Q = \frac{Q_{undersized}}{Q_{no-fault}} \tag{3.4}$$

$$Y_{COP} = \frac{COP_{undersized}}{COP_{no-fault}} \tag{3.5}$$

The correlations for determining normalized cooling capacity and normalized gross COP are given by Eqs. (3.6) and (3.7) and are presented in a graphical form in Figure 3.2. The coefficients are listed in Table 3.6.

$$Y_Q = a_1 + a_2 T_r + a_3 F + a_4 T_r^2 + a_5 T_r F + a_6 F^2 \quad \text{if} \quad T_{OD} \leq T^{dep} \quad \text{or} \quad Y_Q = 1 \ \text{if} \ T_{OD} > T^{dep} \tag{3.6}$$

$$Y_{COP} = b_1 + b_2 T_r + b_3 F + b_4 T_r^2 + b_5 T_r F + b_6 F^2 \quad \text{if} \quad T_{OD} \leq T^{dep} \quad \text{or} \quad Y_Q = 1 \ \text{if} \ T_{OD} > T^{dep} \tag{3.7}$$

Table 3.6. Normalized capacity and COP correlation coefficients for a TXV undersizing fault

Coefficients for Y_Q		Coefficients for Y_{COP}	
a_1	9.1440E-01	b_1	8.4978E-01
a_2	2.0903E-01	b_2	4.0050 E-01
a_3	-5.4122E-01	b_3	-8.4120E-01
a_4	1.2194E-01	b_4	7.5740E-02
a_5	-2.9428E-01	b_5	-3.3105E-01
a_6	-3.0833E-02	b_6	2.0290E-01

A complete and detailed discussion of the TXV undersizing fault correlation development is beyond the scope of this report and is presented by Payne and Kwon (2014).
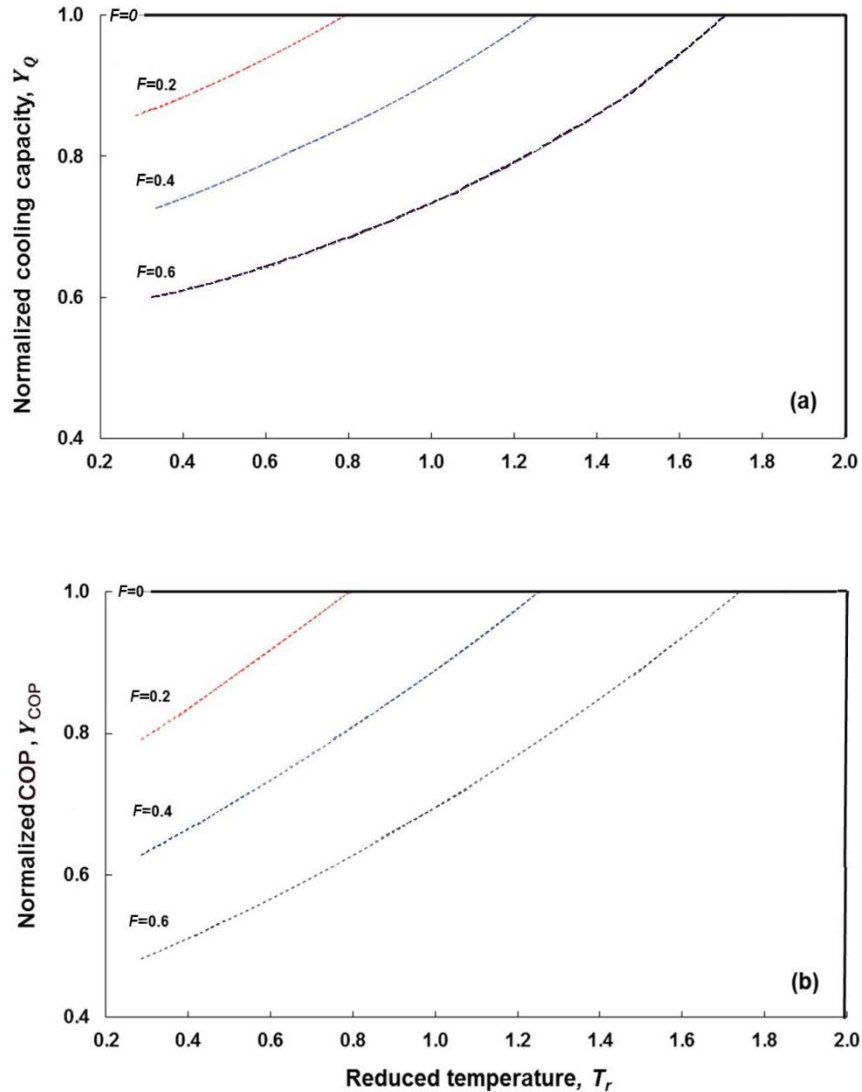
Figure 3.2.   Normalized performance parameters for the cooling mode TXV undersizing fault: (a) capacity, (b) COP

3.2.2 Cooling Mode Charts with Normalized Performance Parameters
Figures 3.3 through 3.8 show variations of the normalized performance parameters with respect to fault levels at five operating conditions. The figures present the measured data points and correlations developed for COP, capacity, SHR, total power and, for some faults, the outdoor unit power. The outdoor unit power is included for improper indoor airflow (AF) and improper liquid line refrigerant subcooling (SC) faults where the trends of the total power and the outdoor unit power were not similar. In some of the figures there is a significant difference between the correlation fits and the actual data points. The correlations were developed for all indoor and outdoor test conditions, and thus the fit sum of squared deviations was minimized. In addition, the normalized value for the heat pump operating with no fault was calculated from the fault-free correlation as presented by Kim et al. (2010); therefore, no-fault tests may actually have normalized values somewhat different from unity due to the inability of the no-fault correlation to predict the no-fault parameter exactly. Scatter of normalized no-fault data around unity indicates measurement uncertainty, correlation uncertainty, and uncertainty caused by different system

installations. The data for Figures 3.6 and 3.8 were collected after the system was removed and re-installed in the test chambers; therefore, one would expect more scatter in the normalized no-fault correlations due to this installation repeatability uncertainty. This installation repeatability uncertainty is also indicative of what could be seen in field installations when applying the same no-fault correlations from system to system.

Figure 3.3 shows the normalized parameters at a reduced and increased indoor airflow. For the studied airflow range from -50 % to +20 % of the nominal value, the change in outdoor unit power ranged from -3 % to 0 %, respectively, with small variations between different operating conditions. Total power varied from -5 % to 2 % within the same range of airflow rate, which indicates the varied power of the indoor fan at this fault. COP and capacity were markedly degraded at a decreased airflow and somewhat improved at the increased airflow above the nominal level; however, these increases in COP and capacity were associated with a significant increase in SHR, which may not be a desirable change from the homeowner's comfort point of view. The difference between total power and outdoor unit power is due to the power of the indoor blower, which was nominally 430 W. Outdoor unit power was relatively constant under this fault. As a result, COP slightly increased at the max fault level by the increased indoor airflow.

Figures 3.4 and 3.5 show the variation of the normalized values for refrigerant charge faults. The changes in COP and total capacity for refrigerant undercharge are larger than those for refrigerant overcharge. A 30 % undercharge reduced capacity by almost 15 % on average reducing COP by 12 % while a 30 % overcharge produced little reductions or small increases in capacity with 6 % greater total power and 3 % reduced COP on average because of the increased discharge pressure. In case of different outdoor temperature conditions, COP and capacity increased as the outdoor temperature increased for the undercharged condition. Farzad et al. (1990) also showed that higher refrigerant flow rate is one reason for the higher capacity at higher outdoor temperatures for the conditions of undercharge.

In this study, a subcooling temperature of 4.4 °C (8.0 °F) was regarded as the no-fault condition under the considered test conditions. Figure 3.6 shows the effects of increased subcooling at the TXV inlet. The departure of the normalized values of COP and cooling capacity from the correlations in the figure are mostly due to the TXV attempting to correct mass flow rate (reduce effective orifice size) as subcooling increases. If more data were available with subcooling being varied randomly from high to low values, hysteresis effects and TXV hunting effects would be better captured. COP and capacity normalized correlations for higher levels of subcooling still represent the general trends in system performance. Increased subcooling is a symptom of excessive refrigerant charge, and it has the same effect; higher subcooling leads to reduced condensing area and increased condensing pressure. In the studied heat pump, refrigerant overcharging by 30 % corresponded to approximately doubling of refrigerant subcooling. For this level of fault the COP degradation was within 4 %. For the highest subcooling fault of 181 % of the nominal value, the impact on the capacity was minor but the outdoor unit power increased by 15 %, which resulted in a similar decrease in the COP.

Figure 3.7 shows the variation of the normalized values for chosen performance parameters versus non-condensable gas (NC) fault level. Non-condensable gases increase the condensing pressure above that corresponding to the saturation pressure of the refrigerant at the same temperature due to the partial pressure of the NC components. As a result, increased total power consumption and decreased COP can be seen in the Figure 3.7. Maximum degradation of COP at the 20 % fault level was about 5 % for the condition of T_{ID}=26.7 °C (80.0 °F) and T_{OD}=27.8 °C (82.0 °F).

Figure 3.8 shows the variation of the normalized values for chosen performance parameters for the line voltage variation fault conditions. A line voltage of 208 V was set as the no-fault condition. Total external static pressure for the indoor air handler was set at 125 Pa (0.5 in H_2O) at the no-fault line voltage, which produced a nominal indoor fan power demand of 430 W. As voltage increased, fan speed and static

pressure increased thus producing increased fan power. Total power consumption increased almost linearly as the fault level increased. The fan power increased more than the compressor power when the voltage was increased. An average increase of 27 % for the fan power and 9 % for the compressor power occurred at the max fault level. At fault levels over 20%, the degradation of COP is greater than 10 %.

The presented measurements for the cooling mode indicate that the refrigerant undercharge fault has the highest potential for degrading air conditioner efficiency. For 30 % percent undercharge – a fault level commonly observed during field surveys – the system efficiency is decreased between 7 % and 15 %, depending on operating conditions.

A reduction of the airflow rate by 30 % (also a commonly observed fault) can reduce the efficiency by 6 %, and this level of degradation persists independently of operating conditions. Refrigerant overcharging by 30 % resulted in COP degradation on the order of 4 %. COP degradation within 3 % was measured for improper electric voltage and non-condensable gas faults. The non-condensable gas fault can be misdiagnosed in the field as refrigerant overcharge, which may prompt a serviceman to remove some of the refrigerant from the system, thus triggering an undercharge fault.
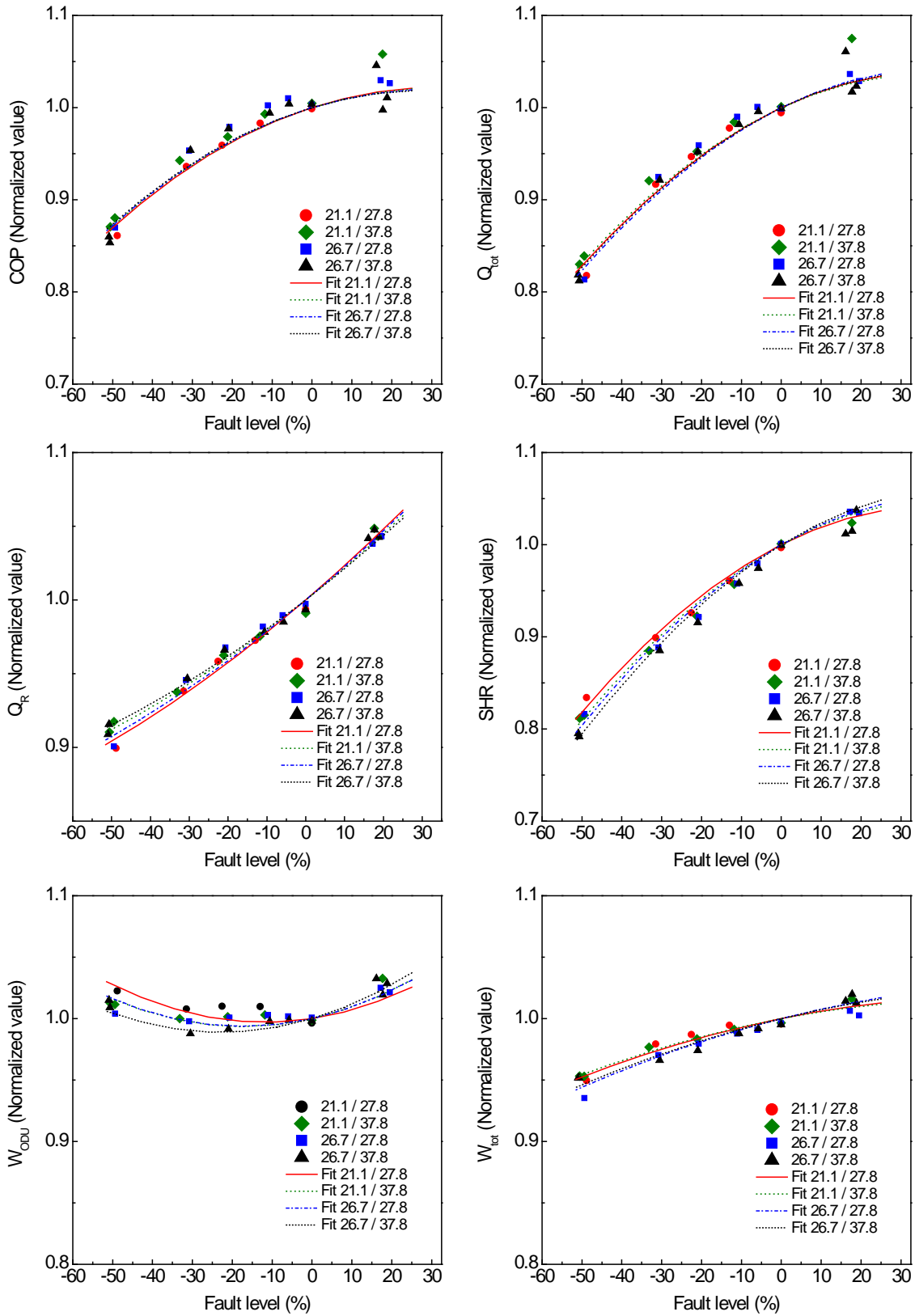
Figure 3.3. Normalized cooling performance parameters for improper indoor airflow
(The numbers in the legend denote test conditions, T_{ID} (°C)/ T_{OD} (°C))

17
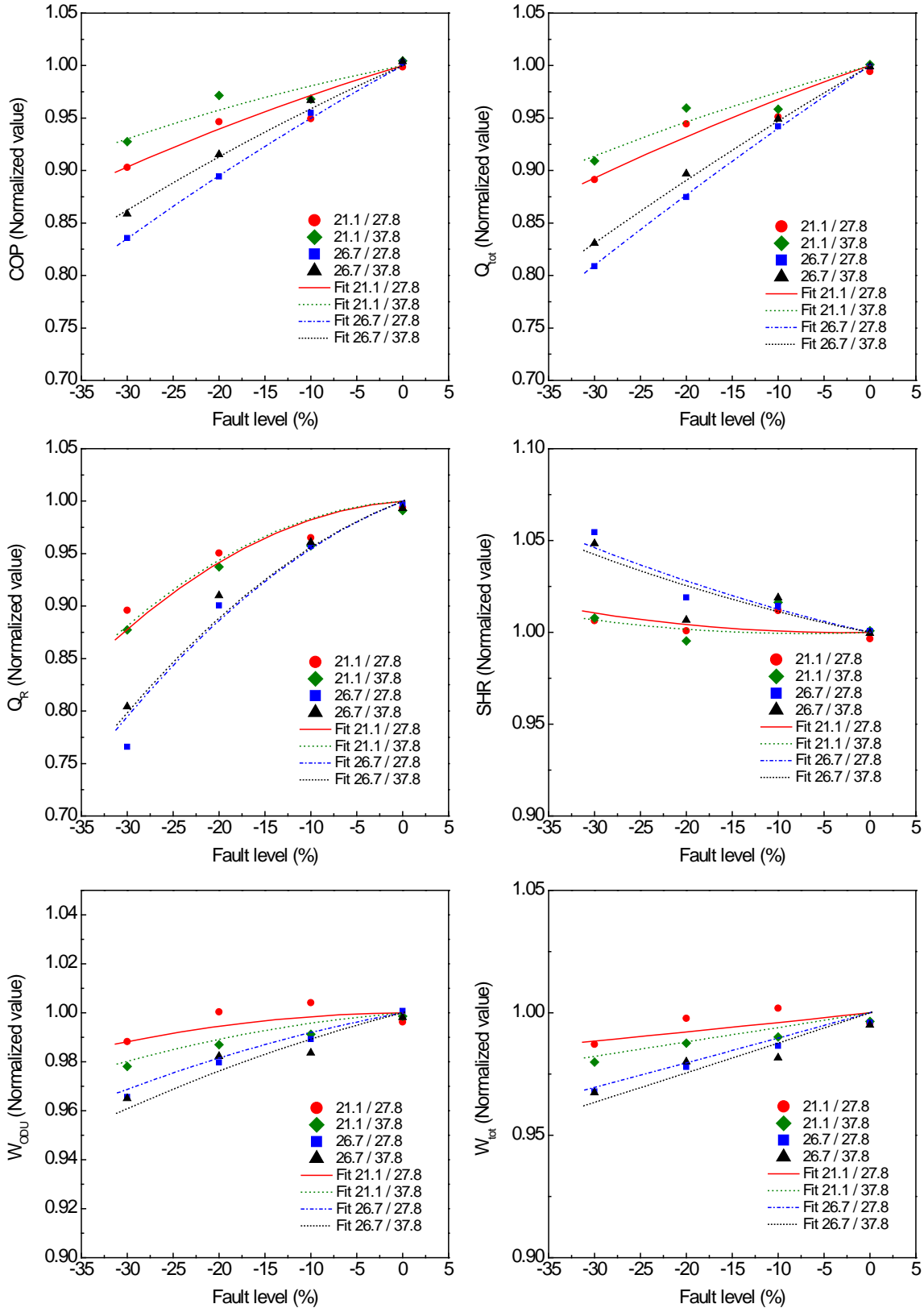
Figure 3.4. Normalized cooling performance parameters for refrigerant undercharge
(The numbers in the legend denote test conditions, T_{ID} (°C)/ T_{OD} (°C))
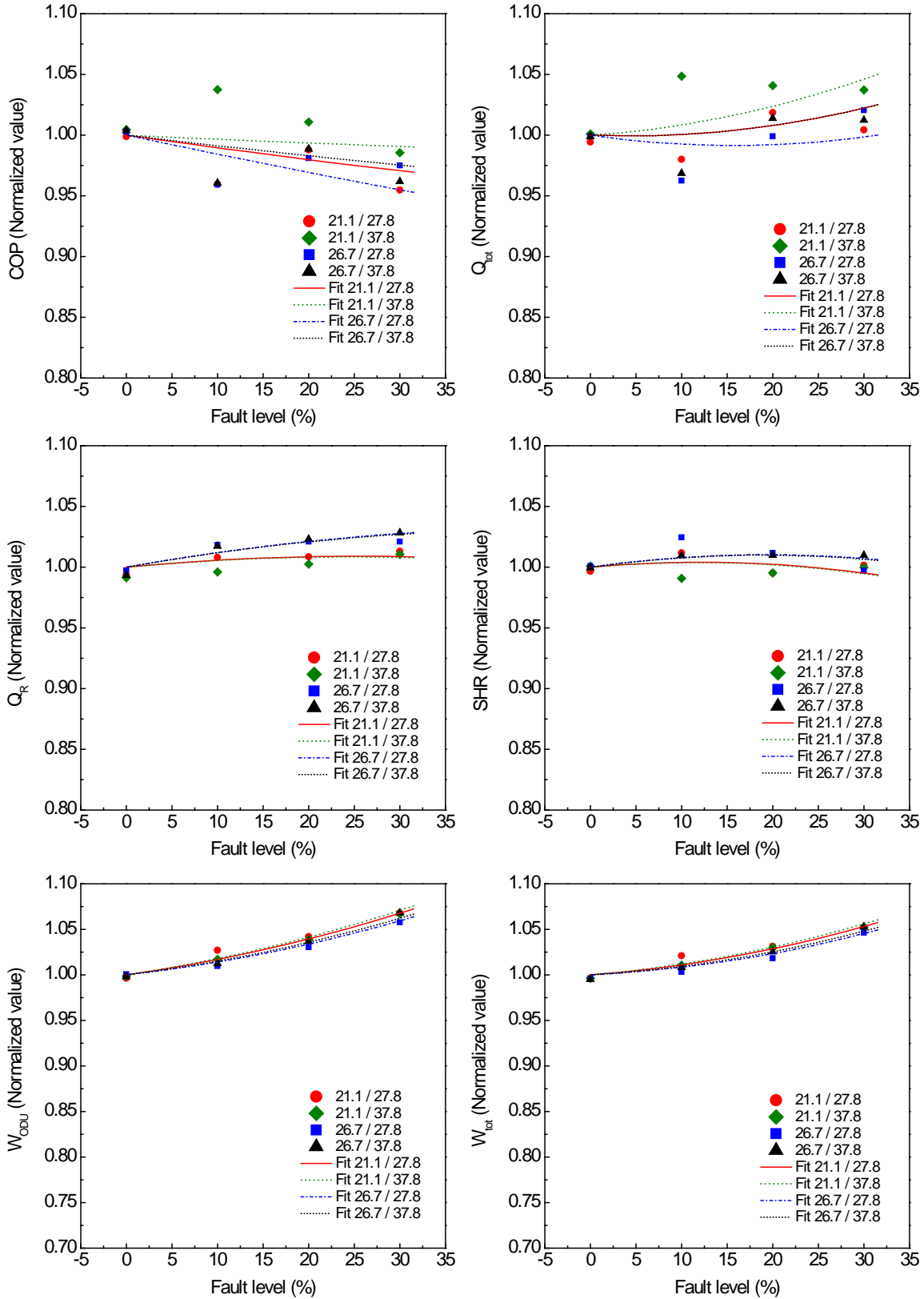
Figure 3.5. Normalized cooling performance parameters for refrigerant overcharge
(The numbers in the legend denote test conditions, T_{ID} (°C)/ T_{OD} (°C))

19
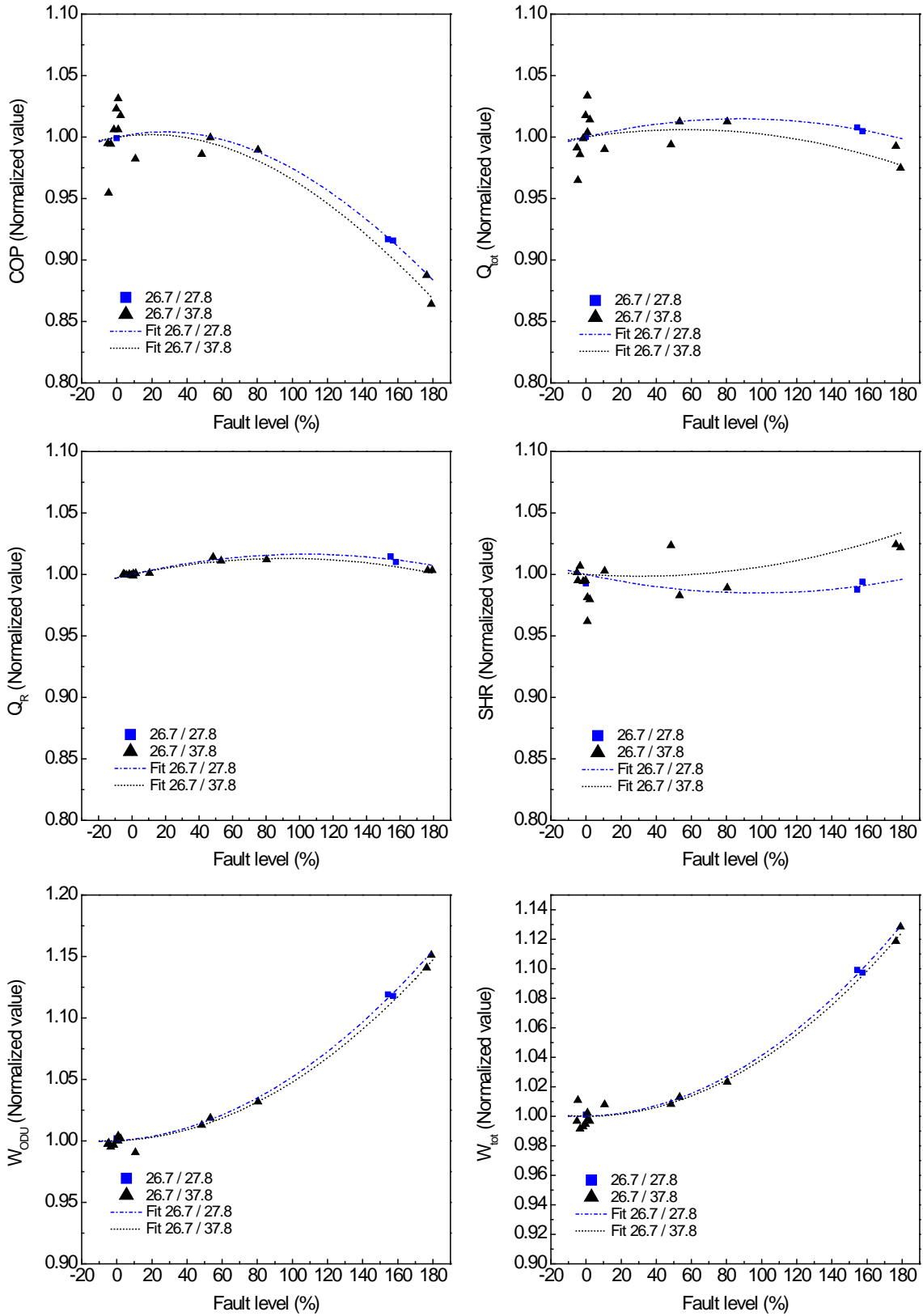
Figure 3.6. Normalized cooling performance parameters for improper liquid line refrigerant subcooling
(The numbers in the legend denote test conditions, T_{ID} (°C)/ T_{OD} (°C))
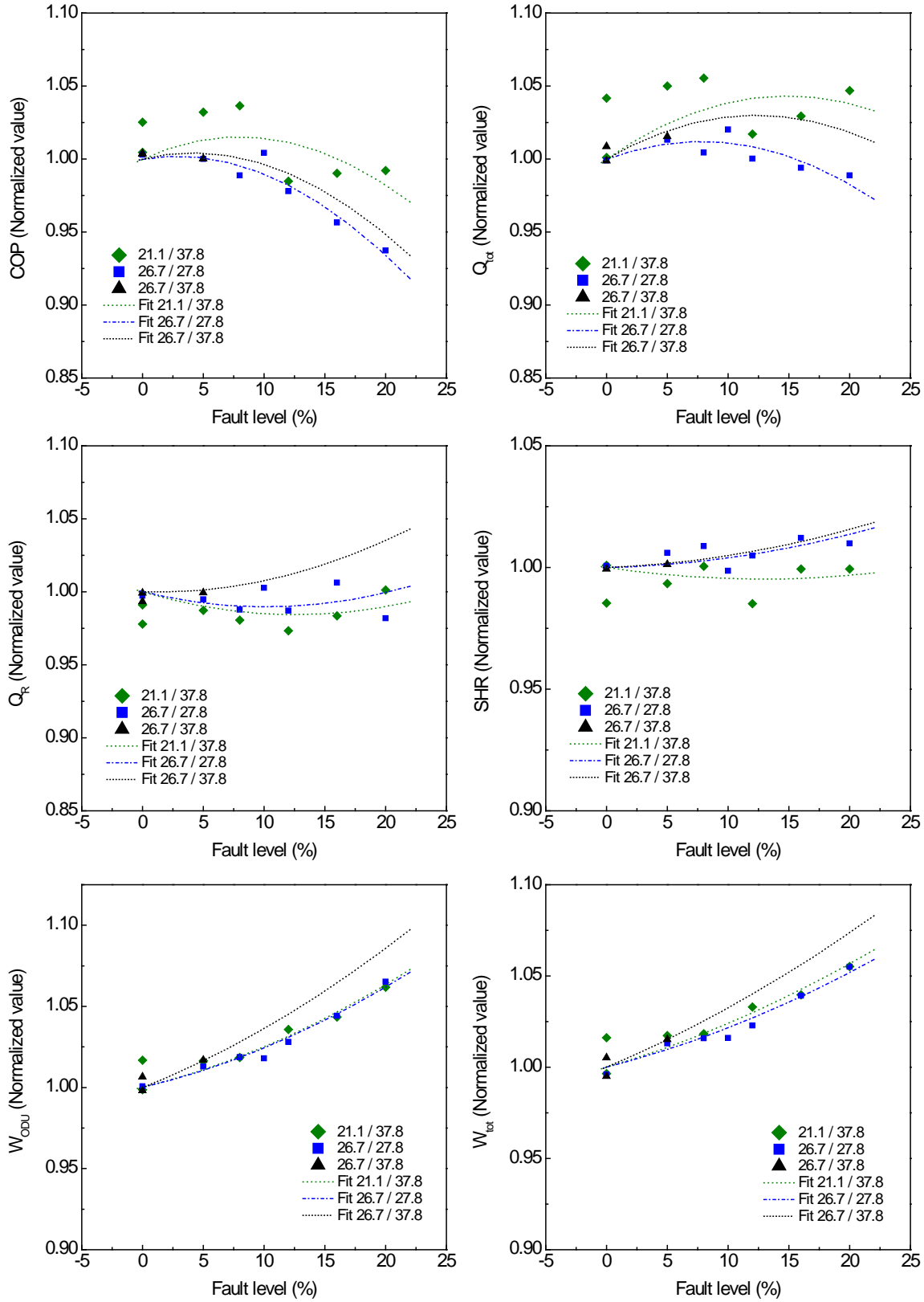
Figure 3.7. Normalized cooling performance parameters for the presence of non-condensable gas
(The numbers in the legend denote test conditions, T_{ID} (°C)/ T_{OD} (°C))
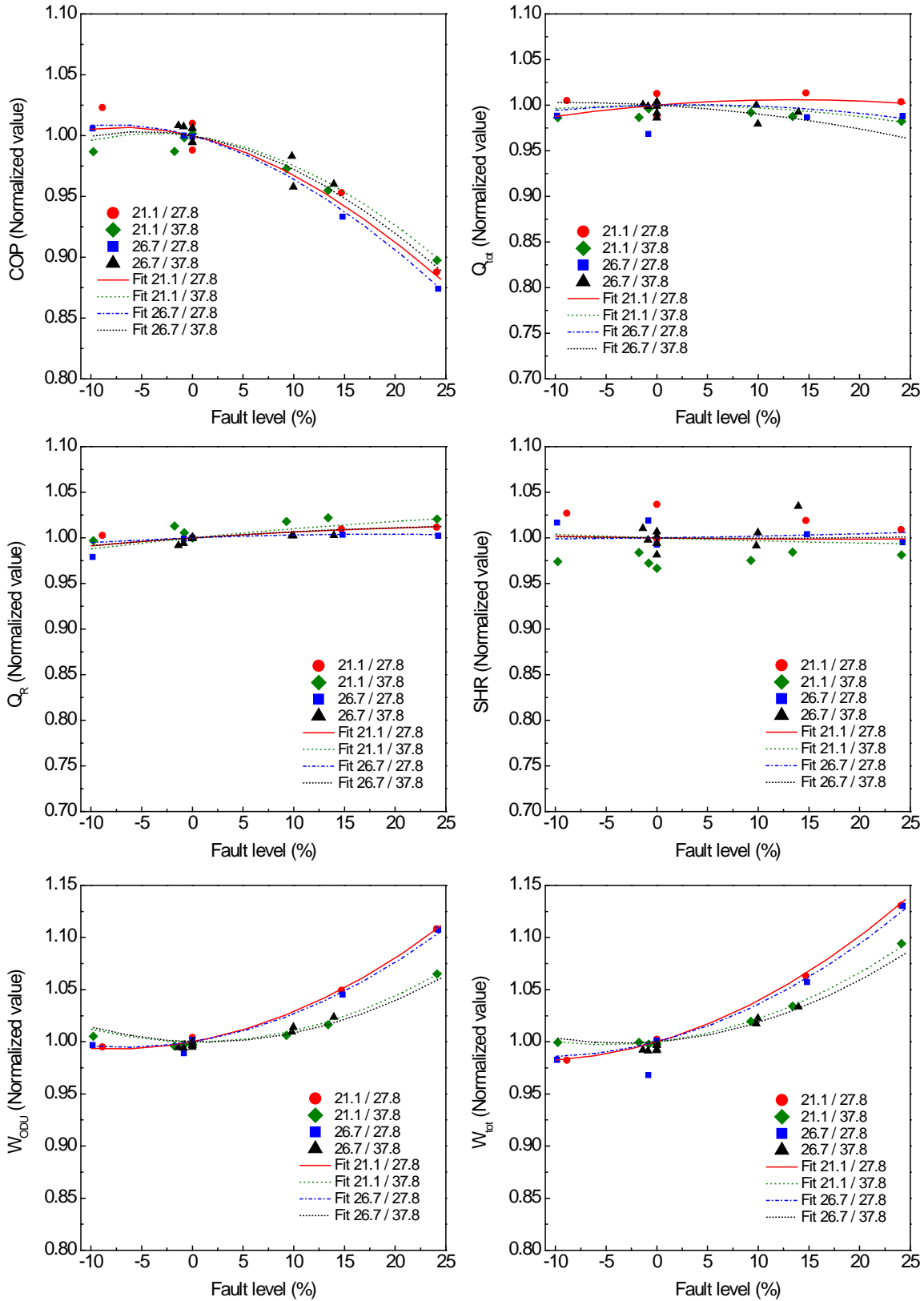
Figure 3.8. Normalized cooling performance parameters for improper electric line voltage
(The numbers in the legend denote test conditions, T_{ID} (°C)/ T_{OD} (°C))

22

3.3 Fault Effects on Heating Mode Performance

3.3.1 Heating Mode Normalized Performance Parameters and Correlation

The heating mode tests considered the effect of faults on five performance parameters: coefficient of performance (COP), total heating capacity (Q_{tot}, includes the indoor fan heat), refrigerant-side heating capacity (Q_R, does not include the indoor fan heat), outdoor unit power (W_{ODU}, includes the compressor, outdoor fan, and controls powers), and total power (W_{tot}, includes W_{ODU} and indoor fan power). These parameters are presented in a dimensionless, normalized format obtained by dividing these parameter values as obtained for the heat pump operating under a selected fault by the no-fault value. The normalized parameters were correlated as a function of outdoor dry-bulb temperature (T_{OD}) and fault level (F). These two parameters were the only values varied for the heating mode tests; indoor dry-bulb temperature did not vary enough to use in the heating mode correlations.

$$Y = \frac{X_{\text{fault}}}{X_{\text{no-fault}}} = 1 + (a_1 + a_2 T_{OD} + a_3 F) \cdot F \qquad (3.8)$$

where a_1, a_2, and a_3 are correlation coefficients, X_{fault} and $X_{no\text{-}fault}$ are performance parameters for a faulty and fault-free heat pump, and Y is a dimensionless parameter representing the ratio of the faulty performance from that of the fault-free heat pump.

Tables 3.7 shows the correlation coefficients. They were determined by means of a multivariate polynomial regression method using the normalized values of performance parameters determined from heat pump test data. If the heat pump is fault free, values of all normalized parameters equal unity.

3.3.2 Heating Mode Charts with Normalized Performance Parameters

Figure 3.9 shows the effects of reduced airflow over the indoor coil during heating mode operations. The airflow rate through the indoor heat exchanger was controlled by changing the speed of the nozzle chamber booster fan. As shown in the graphs, effects of this fault condition for COP and power are noticeable. Especially, for the higher outdoor temperature condition (T_{OD}=8.3 °C (47 °F)) with a 50 % reduced airflow rate, COP was degraded by over 30 % and total power increased by more than 20 %.

Figure 3.10 shows the effects of refrigerant undercharge. At the maximum fault level of 30 %, COP decreased by more than 8 % for the higher outdoor temperature condition (8.3 °C (47 °F)). The decrease was greater for the lower temperature lift case due to the lower pressure ratio and resulting lower mass flow rate potential (pressure drop) across the expansion valve as compared to the -8.3 °C (17 °F) case. Mass flow rate is proportional to the square root of the pressure drop. Therefore the reduction in mass flow rate due to removing refrigerant and lowering liquid line subcooling (lowering liquid line pressure) will have a greater effect upon mass flow rate at higher condenser pressure (higher outdoor temperatures). Capacity reduction had a greater effect upon COP than compressor power demand due to undercharge; refrigerant-side capacity decreased by an average of 22 % while outdoor unit power demand decreased an average of only 5 % for this maximum fault level and 8.3 °C (47 °F) test condition.

Figure 3.11 shows the effects of refrigerant overcharge. The control effect of the TXV is seen in the refrigerant-side capacity; capacity remains nearly constant (±1 %) while compressor power demand increases to approximately 15 % at 30 % fault level. The TXV maintains outdoor coil exit superheat by increasing pressure drop and limiting mass flow. Compressor power demand increases, being more pronounced at the lower temperature lift (lower pressure ratio), highest outdoor temperature. At the lower pressure ratio case, system capacity and refrigerant mass flow are already greater than the higher pressure ratio case, and the addition of refrigerant produces a greater change in power demand for a given fault level.

23

Table 3.7. Correlations for non-dimensional performance parameters in the heating mode

Fault	Performance Parameter Y	$Y=1+(a_1 + a_2 T_{OD} + a_3 F)\cdot F^*$			FSE**
		a_1	a_2	a_3	
Improper indoor airflow rate (AF)	COP	$Y_{COP} = Y_{Qtot} / Y_{Wtot}$			3.27E-02
	Q_{tot}	0.1545961	0.0078768	-0.1746421	2.72E-02
	Q_R	0.0009404	0.0065171	-0.3464391	1.82E-02
	W_{ODU}	-0.177359	-0.0125111	0.4784914	1.21E-02
	W_{tot}	0.0311053	-0.009332	0.7942998	2.87E-02
Refrigerant undercharge (UC)	COP	$Y_{COP} = Y_{Qtot} / Y_{Wtot}$			2.68E-02
	Q_{tot}	-0.104922	0.0156348	-1.3702726	8.02E-03
	Q_R	-0.0338595	0.0202827	-2.6226343	2.55E-02
	W_{ODU}	0.0615649	0.0044554	-0.2598507	8.79E-03
	W_{tot}	0.0537015	0.004334	-0.2272758	7.85E-03
Refrigerant overcharge (OC)	COP	$Y_{COP} = Y_{Qtot} / Y_{Wtot}$			6.08E-03
	Q_{tot}	-0.1198701	-0.0004505	0.5052803	5.20E-03
	Q_R	-0.0029514	0.0007379	-0.0064112	3.14E-03
	W_{ODU}	-0.0594134	0.0159205	1.8872153	9.19E-03
	W_{tot}	-0.053594	0.0140041	1.6948771	8.43E-03
Improper liquid line refrigerant subcooling (SC)	COP	$Y_{COP} = Y_{Qtot} / Y_{Wtot}$			1.77E-02
	Q_{tot}	-0.0369891	0.0014081	0.0113751	1.06E-02
	Q_R	-0.0389621	0.0019259	0.0079344	1.41E-02
	W_{ODU}	0.1353483	-0.001264	0.008241	8.45E-03
	W_{tot}	0.1023326	-0.0007392	0.0128456	6.11E-03
Noncondensable gas (NC)	COP	$Y_{COP} = Y_{Qtot} / Y_{Wtot}$			9.69E-03
	Q_{tot}	0.0852956	0.0058473	-0.9522349	9.37E-03
	Q_R	-0.2081656	0.0058006	0.6035798	2.48E-03
	W_{ODU}	0.181571	0.0008425	0.6093669	3.95E-03
	W_{tot}	0.1840392	-0.0001309	0.3935121	3.92E-03
Improper line voltage (VOL)	COP	$Y_{COP} = Y_{Qtot} / Y_{Wtot}$			1.13E-02
	Q_{tot}	0.1107829	-0.0040167	-0.1347848	9.87E-03
	Q_R	0.0912687	-0.0006155	-0.2343559	5.60E-03
	W_{ODU}	0.1604092	0.0011052	0.9262117	1.80E-03
	W_{tot}	0.283868	0.0009125	0.7759193	3.61E-03

* All temperatures are in Celsius
** FSE (fit standard error) equals the square root of the sum of the squared errors divided by the degrees of freedom

Refrigerant overcharge demonstrates itself in increased refrigerant subcooling in the liquid line. When subcooling was doubled from its nominal value (a fault level of 100 %), compressor power demand increased by approximately 15 % with little change in capacity (Figure 3.12). This resulted in an almost 12 % decrease in COP. Increased subcooling (increased refrigerant charge) affects compressor power demand more than capacity due to the TXV control of evaporator exit superheat.

Figure 3.13 shows the effects of non-condensable gas. The non-condensable gas will accumulate in the condenser (indoor coil) and thus reduce the heat transfer area available and raise the condenser pressure in direct proportion to the volume of the non-condensable gas. At the highest fault level of approximately 20 %, the COP decreases by approximately 8 % at the lowest outdoor test temperature. The non-condensable gas appears to have equal effect upon compressor power demand at all fault levels and outdoor temperatures, while capacity is more affected at the higher pressure ratio produced at the lowest outdoor temperature.

Figure 3.14 shows the effects of varying the system working voltage above and below the nominal value of 208 VAC. The changes in compressor power demand are a result of increased evaporator refrigerant saturation temperature at the higher indoor airflow rates. Changing the supply voltage changes all of the electric motors' rotational speeds; therefore, lowering the voltage is equivalent to reducing compressor pumping capacity while leaving heat transfer area constant. At higher voltages, the higher compressor

speed produces more of an effect on power demand than the indoor airflow rate produces on capacity. The TXV regulates refrigerant flow to maintain superheat at the higher indoor airflow rates. Capacity increases less than 2 % at the highest voltage while compressor power demand increases by more than 10 % resulting in an almost 10 % decrease in COP.
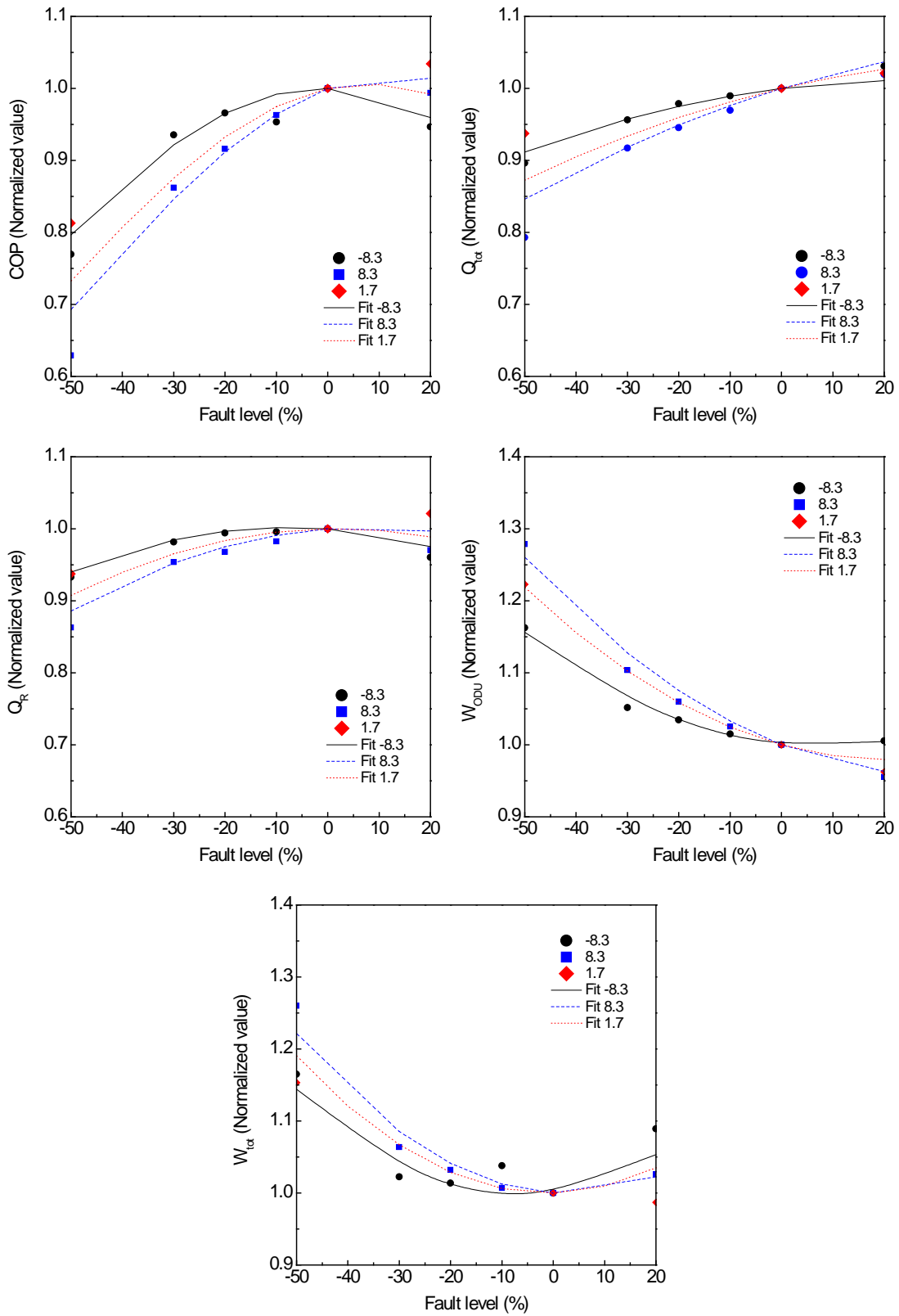
Figure 3.9. Normalized heating performance parameters for improper indoor airflow
(The number in the legend denotes T_{OD} (°C))
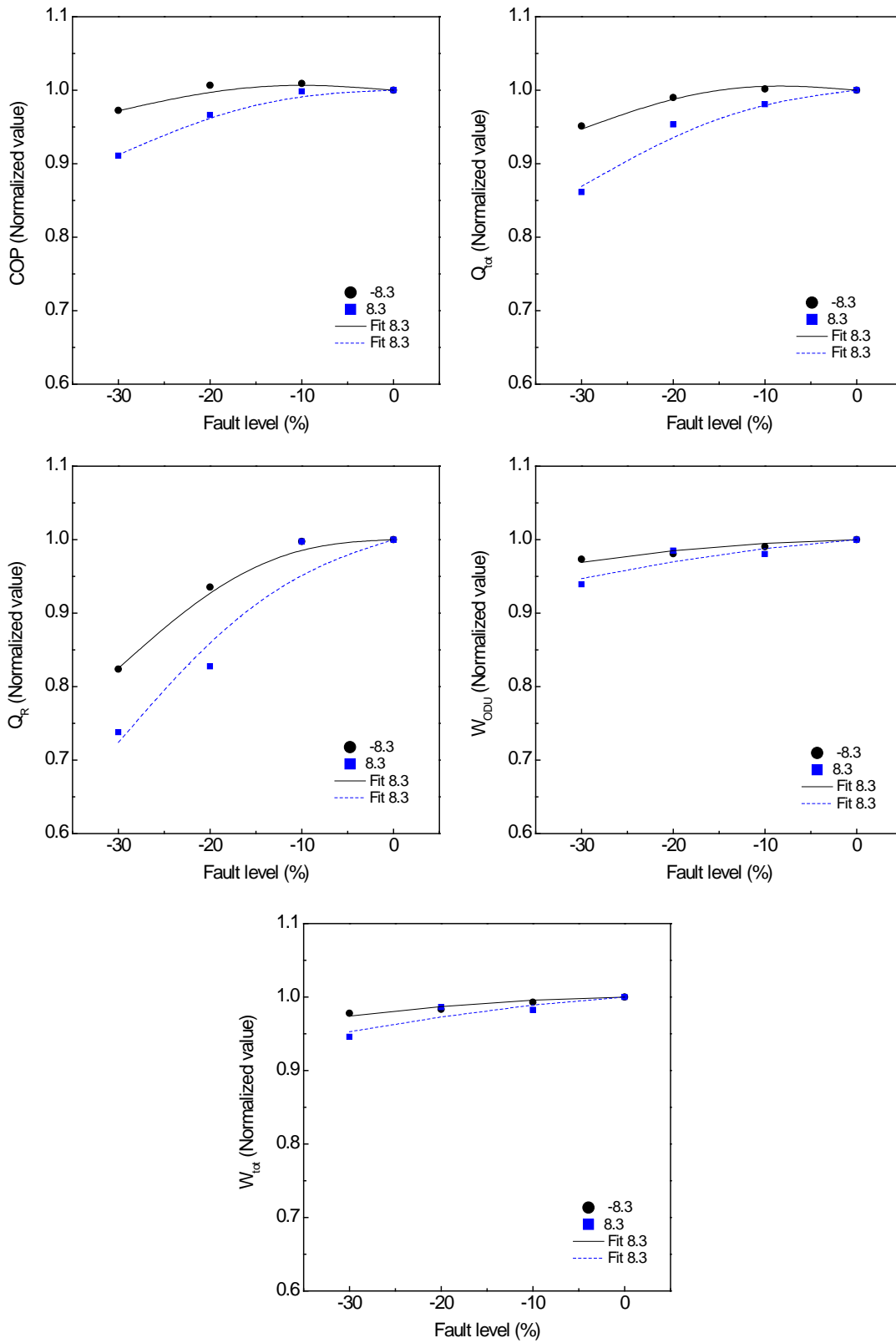
Figure 3.10. Normalized heating performance parameters for refrigerant undercharge
(The number in the legend denotes T_{OD} (°C))

27
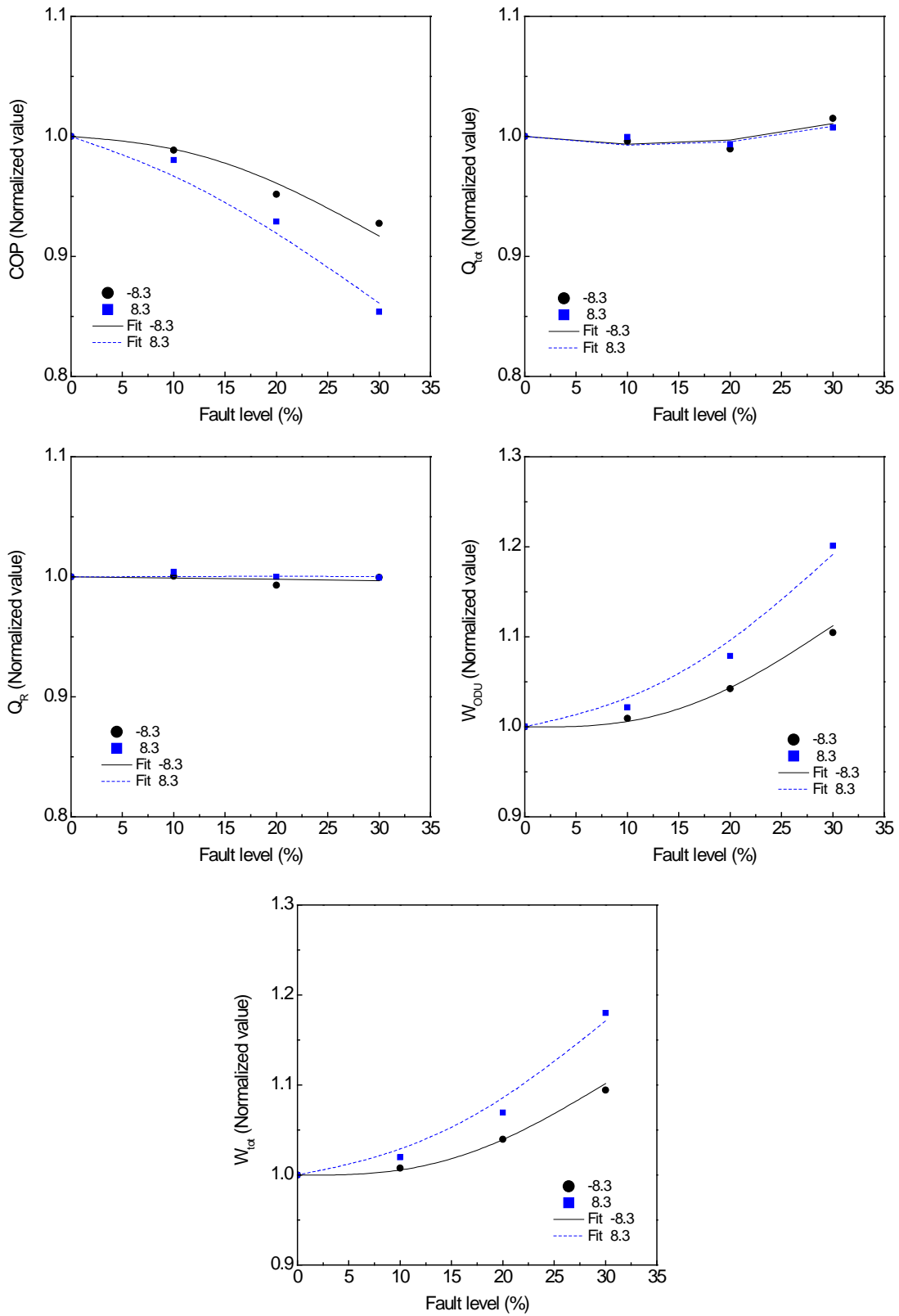
Figure 3.11. Normalized heating performance parameters for refrigerant overcharge
(The number in the legend denotes T_{OD} (°C))

28
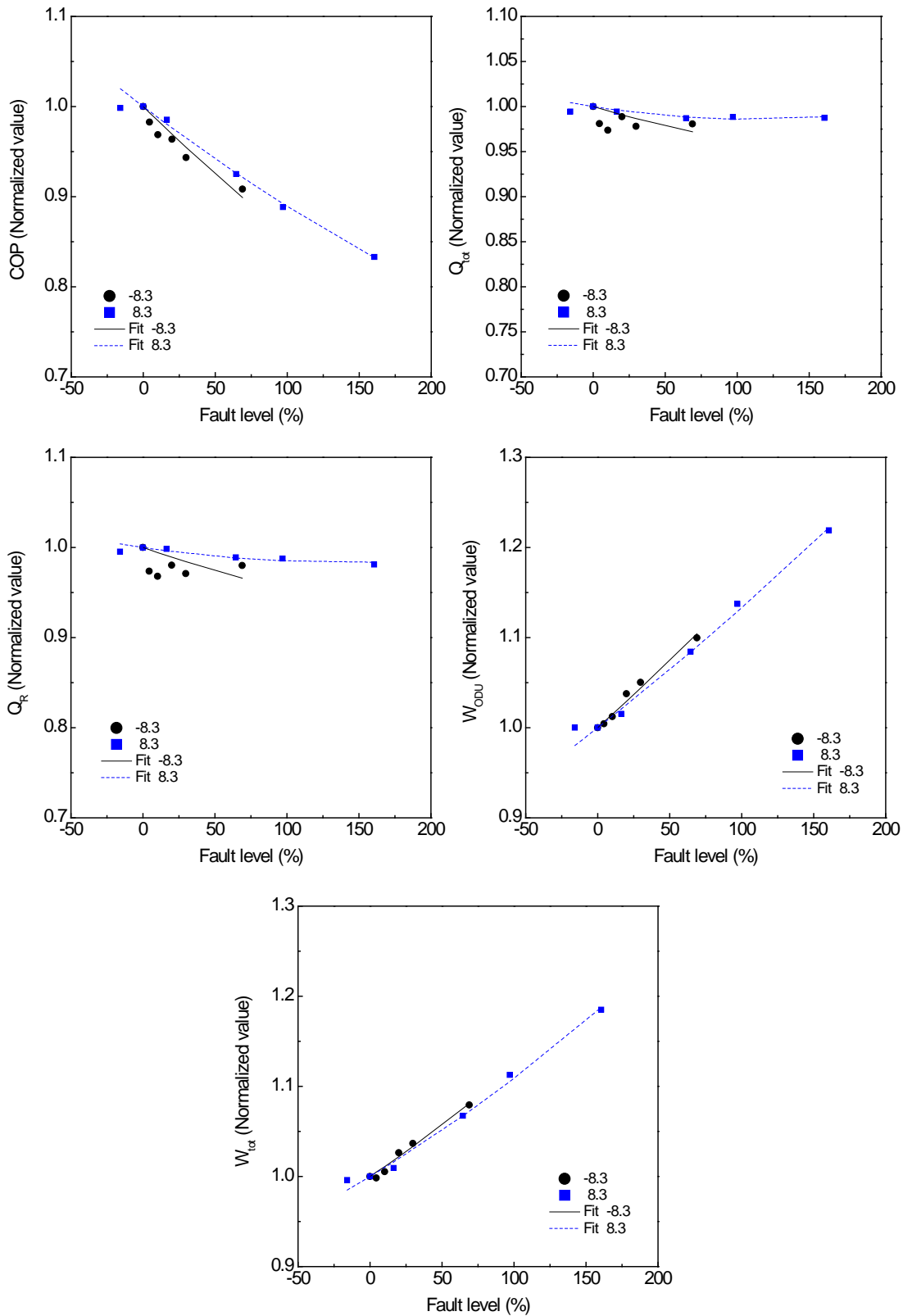
Figure 3.12. Normalized heating performance parameters for improper refrigerant subcooling
(The number in the legend denotes T_{OD} (°C))
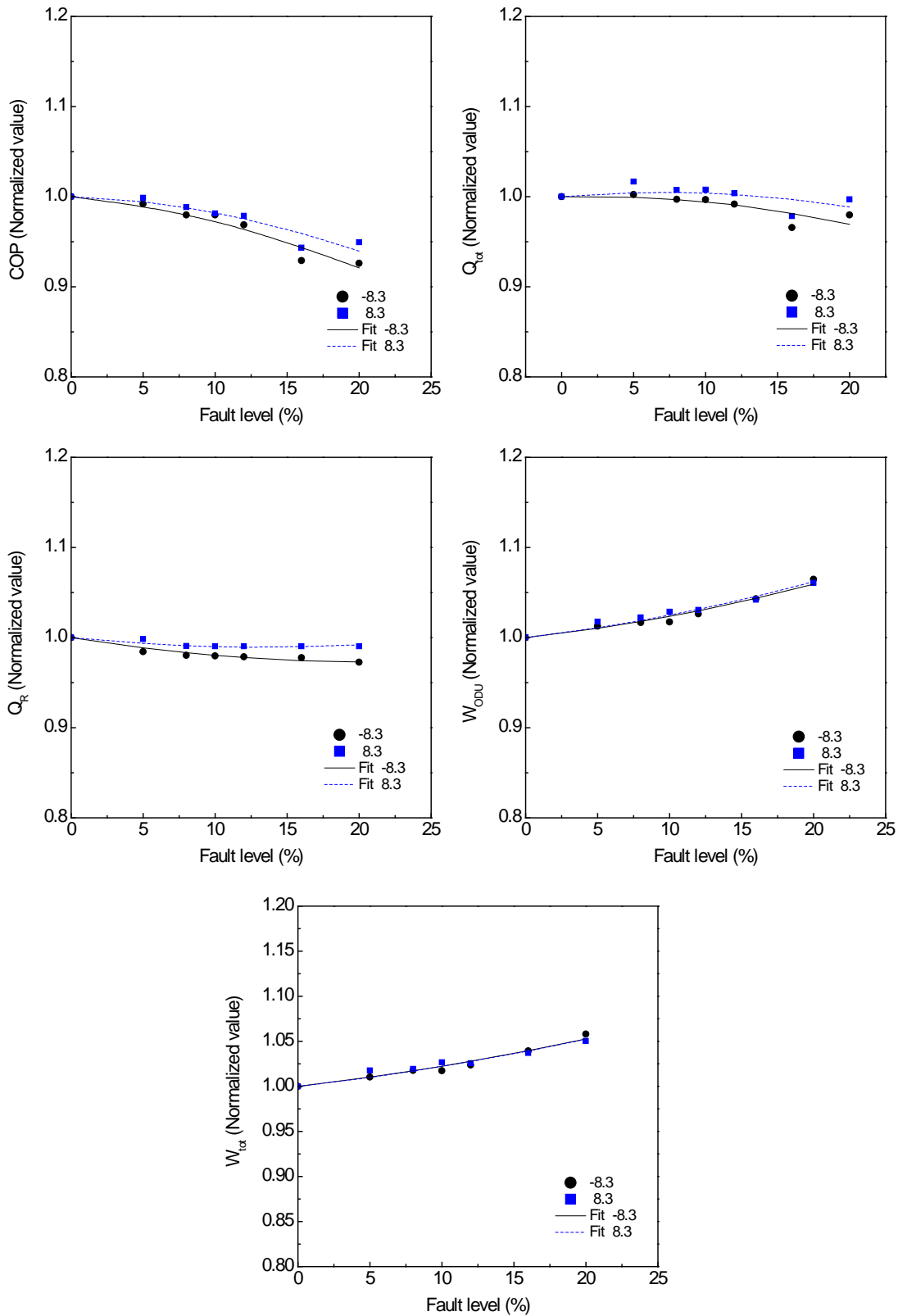
Figure 3.13. Normalized heating performance parameters for the presence of non-condensable gas
(The number in the legend denotes T_{OD} (°C))

30
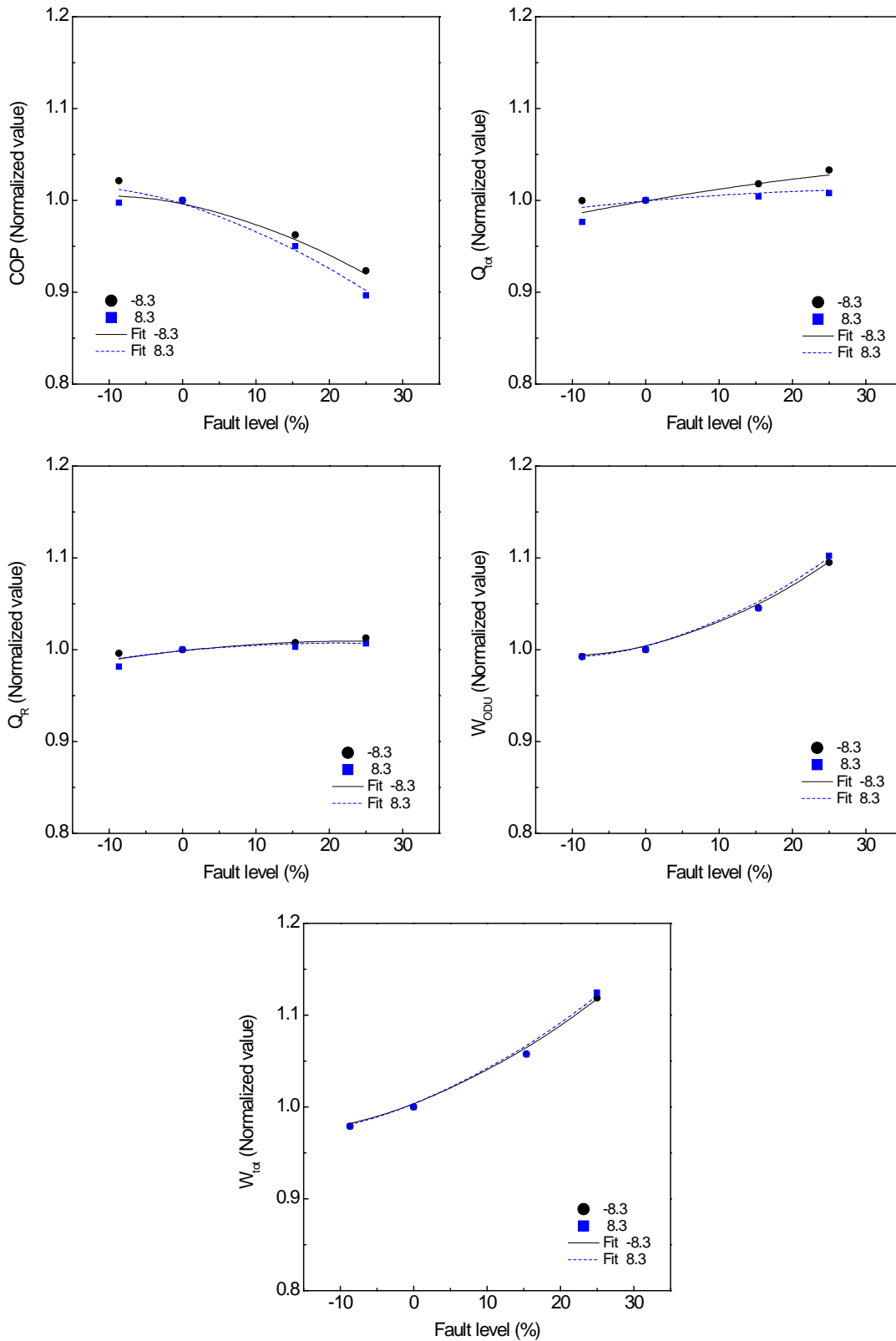
Figure 3.14. Normalized heating performance parameters for improper line voltage
(The number in the legend denotes T_{OD} (°C))

4. BUILDING/HEAT PUMP MODELING APPROACH

4.1 Building/Heat Pump Systems Simulation Models

Several building simulation models are available for modeling residential buildings. Many include well-developed user interfaces aimed at specific audiences – such as residential home energy raters in the United States who seek to determine the Home Energy Rating System score (HERS) (RESNET, 2006). Table 4.1 summarizes the features of these mainstream software tools. Energy Gauge USA, RemRate, and TREAT all have hundreds of users and are widely known in the residential energy efficiency community. However, while these tools include models for commonly-used systems and equipment operating at or near their nominal performance ratings, they do not have the flexibility to consider degraded, abnormal or off-design performance.

Table 4.1. Comparison of residential building simulation software tools

Energy Gauge USA	Fully developed hour-by-hour building simulation model (based on DOE-2.1e). Tool is commonly used by energy raters to develop a Home Energy Rating System (HERS) score. www.energygauge.com Advantages: good well-documented, building model with sound equipment components Disadvantages: no flexibility to add extra correlations or components
RemRATE	Building simulation model (using temperature bin calculations). Tool is commonly used by energy raters to develop a Home Energy Rating System (HERS) score. www.archenergy.com/products/remrate Advantages: good well-documented, building model with models for common equipment components Disadvantages: no flexibility to add extra correlations or components
TREAT	Hourly building simulation model aimed at residential energy analysis, for both single-family and multi-family homes. Used widely in the multi-family energy efficiency sector. www.psdconsulting.com/software/treat Advantages: robust, well-documented, building model focused on multi-family issues Disadvantages: no flexibility to consider alternate technologies

DOE-2 is the original, U.S. federally-funded building simulation model or calculation engine developed in the 1970s that is still used as the basis of some of the mainstream residential software tools (i.e., Energy Gauge USA). The DOE-2 software offers some flexibility but is no longer maintained or supported.

EnergyPlus is a state-of-the-art, very flexible building simulation tool used for research evaluations and mainstream energy analysis and design assistance. Its development is supported by the U.S. Department of Energy (DOE). This detailed calculation engine works at sub-hourly time steps and can consider both residential and commercial buildings.

TRNSYS is a highly flexible transient simulation tool that focuses on thermal systems, primarily aimed at building and HVAC applications (Klein et al., 2007). TRNSYS was originally developed at the University of Wisconsin to simulate the transient performance of solar thermal systems (http://sel.me.wisc.edu/trnsys/). TRNSYS is a modular tool where multiple components can be combined to build up a complex thermal system. TRNSYS includes several components necessary to simulate the transient performance of a building, including building envelope components, HVAC equipment, and utilities to read hourly weather data from TMY files. Because of its flexibility, this tool is uniquely able

to consider new concepts and technologies – such as the research evaluation of this project. The core of the TRNSYS simulation model is the building envelope model based on the Type 56 multi-zone building model. The inputs to Type 56 are defined using the TRNBuild software tool (see Figure 4.1) and then saved in a .BUI file. Type 56 then reads this file at runtime to generate the detailed building description. The building model includes all the basic characteristics of a residential building:

- Heat loss and gains through building walls, roof and floor
- Solar gains through windows
- Interactions between multiple zones (house, attic, rooms)
- Scheduled internal sensible and moisture loads for people, equipment, etc.
- Interactions with the heating, ventilation, and air conditioning equipment
- Scheduled set points for temperature and humidity

Table 4.2 summarizes the advantages and disadvantages for each of these software tools. Because of its flexibility, we selected the building model developed in TRNSYS to study the integrated performance of a heat pump in residential application.

Table 4.2. Comparison of general building calculation models

DOE-2	An hour-by-hour building simulation model developed by the national laboratories in the US in the mid-1970s to predict energy use in commercial and residential buildings (http://gundog.lbl.gov/). DOE-2.1e is no longer under active maintenance, but is still the underlying calculation engine for several software packages, including Energy Gauge. A private software developer (JJ Hirsh and Associates) owns and maintains the newest version of the DOE-2.2 calculation engine and the widely used interface program (eQuest). http://www.doe2.com/ Advantages: well understood, flexible simulation program Disadvantages: no longer updated or supported
EnergyPlus	Flexible building simulation model for commercial and residential buildings. Public domain calculation engine developed by the US Department of Energy (DOE). www.energyplus.gov Advantages: state of the art building model with robust, well-developed equipment components Disadvantages: limited flexibility to add correlations to degrade performance
TRNSYS	Highly flexible, research grade package for analyzing transient thermal systems. Includes pre-developed models for building envelope and other HVAC components. www.trnsys.com Advantages: highly flexible can consider any user-defined equation or component models Disadvantages: difficult to use, and cumbersome to define building envelope details
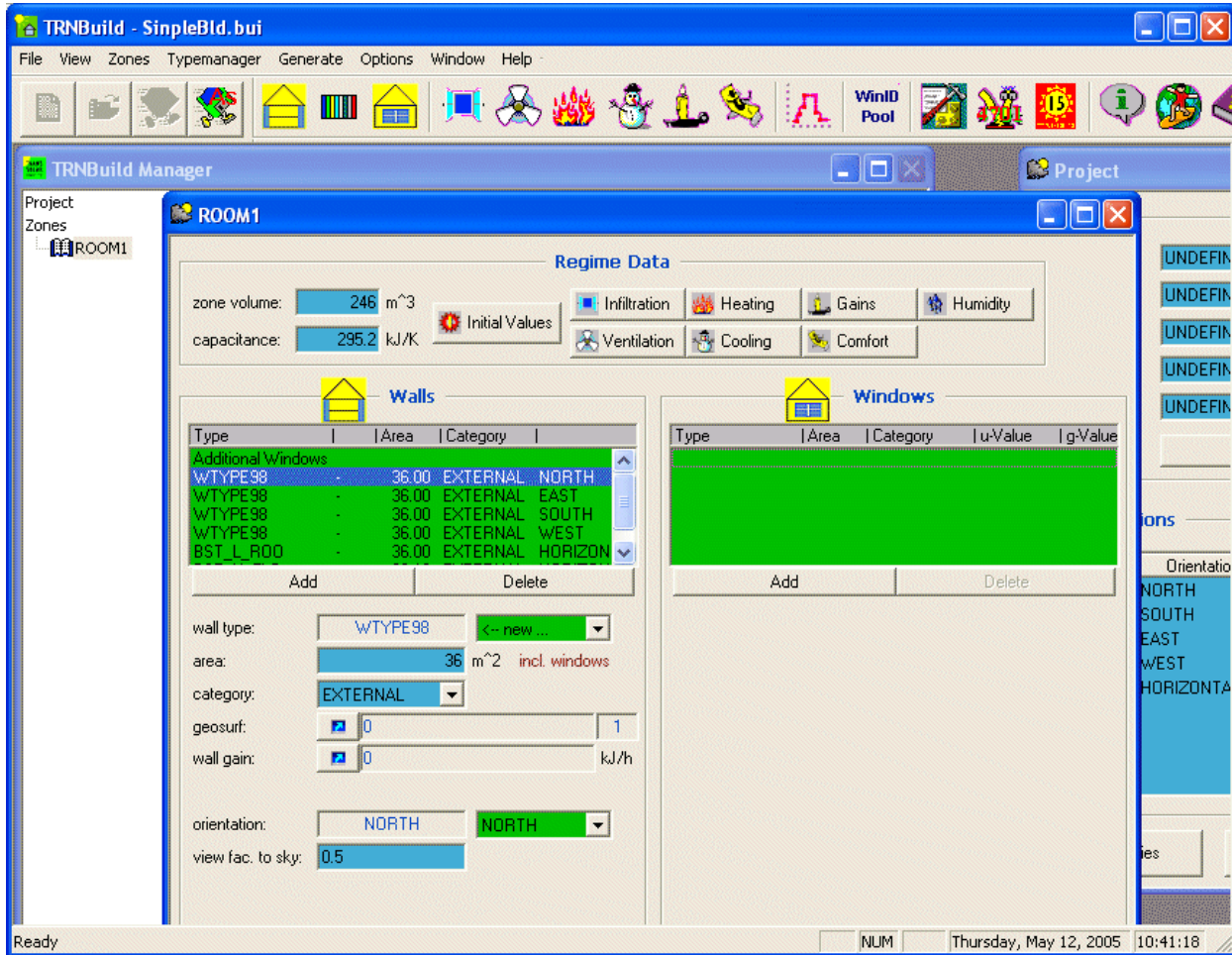
Figure 4.1. Screen shot of TRNBuild used to define the building envelope details

In this study, we used a building model developed in TRNSYS to simulate the integrated performance of heat pumps in residential applications (CDH Energy Corp., 2010). This model was originally applied to simulate an integrated desiccant system's performance (Henderson and Sand, 2003), and it was later refined to consider several issues germane to this residential study, including duct leakage and the part load performance of air conditioners (Henderson et al., 2007) and refrigerant charge impacts (Sachs et al., 2009). The model is driven by typical meteorological year weather data sets TMY3 (Wilcox and Marion, 2008) on a small time-step (e.g., 1.2 minutes). A detailed thermostat model turns the mechanical systems 'on' and 'off' at the end of each time step depending on the calculated space conditions.

4.2 Building and Weather City Definitions
Table 4.3 lists the climates with representative locations and house structures considered in this study. Two houses were modeled: a slab-on-grade house and a house with a basement. The simulated residential buildings corresponded to a code-compliant house with a HERS score of approximately 100 with appropriate levels of insulation and other features corresponding to each climate. The slab-on-grade houses were modeled with ducts located in the attic. The houses with basements were modeled with ducts located in a semi-conditioned space. For Houston, TX, only a slab-on-grade house was studied because houses with basements are rarely built in this location.

34

The selected cities represent each of the International Energy Conservations Code (IECC) climate zones 2 through 6 shown in Figure 4.2, from hot and humid climate to a heating dominated climate. This selection enabled prediction on how different faults will affect air conditioner and heat pump performance in the most prevalent climates in the U.S. TMY3 weather data were used for each location.

Table 4.3. Climates, locations and structures considered

Zone	Climate	Location	Slab-on-grade house	House with basement
2	Hot and humid	Houston, TX	Yes	No
3	Hot and dry climate	Las Vegas, NV	Yes	Yes
4	Mixed climate	Washington, DC	Yes	Yes
5	Heating dominated	Chicago, IL	Yes	Yes
6	Cold	Minneapolis, MN	Yes	Yes
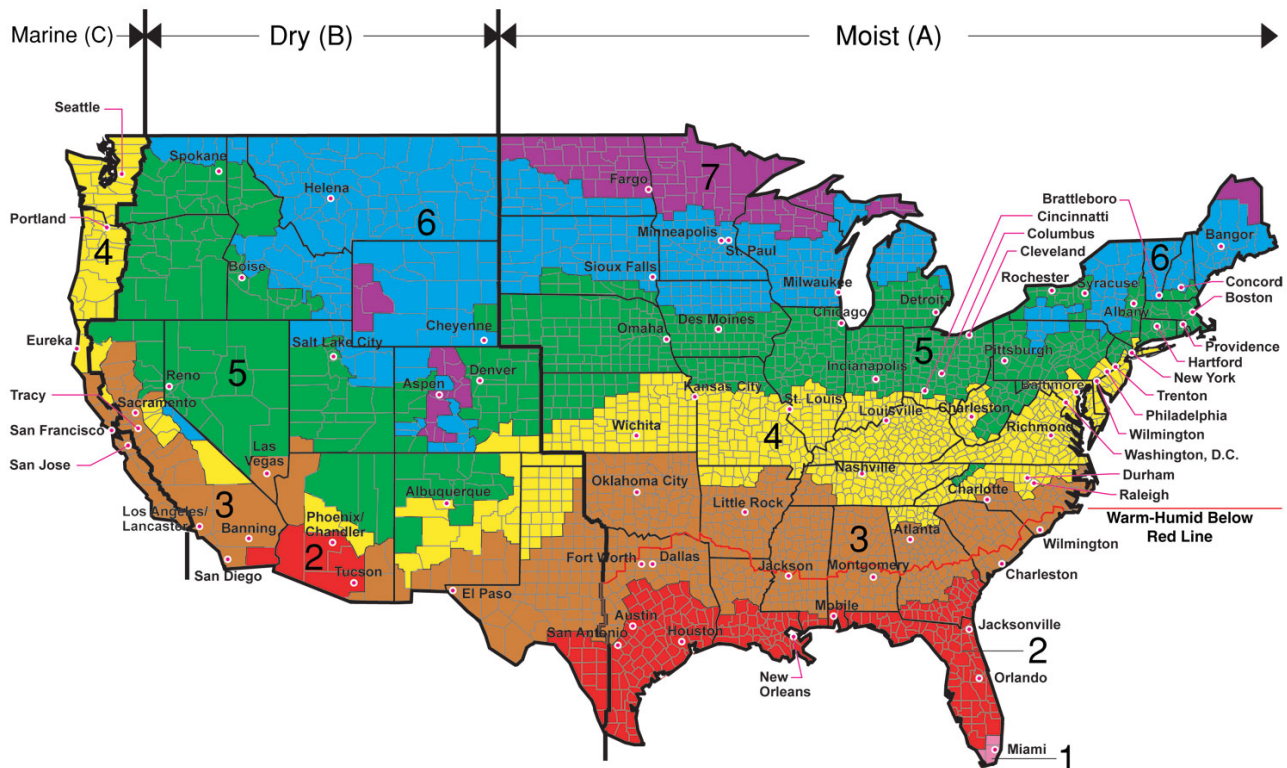
Figure 4.2. IECC climate zone map

4.3 Building and Enclosure Thermal Details

A 185.8 m^2 (2,000 ft^2) three-bedroom house was modeled as a slab-on-grade with a separate attic zone – or a 2-zone model – in TRNSYS Type 56. This house is similar to that simulated by Rudd et al. (2013) for a recently completed ASHRAE research project (RP-1449). Also, a 3-zone model was developed for the house with a basement zone. The basement was not directly conditioned but coupled to the main zone via zone-to-zone air exchange. The characteristics of the buildings are listed in Table 4.4 for each climate.

Table 4.4. Specifications for simulated houses (HERS Index ≈100)

a)   I-P units

Parameter	Houston, TX (Climate Zone 2)	Las Vegas, NV (Climate Zone 3)	Washington, DC (Climate Zone 4)	Chicago, IL (Climate Zone 5)*
Wall insulation R-value (nominal)	13	13	13	19
Cavity	13	13	13	19
Sheathing	0	0	0	0
framing factor	0.23	0.23	0.23	0.23
Ceiling insulation R-value	30	30	38	38
Slab insulation R-value (2' down)	0	0	0	0
Basement Walls	na	na	na	na
Window U-value ($Btu \cdot h^{-1} \cdot ft^{-2} \cdot F^{-1}$)	0.75	0.65	0.40	0.35
Window SHGC	0.40	0.40	0.40	0.40
Building enclosure air leakage (ACH50)	7	7	7	7
Enclosure ELA (in^2)	98.1	98.1	98.1	98.1
Duct air leakage to outside (%)	6% sup, 4% ret	6% sup, 4% ret	6% sup, 4% ret	6% sup, 4% ret
Supply duct area in attic (ft^2)	544	544	544	544
Return duct area in attic (ft^2)	100	100	100	100
Duct R-value	6	6	6	6
SEER, EER	13, 9.6	13, 9.6	13, 9.6	13, 9.6
HSPF, COP	7.7, 2.3	7.7, 2.3	7.7, 2.3	7.7, 2.3
Internal heat gain (lumped)** (people+lighting+appliances)	72.70 kBtu/day	72.70 kBtu/day	72.70 kBtu/day	72.70 kBtu/day
Internal moisture generation	12 lb/day	12 lb/day	12 lb/day	12 lb/day
HERS	106	108	108	107

*This house was also used in simulations for Minneapolis, MN (Climate Zone 6)
**DOE Building America benchmark (Hendron, 2008)

b)   SI units

Parameter	Houston, TX (Climate Zone 2)	Las Vegas, NV (Climate Zone 3)	Washington, DC (Climate Zone 4)	Chicago, IL (Climate Zone 5)*
Wall insulation R(SI)-value (nominal)	2.29	2.29	2.29	3.35
Cavity	2.29	2.29	2.29	3.35
Sheathing	0	0	0	0
framing factor	0.23	0.23	0.23	0.23
Ceiling insulation R(SI)-value	5.38	5.38	6.69	6.69
Slab insulation R(SI)-value (2' down)	0	0	0	0
Basement Walls	na	na	na	na
Window U-value ($W \cdot m^{-2} \cdot K^{-1}$)	4.3	3.7	2.3	2.0
Window SHGC	0.40	0.40	0.40	0.40
Building enclosure air leakage (ACH50)	7	7	7	7
Enclosure ELA (m^2)	0.063	0.063	0.063	0.063
Duct air leakage to outside (%)	6% sup, 4% ret	6% sup, 4% ret	6% sup, 4% ret	6% sup, 4% ret
Supply duct area in attic (m^2)	50.5	50.5	50.5	50.5
Return duct area in attic (m^2)	9.3	9.3	9.3	9.3
Duct R(SI)-value	1.1	1.1	1.1	1.1
SEER (I-P), COP	13, 9.6	13, 9.6	13, 9.6	13, 9.6
HSPF (I-P), COP	7.7, 2.3	7.7, 2.3	7.7, 2.3	7.7, 2.3
Internal heat gain (lumped)** (people+lighting+appliances)	76.70 MJ/day	76.70 MJ/day	76.70 MJ/day	76.70 MJ/day
Internal moisture generation	5.4 kg/day	5.4 kg/day	5.4 kg/day	5.4 kg/day

*This house was also used in simulations for Minneapolis, MN (Climate Zone 6)
**DOE Building America benchmark (Hendron, 2008)

The slab-on-grade house only has perimeter slab insulation in climate zones 4 and 5 (Figure 4.3). For the house with a basement (Figure 4.4), the basement is connected to the main house by openings that are assumed to allow zone-to-zone air exchange of heat and moisture equivalent to 849.4 $m^3 \cdot h^{-1}$ (500 cfm). The basement walls are modeled as 102 mm (4 inch) thick concrete, with R(SI)-1.76 (R-10) exterior foam insulation in climate zones 3, 4 and 5.
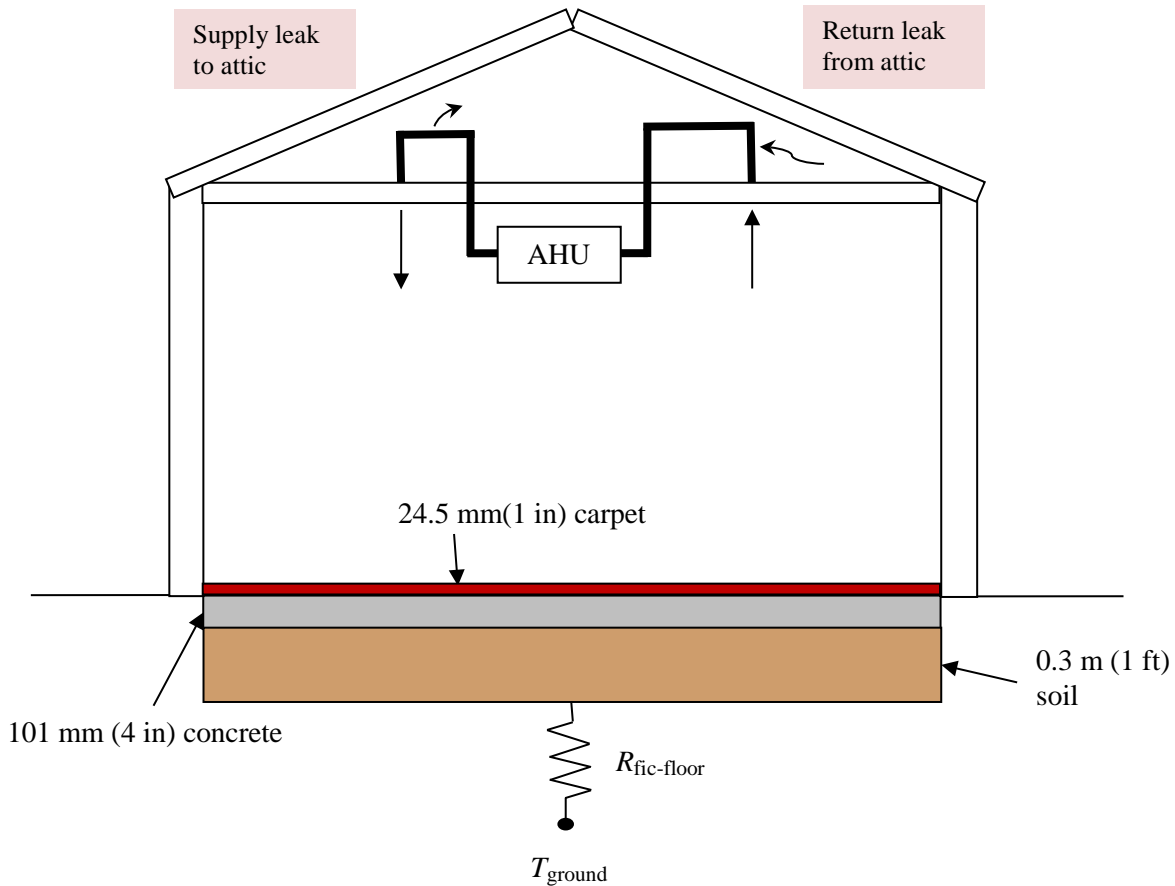
Figure 4.3. Schematic of a slab-on-grade house (ducts located in the unconditioned attic)

Both the slab-on-grade and basement homes are modeled by adding a 'fictitious layer' into the resistance between the zone and ground temperature. This fictitious R-value is added to provide the amount of heat loss through the surfaces determined by the F-factor method ($R_{effective}$) as recommended by Winkelmann (1998). A schematic of this model is shown in Figures 4.3 and 4.4. Tables 4.5 and 4.6 summarize the calculations to determine the necessary R-value for the fictitious layer.

The above-ground portions of the slab-on-grade and basement houses are identical for each climate zone. Each model has exterior walls with layers of drywall, insulation (R(SI)-2.3 (R-13) or R(SI)-3.3 (R-19), depending on the climate zone), and stucco as the outside surface. Windows take up approximately 22 % of all of the exterior walls; 10.2 m^2 (109.6 ft^2) on the north and south facing walls, and 6.5 m^2 (70.4 ft^2) on east and west facing walls.
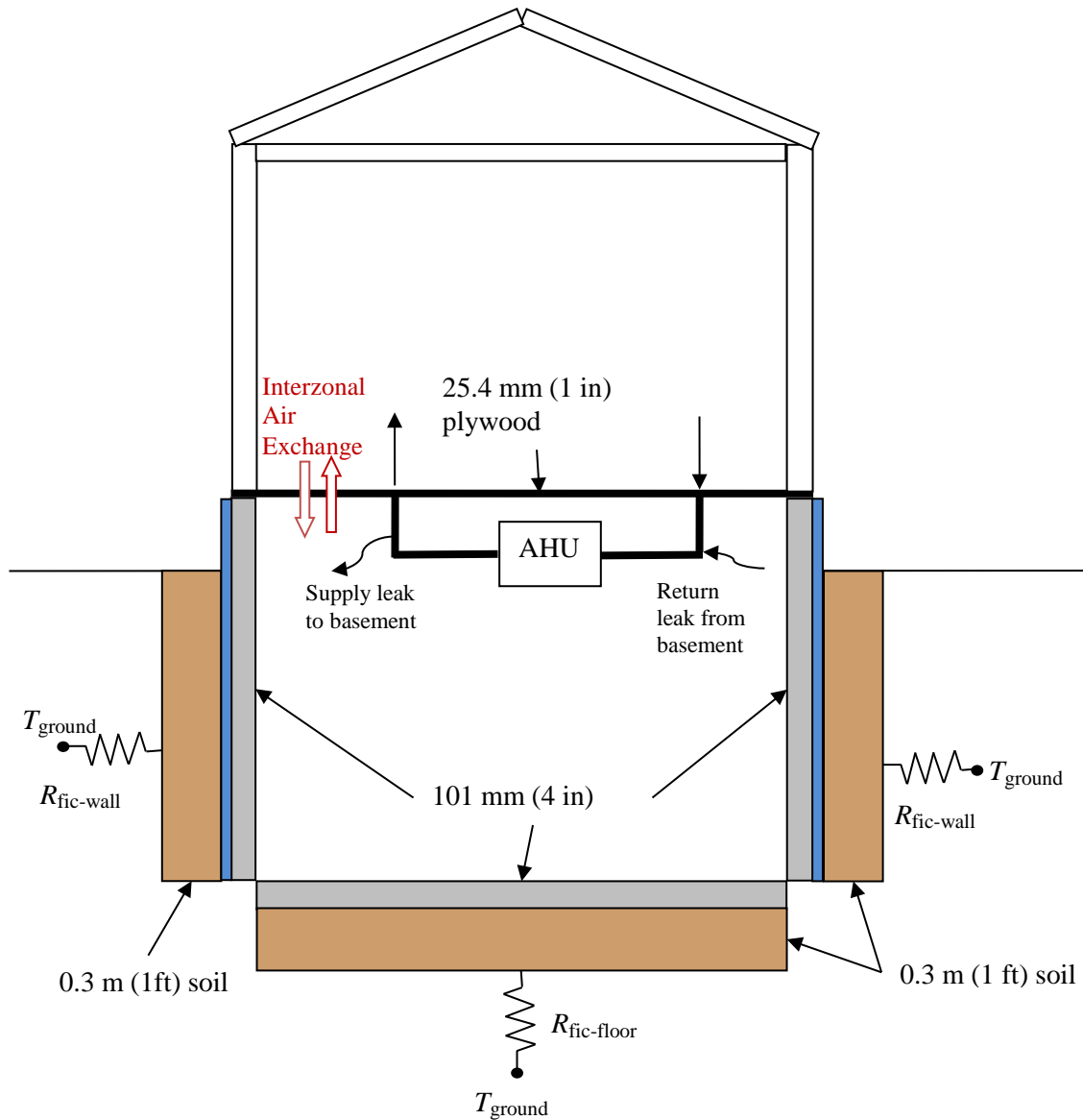
Figure 4.4. Schematic of a house with basement (ducts located in the semi-conditioned basement)

The ceiling (i.e. boundary between main zone and attic) is made up of a layer of drywall, framing and insulation (R(SI)-5.3 (R-30) or R(SI)-6.7 (R-38), depending on climate zone). The attic has gable walls on the east and west sides and roof surface on the north and south sides. The roof is sheathed in plywood and then covered with asphalt shingles. The east and west surfaces (gables) are made up of plywood on the inside surface with stucco on the outside surface.

Table 4.5. Calculation of R-values for basement walls and floor

Basement Wall						
Material	Thickness		Resistance		Total R-Value	
					R(SI)	R
	m	ft	$K \cdot m \cdot W^{-1}$	$h \cdot ft \cdot °F \cdot Btu^{-1}$	$K \cdot m^2 \, W^{-1}$	$h \cdot ft^2 \cdot °F \cdot Btu^{-1}$
Concrete	0.10	0.33	0.775	1.33	0.0775	0.44
Soil	0.30	1.00	1.18	2.01	0.354	2.00
Foam	0.035	0.115	25.1	43.5	0.881	5.00
R_{fic}	Massless				0.111	0.63
				$R_{effective}$	1.42	8.08

Basement Floor						
Material	Thickness		Resistance		Total R-Value	
					R(SI)	R
	m	ft	$K \cdot m \cdot W^{-1}$	$h \cdot ft \cdot °F \cdot Btu^{-1}$	$K \cdot m^2 \, W^{-1}$	$h \cdot ft^2 \cdot °F \cdot Btu^{-1}$
Concrete	0.10	0.33	0.775	1.33	0.0775	0.44
Soil	0.30	1.00	1.18	2.01	0.354	2.00
R_{fic}	Massless				3.26	18.5
				$R_{effective}$	3.69	20.95

Table 4.6. Calculation of R-values for slab-on-grade floor

Slab Resistance – Climate Zones 2 and 3						
Material	Thickness		Resistance		Total R-Value	
					R(SI)	R
	m	ft	$K \cdot m \cdot W^{-1}$	$h \cdot ft \cdot °F \cdot Btu^{-1}$	$K \cdot m^2 \, W^{-1}$	$h \cdot ft^2 \cdot °F \cdot Btu^{-1}$
Carpet	0.025	0.083	14.52	25.13	0.363	2.06
Concrete	0.10	0.33	0.775	1.33	0.0775	0.44
Soil	0.30	1.00	1.18	2.01	0.354	2.01
R_{fic}	Massless				0.958*	5.44*
				$R_{effective}$	1.75	9.95

Slab Resistance – Climate Zones 4 and 5						
Material	Thickness		Resistance		Total R-Value	
					R(SI)	R
	m	ft	$K \cdot m \cdot W^{-1}$	$h \cdot ft \cdot °F \cdot Btu^{-1}$	$K \cdot m^2 \, W^{-1}$	$h \cdot ft^2 \cdot °F \cdot Btu^{-1}$
Carpet	0.025	0.083	14.52	25.13	0.363	2.06
Concrete	0.10	0.33	0.775	1.33	0.0775	0.44
Soil	0.30	1.00	1.18	2.01	0.354	2.01
R_{fic}	Massless				2.19*	12.42*
				$R_{effective}$	2.98	16.93

*The difference in R_{fic} between climate zones 2/3 and 4/5 is due to the perimeter insulation of the slab in climate zones 4 and 5.

4.3.1 Building Enclosure Air Leakage

The AIM-2 infiltration model (Walker and Wilson, 1998; ASHRAE, 2009a) relates infiltration to wind and indoor-outdoor temperature difference for each time step. All simulations in this study used coefficients representing shelter from buildings located across the street. An equivalent leakage area (ELA) of 0.0633 m^2 (98.1 in^2) was chosen to provide the desired seven air changes per hour (ACH) at 50 pascal pressure differential (ACH50 for the main zone in each building model).

The attic used the same AIM-2 equations to determine leakage as a function of wind and temperature difference. The attic ELA was set to be 0.366 m^2 (567 in^2) for each of the climate zones, or about 5 times the leakage rate for the HERS 100 house (Fugler, 1999). In houses with basements, that zone was assumed to have no leakage to outdoors.

4.3.2 Duct Leakage and Thermal Losses

For the slab-on-grade houses, the ducts were modeled to be in the attic space and all the air leakage and thermal losses/gains go into that zone. The details of the duct model are given in Appendix A. For houses with basements, there is no duct leakage to the attic (all leaks are assumed to be into the conditioned space, so they are ignored). Duct leakage was assumed to be 10 % of flow, or 6 % on the supply side and 4 % on the return side. Duct insulation was assumed to be R(SI)-1.1 (R-6) with a supply duct area of 50.5 m^2 (544 ft^2) and a return duct area of 9.3 m^2 (100 ft^2) for a 10.6 kW (3-ton) unit. The duct areas were increased and decreased proportionally based on the size (or nominal tonnage) of the heat pump unit.

4.3.3 Moisture and Thermal Gains

The scheduling or profile of internal heat and moisture generation was taken from the Building America Benchmark Definition (Hendron, 2008). Sensible gains from all sources were assumed to be 76.7 MJ/day (72.7 kBtu/day).

Internal moisture generation from all sources was specified as 5.4 kg/day (12 lb/day), or less than half of the ASHRAE Standard 160 moisture generation rate of 14.2 kg/day (31.2 lb/day) for a three-bedroom house (ASHRAE, 2009b). The ASHRAE 160 value is meant to be a 'worst case' design condition and therefore would not be expected to correspond to average conditions.

4.3.4 Moisture and Thermal Capacitance

Moisture storage in the building materials and furnishings and the rate of mass transfer into storage are important hygrothermal parameters affecting the diurnal swings in indoor humidity. Building material moisture storage was modeled with a simple lumped parameter method with mass factor added to the air node in the zone model:

$$C \ \frac{dw_i}{dt} = m \cdot (w_i - w_o) + Q_{internal} - Q_{AC,latent} \tag{4.1}$$

The moisture capacitance term is usually set to a multiple of the air mass inside the house. The Florida Solar Energy Center used more detailed moisture models including Effective Moisture Penetration Depth (EMPD) to show that reasonable factors for the air mass multiplier are 20 to 30 times the air mass (EPA, 2001).

As a result of the calibration efforts (Appendix C in Rudd et al., 2013), a 30x multiplier for moisture capacitance was used for the main zone and the basement. The attic used a moisture capacitance factor of 15x.

Thermal capacitance was simulated by adding internal walls to the model with 371.6 m^2 (4000 ft^2) of exposed wall surface area. The thermal mass of the air node was also increased by a factor of 20 to 12,331 kJ·K^{-1} (6494 Btu·F^{-1}) to reflect the impact of furniture and other material in the space. The attic was assumed to have a thermal capacitance of 1x and the basement (where applicable) was assumed have a thermal capacitance multiplier of 10x.

4.3.5 Window Performance
The window model in Type 56 uses the window parameters generated by LBNLs WINDOW5 software, which is considerably more detailed than the NFRC rating values generally used in residential practice and building codes. The LBNL WINDOW5 inputs for this project were determined following the methodology developed by Arasteh et al. (2009) for use in EnergyPlus.

4.4 Mechanical Ventilation
The only mechanical ventilation option considered in this study is an exhaust fan. The fan operated continuously to provide sufficient ventilation to the house. Figure 4.5 shows the airflow configuration used in this study. The fans provided an average rate of 98.5 m^3·h^{-1} (58 cfm) required by ASHRAE Standard 62.2 (ASHRAE, 2013) for the 185.8 m^2 (2000 ft^2) three-bedroom house. The exhaust fan power was assumed to be 0.85 kJ·m^{-3} (0.4 W·cfm^{-1}).
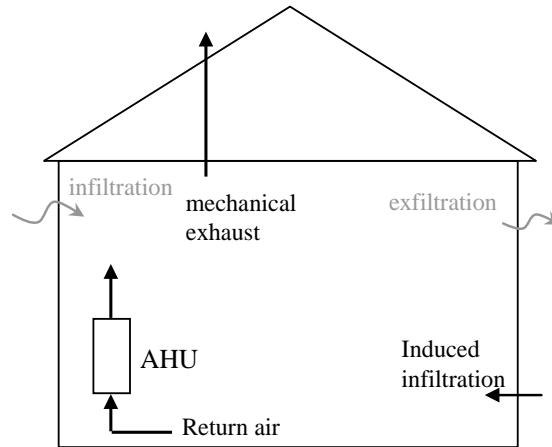
Figure 4.5. Schematic of a mechanical exhaust system

The combined impact of infiltration, ventilation, and duct leakage were considered by using the equations below. The duct leakage was always a net out, so that additional net flow was an exhaust.

V_{in} = incoming ventilation flow
V_{out} = sum of all exhaust flows (exhaust fan, net duct leakage, etc.)
$V_{balanced}$ = MIN (V_{in}, V_{out})
$V_{unbalanced}$ = MAX (V_{in}, V_{out}) − $V_{balanced}$
V_{inf} = infiltration flow calculated for building for the timestep
$V_{combined}$ = MAX ($V_{unbalanced}$, V_{inf} + 0.5·$V_{unbalanced}$) + $V_{balanced}$

The net mechanical inlet flows were subtracted from $V_{combined}$ to determine the remaining non-mechanical ventilation (or infiltration) rate acting on the building envelope. A mass balance tracked CO_2 levels in the space and confirmed the net impact of ventilation to be similar between the cases.

41

4.5 Air Flow Imbalance

Duct leakage is often exacerbated by interactions with building envelope leakage, depressurization caused by exhaust fan operation, and supply and return imbalances caused by closing interior doors (for central return systems). Cummings and Tooley (1989) and Modera (1989) both showed that the pressures induced by air handlers were much greater than the naturally-induced pressures from wind and stack effects in cooling dominated climates. Pressure mapping by Cummings and Tooley (1989) also showed that the supply/return imbalances caused by closing interior doors were also substantial.

One option for considering these interactions is to use a multi-zone, flow-pressurization model such as CONTAM 3.0 (Walton and Dols, 2010). A model can be developed to evaluate the interactions of building envelope leakage paths, duct leakage, and zone pressurization with the supply air (when doors are closed). These models can track airflow but cannot consider the thermal performance of the building envelope nor the energy use of the space-conditioning systems.

In a small time-step thermal building simulation model, it is possible to properly account for the combined effects of 'unbalanced' duct leakage, unbalanced ventilation, and infiltration using a simpler approach. The following procedure accounts for the interactions of unbalanced ventilation and duct leakage with infiltration. The calculation is based on the approach summarized in Barnaby and Spitler (2004) as well as the ASHRAE Handbook of Fundamentals, Chapter 17 (ASHRAE 2009a):

V_{in} = incoming ventilation airflow
V_{out} = sum of all exhaust airflows (exhaust fan, supply duct leaks, etc.)
$V_{balanced}$ = MIN (V_{in}, V_{out})
$V_{unbalanced}$ = MAX (V_{in}, V_{out}) − $V_{balanced}$
V_{inf} = infiltration flow calculated for building for the timestep
$V_{combined}$ = MAX ($V_{unbalanced}$, V_{inf} + 0.5· $V_{unbalanced}$) + $V_{balanced}$

4.6 Heat Pump Specifications and Modeling

A conventional heat pump unit with a 13 SEER and 7.7 HSPF rating was used in the simulations. The cyclic degradation coefficient, C_D, of the heat pump was 0.15 in both cooling and heating. The required size of the unit was determined for each climate using ACCA Manual J (ACCA 2011a). Houses in Houston and Las Vegas had a heat pump with cooling capacity of 10.6 kW (3 ton) and 12.3 kW (3.5 ton), respectively. The Washington, D.C., Chicago, and Minneapolis houses had 8.8 kW (2.5-ton) units.

The detailed heat pump model required separate inputs for the gross COP at nominal conditions, sensible heat ratio (SHR), and indoor fan power. Table 4.7 lists the rated parameters and corresponding inputs to the heat pump model. The fan power assumed for rated conditions and used to calculate SEER is listed along with the actual fan power assumed for operation. The fan power at rated conditions was assumed to be 0.53 kJ·m^{-3} (0.25 W·cfm^{-1}), while the actual fan power was 1.06 kJ·m^{-3} (0.5 W·cfm^{-1}).

Table 4.7. Heat pump cooling characteristics

Unit Description	Rated Performance			Input Parameters		
SEER 13 unit; Single-speed PSC fan motor	Rated SEER Btu·W^{-1}·h^{-1}	Rated COP	Rated Fan Power kJ·m^{-3}	Gross COP	Actual Fan Power kJ·m^{-3}	SHR
	13	2.81	0.53	4.05	1.06	0.77

<u>Note</u>: Gross COP is a ratio of gross cooling capacity (refrigerant-side capacity) and outdoor unit power (includes compressor, outdoor fan, and controls powers) at the nominal rating point: 35 °C (95 °F) outdoor dry-bulb temperature , 26.7 °C/19.4 °C (80 °F/67 °F) indoor dry-bulb/wet-bulb temperature, and 217.4 m^3·h^{-1}kW^{-1} (450 cfm/ton) supply airflow.

The airflow in the cooling and heating mode was assumed to be 181.1 $m^3 \cdot h^{-1} \cdot kW^{-1}$ (375 cfm/ton). Data from the laboratory testing at NIST was used to correct the normalized fan power from the nominal value of 1.06 $kJ \cdot m^{-3}$ (0.5 $W \cdot cfm^{-1}$) as the airflow changes from the nominal value of 181.1 $m^3 \cdot h^{-1} \cdot kW^{-1}$ (375 cfm/ton). The data showed a linear trend. The best fit to the measure data (Eq. 4.2) was used to predict the variation in fan power as the airflow varies.

$$\left(\frac{W_{fan}}{V}\right) = 1.06 - \left[\left(\frac{V}{Q_{tot}}\right) - 181.1\right] \cdot 0.00316 \qquad (4.2)$$

where $\left(\dfrac{W_{fan}}{V}\right)$ = normalized fan power from the nominal value, $kJ \cdot m^{-3}$

$\left(\dfrac{V}{Q_{tot}}\right)$ = airflow to system capacity ratio, $m^3 \cdot h^{-1} \cdot kW^{-1}$

The heating performance for the heat pump used the generic performance curves developed for EnergyGauge (Parker et al., 1999). The generic model is based on catalog data from a series of single-speed heat pump products (ranging from 10 to 14.5 SEER) and was shown to be appropriate over a range of heat pump efficiency levels. The generic model predicts the variation in heating capacity and power input as a function of outdoor dry-bulb temperature, indoor entering temperature, and the airflow ratio (actual airflow divided by nominal airflow).

The impact of defrost operation was determined by the defrost degradation function shown in Figure 4.6, which is also used in EnergyGauge. This simple function[1] predicts the degradation as a function of outdoor dry-bulb temperature for a time-initiated, temperature-terminated defrost controller. The impact of defrost starts at temperatures below 8.3 °C (47 °F), peaks at 11 % by 2.8 °C (37 °F), and tapers off to 7.5 % at lower ambient temperatures. For comparison, the graph also includes the degradation rate implied by ASHRAE Standard 116 (ASHRAE, 2010).

The heat pump gross COP at 8.3 °C (47 °F) was 2.7. The nominal gross heating capacity, also at 8.3 °C (47 °F), was 10 % greater than the nominal gross cooling capacity. A supplemental 10 kW electric heater was activated if the space temperature dropped 0.28 °C (0.5 °F) below the heating set point or to 20.3 °C (68.5 °F) in Chicago, Washington, DC, and Minneapolis. The degraded performance of a heat pump due to faults was modeled by applying the heat pump normalized performance parameters described in Section 3.

Table 4.8 lists thermostat set points for heating and cooling. The 21.1 °C (70 °F) heating set point was selected as appropriate for temperate climates, while the 22.2 °C (72 °F) set point was deemed as more appropriate for the warmer climates. The cooling set point of 25.6 °C (78 °F) was selected as most consistent with homeowner preferences in warm climates. In colder climates 24.4 °C (76 °F) was used.

The impact of thermostat deadband and anticipator were explicitly considered in this short time-step model in the cooling mode as per Henderson (1992). The deadband was ±0.56 °C (1.0 °F) around the desired temperature point. The anticipator temperature gain was 1.4 °C (2.5 °F), and the time constant of the anticipator was 90 seconds. The sensing element of the thermostat had a time constant of 300 seconds. The result was the temperature 'droop' with runtime fraction of about 1.1 °C (2.0 °F). In the heating mode a simple deadband of ±0.6 °C (1.0 °F) around the set point was used without an anticipator or sensing element time constant.

---

[1] Actually, defrost is a function of both temperature and ambient humidity. While more sophisticated defrost models are available in EnergyPlus (see the 2012 Engineering Reference Manual), these approaches were found to have flaws and could not be successfully implemented here for this study.
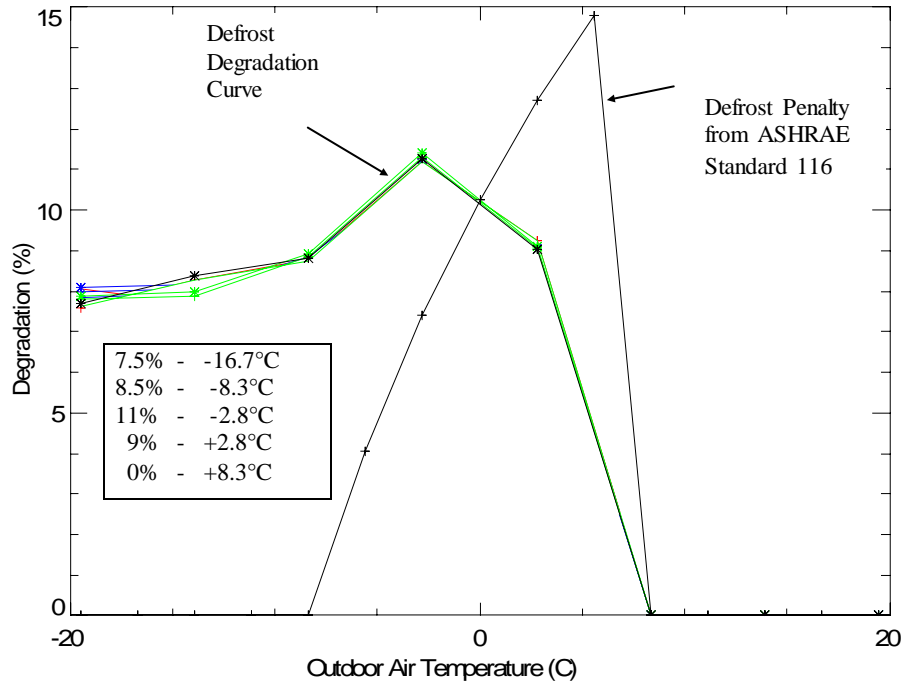
Figure 4.6. Capacity degradation due to defrost as a function of outdoor temperature
(The different color lines on the plot show the defrost degradation from catalog data. The table of values summarizes the average values used in the simulations.)

Table 4.8. Thermostat cooling and heating set points

Zone	Location	Cooling Set Point °C (°F)	Heating Set Point °C (°F)
2	Houston, TX	25.6 (78)	22.2 (72)
3	Las Vegas, NV		
4	Washington, DC	24.4 (76)	21.1 (70)
5	Chicago, IL		
6	Minneapolis, MN		

4.7 Cost of Electricity
Total heat pump operating costs were determined using the electric rates listed in Table 4.9.

Table 4.9. Cost of electricity

Zone	Location	Electric Utility	Cost	
			$/MJ	$/kWh
2	Houston, TX	Entergy	0.306	0.085
3	Las Vegas, NV	NV Energy	0.454	0.126
4	Washington, DC	Pepco	0.508	0.141
5	Chicago, IL	ComEd	0.461	0.128
6	Minneapolis, MN	Northern States Power	0.389	0.108

Note: Electric costs are from Form 826 data for local utility in 2010 for residential sector (EIA, 2012)

5. SIMULATIONS OF BUILDING/HEAT PUMP SYSTEMS WITH INSTALLATION FAULTS

Section 4.2 discussed the IECC climate zones and baseline houses considered in this study. The selected house options include a slab-on-grade house and a house with a basement for Las Vegas, Washington, DC, Chicago, and Minneapolis, and a slab-on-grade house only for Houston.

The following sections present results of annual simulations of energy consumption for a heat pump operating under different levels of different installation faults. These annual simulations focused on performance issues of the house/heat pump systems related to heat pump capacity and energy consumption while maintaining the target indoor dry-bulb temperature (shown in Table 4.8) within the temperature band imposed by the thermostat. For a few faults, we performed additional annual simulations with a lowered thermostat set-point temperature to mimic this common response to elevated indoor humidity levels caused by installation faults.

Results of annual simulations of energy consumptions are presented in the format consistent with Table 5.1. The threshold 55 % relative humidity value used in the third column was selected as the level above which humidity might start to be a concern. This threshold is slightly lower than the limit of 60 % relative humidity, which has historically been identified as the space condition where mold growth can occur in the building envelope (Sterling et al., 1985). The 'Space Temp Max' column contains the highest indoor temperature reached during the cooling season. The column 'AC Energy' contains the energy used by the compressor and outdoor fan to provide cooling; the column 'Htg Energy' contains the energy used by the compressor, outdoor fan, and backup heat to provide heating; and the column 'AHU Fan Energy' contains the energy used by the indoor fan during the whole year. The column 'TOTAL ENERGY' contains the total energy used by the heat pump throughout the entire year, which consists of the energy use listed in the three previous columns, and the energy used by the home exhaust fan.

5.1 Annual Energy Consumption in Baseline Houses

Table 5.1 presents simulation results of the annual heat pump operating energy consumption, energy cost, and relative energy cost referenced to that of the slab-on-grade house for each locality. The energy use of the basement house is from 17 % to 19 % lower than that for the slab-on-grade house in most climates. Most of this difference is due to duct leakage: the basement house has the ducts in the basement (with no losses) instead of ducts in the attic for the slab-on-grade house with the assumed typical leakage of 10 % (Section 4.3.2).

Table 5.1 also includes results from additional runs for the slab-on-grade house without duct leakage (i.e., treated as ducts in the conditioned space) denoted in the table as 'Slab, Ducts Inside'. When the duct leakage and duct thermal losses are eliminated, the slab-on-grade and basement houses perform within 3 % for Las Vegas and within 9 % for the cold climates. The basement house does have higher energy use in the colder climates.

Table 5.1. Annual energy consumption and cost in baseline houses

		Hours Above 55 % RH	Space Temp Max (C)	AC Runtime (h)	Htg Runtime (h)	Backup Heat Runtime (h)	AHU Fan Runtime (h)	AC COP (-)	AC SHR (-)	AC Energy (MJ)	Htg Energy (MJ)	AHU Fan Energy (MJ)	TOTAL ENERGY (MJ)	Total Costs	Relative Energy
Houston	Slab-on-Grade	1,512	26.6	1,981	749	5.1	2,730.5	4.3	0.785	16,660	8,537	5,529	31,457	$743	100%
	Basement														
	Slab, Ducts inside	1,715	25.2	1,555	588	0.3	2,142.9	4.3	0.789	13,007	6,623	4,339	24,700	$583	79%
Las Vegas	Slab-on-Grade	-	27.0	1,966	865	0.3	2,831.1	3.7	0.999	20,531	11,251	6,687	39,200	$1,372	100%
	Basement	-	25.3	1,552	718	0.3	2,269.9	3.7	1.000	16,107	9,407	5,362	31,607	$1,106	81%
	Slab, Ducts inside	-	25.3	1,536	668	0.3	2,204.5	3.7	1.000	15,941	8,763	5,207	30,642	$1,072	78%
Washington, DC	Slab-on-Grade	253	25.1	1,207	1,971	89.0	3,178.0	4.5	0.809	8,098	21,759	5,363	35,952	$1,408	100%
	Basement	654	24.0	742	1,907	27.0	2,649.5	4.4	0.775	5,008	19,120	4,471	29,330	$1,149	82%
	Slab, Ducts inside	280	24.1	944	1,532	12.9	2,476.3	4.4	0.801	6,301	15,111	4,179	26,322	$1,031	73%
Chicago	Slab-on-Grade	189	25.0	1,031	2,833	281.2	3,863.9	4.5	0.827	6,816	37,118	6,520	51,186	$1,820	100%
	Basement	289	24.0	631	2,785	129.8	3,416.1	4.4	0.797	4,198	31,565	5,765	42,259	$1,503	83%
	Slab, Ducts inside	203	24.0	815	2,288	70.0	3,103.7	4.5	0.819	5,369	24,753	5,238	36,092	$1,283	71%
Minneapolis	Slab-on-Grade	13	25.2	897	3,432	612.5	4,328.9	4.5	0.846	5,912	55,105	7,305	69,053	$2,072	100%
	Basement	61	24.0	515	3,424	354.2	3,939.8	4.4	0.810	3,428	46,239	6,648	57,048	$1,711	83%
	Slab, Ducts inside	15	24.1	711	2,902	216.9	3,613.5	4.5	0.838	4,670	36,410	6,098	47,909	$1,437	69%

5.2 Simulation with Single Faults

5.2.1 Studied Faults

Table 5.2 summarizes the studied faults and their level values used in simulations.

Table 5.2. Studied faults in the cooling and heating mode

Fault Type	Fault Levels (%)	
	Cooling mode	Heating mode
Heat Pump Sizing (SIZ)	-20, 25, 50, 75, 100	-20, 25, 50, 75, 100
Duct Leakage (DUCT)	0, 10, 20, 30, 40, 50	0, 10, 20, 30, 40, 50
Indoor Coil Airflow (AF)	-36, -15, 7, 28	-36, -15, 7, 28
Refrigerant Undercharge (UC)	-10, -20, -30	-10, -20, -30
Refrigerant Overcharge (OC)	10, 20, 30	10, 20, 30
Excessive Refrigerant Subcooling (SC)	100, 200	-
Non-Condensable Gases (NC)	10, 20	10, 20
Electric Voltage (VOL)	-8, 8, 25	-8, 8, 25
TXV Undersizing (TXV)	-60, -40, -20	-

5.2.2 Effect of Heat Pump Sizing

Changing the size of the heat pump for a given house – either undersizing or oversizing – impacts the heat pump performance in several ways:

- Cycling losses increase as the unit gets larger; the unit runs for shorter periods and the degraded performance at startup has more impact (parameters used in simulations are: time constant = 45 seconds, or $C_D \sim 0.15$).
- In the cooling mode, the shorter run periods impact the moisture removal capability (i.e., ability to control indoor humidity levels) because operational steady-state conditions are an even smaller portion of the runtime fraction.
- In the cooling mode, continuous fan operation with compressor cycling greatly increases moisture evaporation from the cooling coil. However, this impact is minimal with auto fan control (indoor fan time 'on' and 'off' the same as that of the compressor), since only a small amount of evaporation occurs with the assumed 4 % airflow during the off-cycle with the indoor fan off.   If the air conditioner controls include an off-cycle fan delay – that keeps the fan on for 30-90

seconds after the compressor stops – then the impact of off-cycle evaporation is in between these two extremes (Shirey et al., 2006).   The results in this study assumed auto fan operation with no fan delay.

- In the heating mode, the backup heater runtime is lower for the oversized unit since the larger heat pump meets more of the winter heating needs.

Heat pump sizing also affects the level of duct losses. This study considered two heat pump sizing scenarios with regard to the sizing of the air duct. In scenario (1), the heat pump and air duct are proportionally undersized or oversized, i.e., the duct flow area increases proportionally to the increase of heat pump capacity. As a result, the air mass flux through the duct remains unchanged, and the duct surface area increases with the square root of capacity ratio (unit capacity/design building load). The duct losses to the attic (thermal and air leak losses) tend to increase with the unit size since the surface area of the duct and the amount of airflow increases; however, the lower indoor fan runtime associated with an oversized heat pump has the opposing influence (reduces duct losses to the attic) since in the model the losses only occur when the fan is 'on'. Not included in this analysis is the impact that oversizing has on moisture control, especially at part load (see Sonne et al. (2006) for an in-depth review on this topic).

In scenario (2), the duct has been sized for a heat pump of nominal capacity and remains unchanged for different size heat pumps. When the heat pump is oversized, the fan speed is increased but the airflow does not reach the target flow rate because the unit is not capable of overcoming the increased external static pressure. Since the indoor fan works against increased static pressure, the fan power changes per the fan curve, i.e., fan power increases with an increasing unit size. The increased pressure in the duct increases the duct leakage. Table 5.3 shows the realized airflow per unit capacity, external static pressure, and duct leakage for scenario (1) and scenario (2).

Table 5.4 compares the effect of 100 % oversizing on the cooling and the heating performance for the slab-on-grade house for the five studied cities and two oversizing scenarios. For scenario (1) - duct size changes - oversizing degrades the cooling COP only modestly (about 2 %). The thermostat has 'droop' that causes the average space temperature to drop by (1.1 ~ 1.7) °C ((2 ~ 3) °F) with lower runtime fractions. In addition, the larger ducts have more losses to the uninsulated attic, but the shorter indoor runtime has the opposing effect. The net effect is that the energy use in the cooling mode increases by (2 ~ 3) %. In the heating mode, the larger heat pump meets more of the space heating load, so less operation of the inefficient auxiliary resistance heater is required. As a result, the heating energy decreases by (3 ~ 4) % in the cooling-dominated climates and almost 9 % in the heating-dominated climates. Overall, the total annual energy use is barely affected in the cooling-dominated climates and decreases in the heating dominated climates by about 4 %. Note, that the simulations in this section use a duct leakage rate of 10 %, which is assumed to be a 'no fault' installation condition. For scenario (2) - no change in duct size -, the increased fan power (while working against increased static pressure) and fan heat added to the load are the main factors contributing to the significant increase in energy used in cooling-dominated climates (Houston, Las Vegas, Washington, DC).

Tables 5.3. Indoor airflow information for heat pump sizing scenario (1) and scenario (2)

a) SI units	Heat Pump Sizing (%)	Fan Speed (%)	Normalized Airflow ($m^3 \cdot h^{-1} \cdot kW^{-1}$)	Normalized Fan Power ($kJ \cdot m^{-3}$)	Static Pressure (Pa)	Duct Leakage (%)	
						Supply	Return
Scenario (1): Duct size changes proportionally with HP size	80	100	181.1	1.06	167	6	4
	100	100	181.1	1.06	167	6	4
	125	100	181.1	1.06	167	6	4
	150	100	181.1	1.06	167	6	4
	175	100	181.1	1.06	167	6	4
	200	100	181.1	1.06	167	6	4
Scenario (2): Duct size stays the same as HP size changes	80	90	202.4	0.80	137	5.4	3.6
	100	100	181.1	1.06	167	6.0	4.0
	125	115	168.1	1.45	224	7.0	4.6
	150	120	145.5	1.68	249	7.3	4.9
	175	125	130.9	1.90	274	7.7	5.1
	200	130	120.8	2.11	299	8.0	5.4

b) I-P units	Heat Pump Sizing (%)	Fan Speed (%)	Normalized Airflow (cfm/ton)	Normalized Fan Power ($W \cdot cfm^{-1}$)	Static Pressure (inch)	Duct Leakage (%)	
						Supply	Return
Scenario (1): Duct size changes proportionally with HP size	80	100	375	0.50	0.76	6	4
	100	100	375	0.50	0.76	6	4
	125	100	375	0.50	0.76	6	4
	150	100	375	0.50	0.76	6	4
	175	100	375	0.50	0.76	6	4
	200	100	375	0.50	0.76	6	4
Scenario (2): Duct size stays the same as HP size changes	80	90	419	0.38	0.55	5.4	3.6
	100	100	375	0.50	0.67	6.0	4.0
	125	115	348	0.68	0.90	7.0	4.6
	150	120	301	0.79	1.00	7.3	4.9
	175	125	271	0.89	1.10	7.7	5.1
	200	130	250	0.99	1.20	8.0	5.4

Table 5.4. Effect of 100 % unit oversizing on annual energy use for a slab-on-grade house for scenario (1) and scenario (2)

Scenario (1): Duct size changes proportionally with HP size	Cooling COP (%)	Cooling Load (%)	Cooling Energy (%)	Heating Energy (%)	Total Energy (%)
Houston	-2.0	1.2	3.3	-4.1	0.9
Las Vegas	-2.5	-0.6	1.9	-3.3	0.1
Washington	-1.9	0.3	2.2	-7.9	-3.6
Chicago	-1.8	0.0	1.8	-8.9	-4.6
Minneapolis	-1.7	0.2	2.0	-8.6	-4.3

Scenario (2): Duct size stays the same as HP size changes	Cooling COP (%)	Cooling Load (%)	Cooling Energy (%)	Heating Energy (%)	Total Energy (%)
Houston	-10.3	9.6	22.2	-0.6	24.2
Las Vegas	-11.9	5.6	19.8	2.2	21.7
Washington	-10.3	9.6	22.1	-10.9	8.0
Chicago	-10.2	10.2	22.7	-13..5	2.1
Minneapolis	-10.2	10.8	23.4	-14.2	-0.9

Tables 5.5 and 5.6 show in detail the effect of heat pump sizing on the total energy performance for scenario (1). The impact of oversizing is modest for the house with the basement (Table 5.6) since the ducts are in the conditioned space. In this case, oversizing increases cooling energy because of efficiency losses from cyclic degradation, therefore overall energy use in cooling-dominated locations such as Houston and Las Vegas increases. In the heating-dominated climates, such as Chicago, the heating energy is affected by cyclic degradation as well; however, the larger heat pump meets more of the heating load, which reduces the need for backup heating. The net effect is a slight decrease in overall energy use. For the slab-on-grade house (Table 5.5) the impact of duct leakage further complicates the situation. In addition to the factors discussed for the house with the basement, oversized heat pumps have reduced runtimes, which reduce duct losses and result in a less energy being used than by the baseline system. Combining all effects, the net impact on energy use in Houston and Las Vegas is neutral. In Chicago, oversizing actually reduces energy use by as much as 5 % for the slab-on-grade house.

Tables 5.7 and 5.8 show in detail the effect of sizing on the total performance for scenario (2), and Figures 5.1 and 5.2 show relative energy input for the slab-on-grade house and house with a basement, respectively. The indoor fan power changes associated with heat pump sizing have proportionally bigger impact in the basement house then the slab-on-grade house since the cooling loads are smaller. In heating, the added fan power from oversizing in the basement house attenuates the drop in heating energy. The houses located in cooling dominated climates use less energy when the heat pump is undersized because the heat pump does not handle all the cooling load (the indoor temperature increases on hot days). For the heating dominated climates, the energy use is increased because of the significantly increased use of the resistant heater.

Table 5.5. Effect of heat pump sizing on annual energy use for a slab-on-grade house with duct sized to match heat pump size (scenario (1))

Houston	Hours Above 55 % RH	Space Temp Max (C)	AC Runtime (h)	Htg Runtime (h)	Backup Heat Runtime (h)	AHU Fan Runtime (h)	AC COP (-)	AC SHR (-)	AC Energy (MJ)	Htg Energy (MJ)	AHU Fan Energy (MJ)	TOTAL ENERGY (MJ)	Total Costs	Relative Energy
Undersized 20 %	1,521	27.7	2,401	918	15.1	3,319.0	4.4	0.784	16,078	8,710	5,377	30,897	$730	98%
Normal	1,512	26.6	1,981	749	5.1	2,730.5	4.3	0.785	16,660	8,537	5,529	31,457	$743	100%
Oversized 25 %	1,527	25.6	1,606	597	1.0	2,202.5	4.3	0.785	16,901	8,369	5,575	31,577	$746	100%
Oversized 50 %	1,544	25.3	1,347	493	0.3	1,840.0	4.3	0.784	17,012	8,283	5,589	31,616	$746	101%
Oversized 75 %	1,561	25.1	1,162	420	0.2	1,581.6	4.3	0.784	17,119	8,232	5,605	31,687	$748	101%
Oversized 100 %	1,587	25.1	1,022	365	0.2	1,387.3	4.3	0.785	17,213	8,191	5,618	31,754	$750	101%

Las Vegas	Hours Above 55 % RH	Space Temp Max (C)	AC Runtime (h)	Htg Runtime (h)	Backup Heat Runtime (h)	AHU Fan Runtime (h)	AC COP (-)	AC SHR (-)	AC Energy (MJ)	Htg Energy (MJ)	AHU Fan Energy (MJ)	TOTAL ENERGY (MJ)	Total Costs	Relative Energy
Undersized 20 %	-	28.5	2,376	1,095	2.4	3,470.2	3.8	0.999	19,716	11,448	6,559	38,455	$1,346	98%
Normal	-	27.0	1,966	865	0.3	2,831.1	3.7	0.999	20,531	11,251	6,687	39,200	$1,372	100%
Oversized 25 %	-	25.6	1,587	680	0.3	2,267.3	3.7	0.999	20,758	11,070	6,696	39,256	$1,374	100%
Oversized 50 %	-	25.2	1,326	562	0.3	1,887.8	3.7	0.999	20,806	10,983	6,690	39,210	$1,372	100%
Oversized 75 %	-	25.1	1,140	479	0.2	1,618.7	3.7	0.999	20,863	10,927	6,692	39,215	$1,373	100%
Oversized 100 %	-	25.1	1,000	417	0.2	1,417.4	3.6	1.000	20,926	10,877	6,697	39,232	$1,373	100%

Washington, DC	Hours Above 55 % RH	Space Temp Max (C)	AC Runtime (h)	Htg Runtime (h)	Backup Heat Runtime (h)	AHU Fan Runtime (h)	AC COP (-)	AC SHR (-)	AC Energy (MJ)	Htg Energy (MJ)	AHU Fan Energy (MJ)	TOTAL ENERGY (MJ)	Total Costs	Relative Energy
Undersized 20 %	238	25.9	1,480	2,330	147.7	3,810.1	4.5	0.809	7,909	22,789	5,144	36,573	$1,432	102%
Normal	253	25.1	1,207	1,971	89.0	3,178.0	4.5	0.809	8,098	21,759	5,363	35,952	$1,408	100%
Oversized 25 %	276	24.3	974	1,633	46.6	2,606.4	4.4	0.808	8,178	20,958	5,498	35,365	$1,385	98%
Oversized 50 %	280	24.0	815	1,385	22.3	2,199.9	4.4	0.809	8,216	20,487	5,568	35,004	$1,371	97%
Oversized 75 %	287	24.0	701	1,197	9.0	1,898.1	4.4	0.809	8,251	20,223	5,605	34,811	$1,363	97%
Oversized 100 %	303	23.9	616	1,049	1.8	1,664.9	4.4	0.809	8,280	20,044	5,619	34,674	$1,358	96%

Chicago	Hours Above 55 % RH	Space Temp Max (C)	AC Runtime (h)	Htg Runtime (h)	Backup Heat Runtime (h)	AHU Fan Runtime (h)	AC COP (-)	AC SHR (-)	AC Energy (MJ)	Htg Energy (MJ)	AHU Fan Energy (MJ)	TOTAL ENERGY (MJ)	Total Costs	Relative Energy
Undersized 20 %	189	26.0	1,269	3,178	421.6	4,446.0	4.6	0.827	6,690	39,279	6,002	52,703	$1,874	103%
Normal	189	25.0	1,031	2,833	281.2	3,863.9	4.5	0.827	6,816	37,118	6,520	51,186	$1,820	100%
Oversized 25 %	193	24.2	830	2,430	178.3	3,259.1	4.5	0.827	6,863	35,494	6,875	49,963	$1,776	98%
Oversized 50 %	193	24.0	694	2,120	112.0	2,813.7	4.5	0.827	6,892	34,615	7,122	49,361	$1,755	96%
Oversized 75 %	190	24.0	597	1,860	76.2	2,456.5	4.4	0.827	6,916	34,162	7,254	49,065	$1,745	96%
Oversized 100 %	197	23.9	524	1,648	53.4	2,171.7	4.4	0.827	6,941	33,826	7,329	48,828	$1,736	95%

Minneapolis	Hours Above 55 % RH	Space Temp Max (C)	AC Runtime (h)	Htg Runtime (h)	Backup Heat Runtime (h)	AHU Fan Runtime (h)	AC COP (-)	AC SHR (-)	AC Energy (MJ)	Htg Energy (MJ)	AHU Fan Energy (MJ)	TOTAL ENERGY (MJ)	Total Costs	Relative Energy
Undersized 20 %	12	26.1	1,107	3,727	827.2	4,833.6	4.5	0.847	5,819	58,359	6,525	71,436	$2,143	103%
Normal	13	25.2	897	3,432	612.5	4,328.9	4.5	0.846	5,912	55,105	7,305	69,053	$2,072	100%
Oversized 25 %	15	24.3	722	3,066	432.9	3,788.6	4.5	0.846	5,958	52,707	7,992	67,388	$2,022	98%
Oversized 50 %	15	24.1	604	2,735	322.0	3,339.1	4.5	0.846	5,981	51,531	8,452	66,696	$2,001	97%
Oversized 75 %	15	24.0	521	2,440	253.2	2,960.7	4.4	0.847	6,012	50,862	8,743	66,349	$1,990	96%
Oversized 100 %	16	23.9	457	2,195	203.5	2,651.8	4.4	0.848	6,028	50,388	8,950	66,098	$1,983	96%

Table 5.6. Effect of heat pump sizing on annual energy use for a house with basement with duct sized to match heat pump size (scenario (1))

Las Vegas	Hours Above 55 % RH	Space Temp Max (C)	AC Runtime (h)	Htg Runtime (h)	Backup Heat Runtime (h)	AHU Fan Runtime (h)	AC COP (-)	AC SHR (-)	AC Energy (MJ)	Htg Energy (MJ)	AHU Fan Energy (MJ)	TOTAL ENERGY (MJ)	Total Costs	Relative Energy
Undersized 20 %	-	26.0	1,908	898	0.3	2,806.8	3.7	1.000	15,839	9,411	5,305	31,287	$1,095	99%
Normal	-	25.3	1,552	718	0.3	2,269.9	3.7	1.000	16,107	9,407	5,362	31,607	$1,106	100%
Oversized 25 %	-	25.2	1,260	574	0.2	1,834.1	3.6	1.000	16,354	9,413	5,416	31,915	$1,117	101%
Oversized 50 %	-	25.1	1,064	479	0.2	1,542.6	3.6	1.000	16,568	9,430	5,467	32,196	$1,127	102%
Oversized 75 %	-	25.0	920	411	0.2	1,331.1	3.6	1.000	16,735	9,434	5,503	32,404	$1,134	103%
Oversized 100 %	-	24.9	812	360	0.2	1,171.9	3.6	1.000	16,871	9,452	5,537	32,592	$1,141	103%

Washington, DC	Hours Above 55 % RH	Space Temp Max (C)	AC Runtime (h)	Htg Runtime (h)	Backup Heat Runtime (h)	AHU Fan Runtime (h)	AC COP (-)	AC SHR (-)	AC Energy (MJ)	Htg Energy (MJ)	AHU Fan Energy (MJ)	TOTAL ENERGY (MJ)	Total Costs	Relative Energy
Undersized 20 %	647	24.2	914	2,294	62.1	3,208.5	4.4	0.773	4,930	19,645	4,331	29,638	$1,161	101%
Normal	654	24.0	742	1,907	27.0	2,649.5	4.4	0.775	5,008	19,120	4,471	29,330	$1,149	100%
Oversized 25 %	666	23.9	603	1,562	6.5	2,164.2	4.4	0.776	5,085	18,867	4,565	29,249	$1,146	100%
Oversized 50 %	669	23.8	507	1,313	0.5	1,820.1	4.3	0.778	5,142	18,855	4,607	29,336	$1,149	100%
Oversized 75 %	677	23.8	439	1,128	0.1	1,566.8	4.3	0.779	5,196	18,899	4,627	29,454	$1,154	100%
Oversized 100 %	694	23.7	387	986	0.1	1,373.4	4.3	0.780	5,236	18,897	4,635	29,500	$1,155	101%

Chicago	Hours Above 55 % RH	Space Temp Max (C)	AC Runtime (h)	Htg Runtime (h)	Backup Heat Runtime (h)	AHU Fan Runtime (h)	AC COP (-)	AC SHR (-)	AC Energy (MJ)	Htg Energy (MJ)	AHU Fan Energy (MJ)	TOTAL ENERGY (MJ)	Total Costs	Relative Energy
Undersized 20 %	276	24.2	777	3,199	240.2	3,976.0	4.5	0.795	4,131	33,239	5,368	43,470	$1,546	103%
Normal	289	24.0	631	2,785	129.8	3,416.1	4.4	0.797	4,198	31,565	5,765	42,259	$1,503	100%
Oversized 25 %	287	23.9	512	2,351	60.6	2,862.8	4.4	0.799	4,259	30,692	6,039	41,721	$1,483	99%
Oversized 50 %	285	23.8	431	2,010	31.1	2,441.1	4.4	0.800	4,308	30,474	6,179	41,693	$1,482	99%
Oversized 75 %	285	23.8	373	1,745	15.4	2,117.8	4.4	0.801	4,344	30,363	6,254	41,693	$1,482	99%
Oversized 100 %	292	23.7	328	1,541	6.5	1,868.8	4.4	0.803	4,373	30,362	6,307	41,774	$1,485	99%

Minneapolis	Hours Above 55 % RH	Space Temp Max (C)	AC Runtime (h)	Htg Runtime (h)	Backup Heat Runtime (h)	AHU Fan Runtime (h)	AC COP (-)	AC SHR (-)	AC Energy (MJ)	Htg Energy (MJ)	AHU Fan Energy (MJ)	TOTAL ENERGY (MJ)	Total Costs	Relative Energy
Undersized 20 %	61	24.3	635	3,793	551.4	4,428.1	4.4	0.809	3,375	49,371	5,978	59,456	$1,784	104%
Normal	61	24.0	515	3,424	354.2	3,939.8	4.4	0.810	3,428	46,239	6,648	57,048	$1,711	100%
Oversized 25 %	64	24.0	418	2,984	219.1	3,401.9	4.4	0.812	3,480	44,581	7,176	55,969	$1,679	98%
Oversized 50 %	66	23.9	352	2,602	147.8	2,954.8	4.4	0.814	3,520	43,888	7,479	55,619	$1,669	97%
Oversized 75 %	70	23.8	304	2,299	99.1	2,603.2	4.4	0.816	3,548	43,438	7,688	55,405	$1,662	97%
Oversized 100 %	70	23.7	268	2,057	65.8	2,324.7	4.4	0.817	3,570	43,260	7,846	55,408	$1,662	97%

Table 5.7. Effect of heat pump sizing on annual energy use for a slab-on-grade house with fixed duct size (scenario (2))

Houston	Hours Above 55 % RH	Space Temp Max (C)	AC Runtime (h)	Htg Runtime (h)	Backup Heat Runtime (h)	AHU Fan Runtime (h)	AC COP (-)	AC SHR (-)	AC Energy (MJ)	Htg Energy (MJ)	AHU Fan Energy (MJ)	TOTAL ENERGY (MJ)	Total Costs	Relative Energy
Undersized 20 %	1,692	27.6	2,317	906	14.4	3,223.4	4.5	0.790	15,621	8,583	4,292	29,227	$690	93%
Normal	1,512	26.6	1,981	749	5.1	2,730.5	4.3	0.785	16,660	8,537	5,529	31,457	$743	100%
Oversized 25 %	1,443	25.8	1,687	605	1.0	2,292.1	4.3	0.780	17,709	8,481	7,330	34,252	$809	109%
Oversized 50 %	1,320	25.3	1,492	505	0.3	1,996.8	4.1	0.774	18,713	8,470	8,147	36,062	$851	115%
Oversized 75 %	1,244	25.2	1,343	433	0.2	1,775.8	4.0	0.769	19,587	8,482	8,832	37,634	$889	120%
Oversized 100 %	1,205	25.1	1,224	379	0.2	1,602.7	3.9	0.766	20,351	8,483	9,513	39,078	$923	124%

Las Vegas	Hours Above 55 % RH	Space Temp Max (C)	AC Runtime (h)	Htg Runtime (h)	Backup Heat Runtime (h)	AHU Fan Runtime (h)	AC COP (-)	AC SHR (-)	AC Energy (MJ)	Htg Energy (MJ)	AHU Fan Energy (MJ)	TOTAL ENERGY (MJ)	Total Costs	Relative Energy
Undersized 20 %	-	28.3	2,303	1,109	3.0	3,411.4	3.9	1.000	19,197	11,620	5,060	36,608	$1,281	93%
Normal	-	27.0	1,966	865	0.3	2,831.1	3.7	0.999	20,531	11,251	6,687	39,200	$1,372	100%
Oversized 25 %	-	25.9	1,658	708	0.3	2,366.3	3.6	0.999	21,651	11,509	8,447	42,339	$1,482	108%
Oversized 50 %	-	25.2	1,461	588	0.3	2,048.9	3.5	0.997	22,773	11,483	9,346	44,335	$1,552	113%
Oversized 75 %	-	25.2	1,311	505	0.2	1,815.7	3.4	0.995	23,742	11,495	10,108	46,077	$1,613	118%
Oversized 100 %	-	25.2	1,194	442	0.2	1,635.9	3.3	0.993	24,605	11,504	10,878	47,719	$1,670	122%

Washington, DC	Hours Above 55 % RH	Space Temp Max (C)	AC Runtime (h)	Htg Runtime (h)	Backup Heat Runtime (h)	AHU Fan Runtime (h)	AC COP (-)	AC SHR (-)	AC Energy (MJ)	Htg Energy (MJ)	AHU Fan Energy (MJ)	TOTAL ENERGY (MJ)	Total Costs	Relative Energy
Undersized 20 %	326	25.7	1,424	2,266	138.8	3,689.5	4.6	0.816	7,658	22,274	4,795	35,459	$1,389	99%
Normal	253	25.1	1,207	1,971	89.0	3,178.0	4.5	0.809	8,098	21,759	5,363	35,952	$1,408	100%
Oversized 25 %	216	24.4	1,025	1,604	42.9	2,628.8	4.4	0.804	8,581	20,448	7,423	37,184	$1,456	103%
Oversized 50 %	134	24.1	907	1,363	17.4	2,269.7	4.2	0.796	9,077	19,830	8,047	37,685	$1,476	105%
Oversized 75 %	89	24.1	817	1,181	5.6	1,998.2	4.1	0.790	9,511	19,567	8,464	38,273	$1,499	106%
Oversized 100 %	59	24.0	745	1,036	0.7	1,781.8	4.0	0.785	9,892	19,396	8,822	38,841	$1,521	108%

Chicago	Hours Above 55 % RH	Space Temp Max (C)	AC Runtime (h)	Htg Runtime (h)	Backup Heat Runtime (h)	AHU Fan Runtime (h)	AC COP (-)	AC SHR (-)	AC Energy (MJ)	Htg Energy (MJ)	AHU Fan Energy (MJ)	TOTAL ENERGY (MJ)	Total Costs	Relative Energy
Undersized 20 %	187	25.8	1,215	3,123	399.8	4,338.1	4.6	0.836	6,451	38,633	5,807	51,622	$1,835	101%
Normal	189	25.0	1,031	2,833	281.2	3,863.9	4.5	0.827	6,816	37,118	6,520	51,186	$1,820	100%
Oversized 25 %	192	24.3	874	2,398	164.7	3,272.0	4.4	0.821	7,209	34,553	9,278	51,772	$1,841	101%
Oversized 50 %	183	24.1	777	2,086	97.3	2,862.8	4.3	0.811	7,657	33,246	10,145	51,779	$1,841	101%
Oversized 75 %	183	24.0	700	1,829	63.6	2,529.5	4.1	0.803	8,033	32,604	10,640	52,008	$1,849	102%
Oversized 100 %	173	24.0	640	1,623	40.8	2,262.7	4.1	0.798	8,365	32,100	11,041	52,238	$1,857	102%

Minneapolis	Hours Above 55 % RH	Space Temp Max (C)	AC Runtime (h)	Htg Runtime (h)	Backup Heat Runtime (h)	AHU Fan Runtime (h)	AC COP (-)	AC SHR (-)	AC Energy (MJ)	Htg Energy (MJ)	AHU Fan Energy (MJ)	TOTAL ENERGY (MJ)	Total Costs	Relative Energy
Undersized 20 %	16	26.0	1,059	3,673	797.0	4,732.5	4.6	0.857	5,604	57,677	6,432	70,445	$2,113	102%
Normal	13	25.2	897	3,432	612.5	4,328.9	4.5	0.846	5,912	55,105	7,305	69,053	$2,072	100%
Oversized 25 %	13	24.5	761	3,033	408.9	3,793.4	4.4	0.840	6,255	51,321	10,781	69,089	$2,073	100%
Oversized 50 %	11	24.1	677	2,694	293.2	3,371.5	4.3	0.828	6,659	49,336	11,945	68,672	$2,060	99%
Oversized 75 %	8	24.0	612	2,403	224.3	3,014.5	4.1	0.820	7,000	48,228	12,630	68,589	$2,058	99%
Oversized 100 %	5	24.0	560	2,161	171.5	2,720.2	4.0	0.814	7,295	47,255	13,164	68,445	$2,053	99%

Table 5.8. Effect of heat pump sizing on annual energy use for a house with basement with fixed duct size (scenario (2))

Las Vegas	Hours Above 55 % RH	Space Temp Max (C)	AC Runtime (h)	Htg Runtime (h)	Backup Heat Runtime (h)	AHU Fan Runtime (h)	AC COP (-)	AC SHR (-)	AC Energy (MJ)	Htg Energy (MJ)	AHU Fan Energy (MJ)	TOTAL ENERGY (MJ)	Total Costs	Relative Energy
Undersized 20 %	-	25.8	1,835	904	0.3	2,739.1	3.8	1.000	15,274	9,464	4,062	29,531	$1,034	93%
Normal	-	25.3	1,552	718	0.3	2,269.9	3.7	1.000	16,107	9,407	5,362	31,607	$1,106	100%
Oversized 25 %	-	25.2	1,313	591	0.3	1,903.5	3.6	1.000	17,007	9,695	6,773	34,207	$1,197	108%
Oversized 50 %	-	25.1	1,167	497	0.2	1,664.2	3.4	1.000	18,072	9,796	7,564	36,163	$1,266	114%
Oversized 75 %	-	25.1	1,054	429	0.2	1,483.1	3.3	0.999	18,965	9,870	8,223	37,790	$1,323	120%
Oversized 100 %	-	25.0	963	377	0.2	1,340.7	3.2	0.997	19,736	9,918	8,875	39,260	$1,374	124%

Washington, DC	Hours Above 55 % RH	Space Temp Max (C)	AC Runtime (h)	Htg Runtime (h)	Backup Heat Runtime (h)	AHU Fan Runtime (h)	AC COP (-)	AC SHR (-)	AC Energy (MJ)	Htg Energy (MJ)	AHU Fan Energy (MJ)	TOTAL ENERGY (MJ)	Total Costs	Relative Energy
Undersized 20 %	863	24.0	873	2,212	53.8	3,085.1	4.5	0.779	4,734	18,958	4,126	28,550	$1,118	97%
Normal	654	24.0	742	1,907	27.0	2,649.5	4.4	0.775	5,008	19,120	4,471	29,330	$1,149	100%
Oversized 25 %	514	24.0	630	1,535	4.6	2,165.2	4.3	0.775	5,301	18,466	6,135	30,634	$1,200	104%
Oversized 50 %	359	23.9	563	1,302	0.5	1,865.1	4.1	0.768	5,663	18,592	6,610	31,596	$1,238	108%
Oversized 75 %	263	23.9	509	1,128	0.1	1,637.6	4.0	0.764	5,965	18,725	6,900	32,323	$1,266	110%
Oversized 100 %	216	23.8	467	995	0.1	1,461.3	3.9	0.761	6,231	18,818	7,159	32,940	$1,290	112%

Chicago	Hours Above 55 % RH	Space Temp Max (C)	AC Runtime (h)	Htg Runtime (h)	Backup Heat Runtime (h)	AHU Fan Runtime (h)	AC COP (-)	AC SHR (-)	AC Energy (MJ)	Htg Energy (MJ)	AHU Fan Energy (MJ)	TOTAL ENERGY (MJ)	Total Costs	Relative Energy
Undersized 20 %	318	24.1	741	3,119	213.1	3,860.3	4.5	0.804	3,963	32,140	5,292	42,126	$1,498	100%
Normal	289	24.0	631	2,785	129.8	3,416.1	4.4	0.797	4,198	31,565	5,765	42,259	$1,503	100%
Oversized 25 %	263	24.0	536	2,313	54.7	2,848.6	4.3	0.795	4,446	29,982	8,099	43,258	$1,538	102%
Oversized 50 %	237	23.9	480	1,991	28.8	2,470.1	4.2	0.787	4,758	29,840	8,751	44,080	$1,567	104%
Oversized 75 %	224	23.8	435	1,745	13.8	2,179.5	4.1	0.780	5,019	29,858	9,130	44,738	$1,591	106%
Oversized 100 %	213	23.8	398	1,550	6.1	1,948.1	4.0	0.776	5,243	29,944	9,426	45,345	$1,612	107%

Minneapolis	Hours Above 55 % RH	Space Temp Max (C)	AC Runtime (h)	Htg Runtime (h)	Backup Heat Runtime (h)	AHU Fan Runtime (h)	AC COP (-)	AC SHR (-)	AC Energy (MJ)	Htg Energy (MJ)	AHU Fan Energy (MJ)	TOTAL ENERGY (MJ)	Total Costs	Relative Energy
Undersized 20 %	72	24.2	604	3,724	505.2	4,327.8	4.5	0.818	3,230	47,917	6,016	57,894	$1,737	101%
Normal	61	24.0	515	3,424	354.2	3,939.8	4.4	0.810	3,428	46,239	6,648	57,048	$1,711	100%
Oversized 25 %	58	24.0	438	2,943	204.3	3,381.6	4.3	0.808	3,636	43,494	9,633	57,495	$1,725	101%
Oversized 50 %	54	24.0	392	2,580	139.4	2,972.0	4.2	0.798	3,894	42,806	10,527	57,959	$1,739	102%
Oversized 75 %	50	23.9	356	2,297	93.9	2,653.1	4.1	0.791	4,110	42,474	11,075	58,390	$1,752	102%
Oversized 100 %	49	23.8	327	2,067	62.8	2,393.8	4.0	0.786	4,300	42,343	11,497	58,871	$1,766	103%
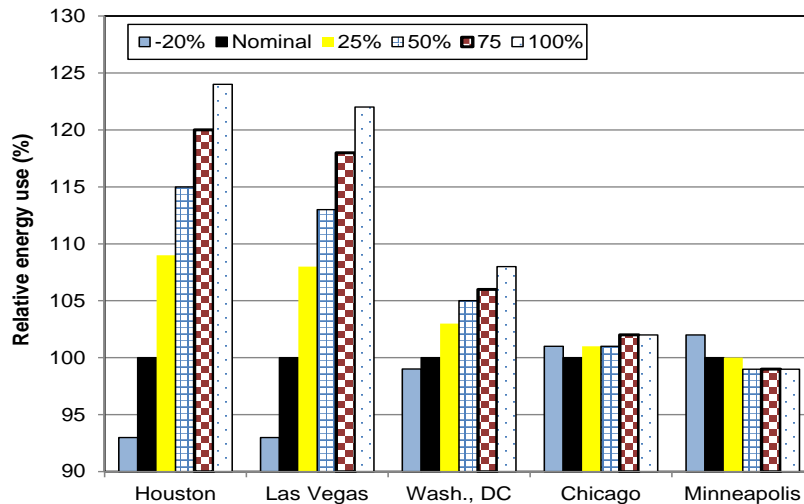
Figure 5.1. Annual energy use for slab-on-grade houses for different heat pump sizings, scenario (2)

53
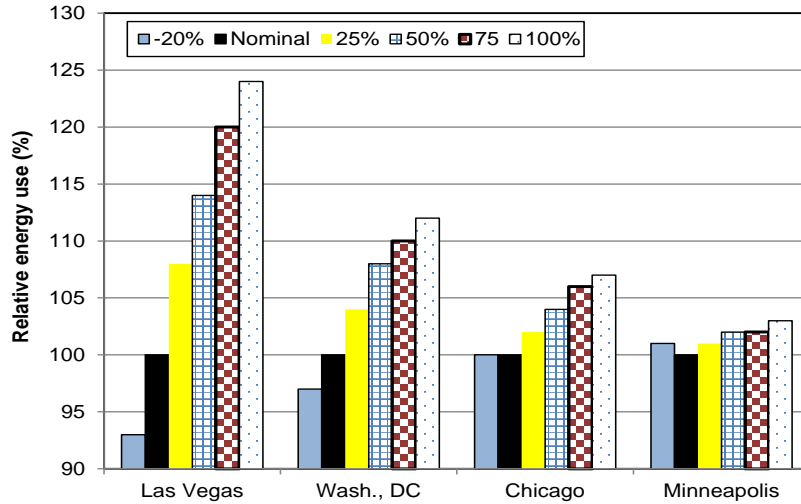
Figure 5.2. Annual energy use for houses with basement for different heat pump sizings, scenario (2)

5.2.3 Effect of Duct Leakage

Per the earlier discussion in Section 4.3.2, the effect of duct leakage has been evaluated only for slab-on-grade houses where ducts were installed in the attic (i.e., in the unconditioned space). The baseline houses include ducts in the attic with a leakage rate of 10 % (leakage distributed 60 % on the supply side and 40 % on the return side) as well as thermal losses through the duct wall. Table 5.9 compares this base case to other levels of duct leakage with the thermostat set at the default set point temperature (Table 4.8). The entry '0 % & No thermal' in the left most column denotes an idealistic installation with zero air leakage and no thermal loss (i.e., an insulation with an infinite R). For all other simulation cases the duct insulation is assumed to be R(SI)-1.1 (R-6).

As expected, the baseline duct losses increase energy use in the baseline houses; our simulations showed a 20 % and 30 % increase for the cooling climates and heating climates, respectively, compared to the 0 % leak case. As the duct leakage increases, energy use increases by at least 8 % for the cooling climates and by 12 % for the heating climates for each 10 % increment in the duct leakage fault. A slight improvement of the cooling COP shown with the increasing fault level is caused by a somewhat higher refrigerant saturation temperature (and pressure) in the evaporator when the air returning to the indoor section is at higher temperature due to duct losses. This COP improvement, however, can't compensate for the significant increase in the cooling load, which is the cause of the increased energy use.

Table 5.10 shows the effect of duct leakage on annual energy use for the slab-on-grade house from lowering the cooling set point by 1.1 °C (2.0 °F). For completeness, the table includes all studied locations, although houses in Houston and Washington, DC, are most likely to be operated at a lowered set point temperature to improve the indoor comfort. Table 5.11 shows simulation results for the indoor set point temperature lowered by an additional 1.1 °C (2.0 °F), i.e., by 2.2 °C (4.0 °F) below the default value for the house in Houston.

Reducing the set point results in a lower number of hours with relative humidity above 55 % for small levels of duct leaks only (Tables 5.10 and 5.11). For large levels of duct leakage, the number of hours with relative humidity above 55 % actually increases. This result is caused by the fact that lowering the set point requires longer operational runtimes (with correspondingly higher energy consumption and duct leakage) and, depending on the ratio of sensible to latent capacities, lowering the indoor temperature may actually increase the relative humidity, although the indoor comfort might improve due to a lower dry-bulb temperature.

Table 5.9. Effect of duct leakage on annual energy use for a slab-on-grade house at default cooling set point

Houston	Hours Above 55 % RH	AC Runtime (h)	Htg Runtime (h)	Backup Heat Runtime (h)	AHU Fan Runtime (h)	AC COP (-)	AC SHR (-)	AC Energy (MJ)	Htg Energy (MJ)	AHU Fan Energy (MJ)	TOTAL ENERGY (MJ)	Total Costs	Relative Energy
0 % & No thermal	1,715	1,555	588	0.3	2,142.9	4.3	0.789	13,007	6,623	4,339	24,700	$583	79%
0 % Leak	1,537	1,794	685	2.1	2,479.0	4.3	0.812	15,046	7,761	5,020	28,559	$674	91%
10 % Leak	1,512	1,981	749	5.1	2,730.5	4.3	0.785	16,660	8,537	5,529	31,457	$743	100%
20 % Leak	1,632	2,160	815	9.4	2,975.1	4.4	0.767	18,179	9,383	6,025	34,317	$810	109%
30 % Leak	1,922	2,327	883	17.5	3,209.7	4.5	0.753	19,574	10,393	6,500	37,198	$878	118%
40 % Leak	2,738	2,489	953	35.5	3,441.7	4.5	0.743	20,922	11,773	6,970	40,397	$954	128%
50 % Leak	3,364	2,649	1,032	61.8	3,681.0	4.6	0.734	22,231	13,578	7,454	43,995	$1,039	140%

Las Vegas	Hours Above 55 % RH	AC Runtime (h)	Htg Runtime (h)	Backup Heat Runtime (h)	AHU Fan Runtime (h)	AC COP (-)	AC SHR (-)	AC Energy (MJ)	Htg Energy (MJ)	AHU Fan Energy (MJ)	TOTAL ENERGY (MJ)	Total Costs	Relative Energy
0 % & No thermal	-	1,536	668	0.3	2,204.5	3.7	1.000	15,941	8,763	5,207	30,642	$1,072	78%
0 % Leak	-	1,817	786	0.3	2,602.5	3.7	1.000	18,952	10,273	6,147	36,104	$1,264	92%
10 % Leak	-	1,966	865	0.3	2,831.1	3.7	0.999	20,531	11,251	6,687	39,200	$1,372	100%
20 % Leak	-	2,114	951	1.2	3,065.4	3.8	0.998	22,081	12,339	7,241	42,393	$1,484	108%
30 % Leak	-	2,261	1,054	3.7	3,315.3	3.8	0.998	23,580	13,718	7,831	45,861	$1,605	117%
40 % Leak	-	2,405	1,170	8.6	3,575.4	3.9	0.997	25,028	15,353	8,445	49,558	$1,735	126%
50 % Leak	-	2,549	1,290	22.7	3,838.7	3.9	0.996	26,444	17,362	9,067	53,605	$1,876	137%

Washington, DC	Hours Above 55 % RH	AC Runtime (h)	Htg Runtime (h)	Backup Heat Runtime (h)	AHU Fan Runtime (h)	AC COP (-)	AC SHR (-)	AC Energy (MJ)	Htg Energy (MJ)	AHU Fan Energy (MJ)	TOTAL ENERGY (MJ)	Total Costs	Relative Energy
0 % & No thermal	280	944	1,532	12.9	2,476.3	4.4	0.801	6,301	15,111	4,179	26,322	$1,031	73%
0 % Leak	175	1,100	1,803	54.5	2,902.7	4.4	0.823	7,361	19,093	4,898	32,084	$1,257	89%
10 % Leak	253	1,207	1,971	89.0	3,178.0	4.5	0.809	8,098	21,759	5,363	35,952	$1,408	100%
20 % Leak	368	1,314	2,133	134.8	3,446.8	4.5	0.799	8,825	24,760	5,817	40,133	$1,572	112%
30 % Leak	523	1,419	2,294	192.5	3,712.5	4.6	0.791	9,528	28,180	6,265	44,704	$1,751	124%
40 % Leak	814	1,523	2,457	270.0	3,979.2	4.6	0.786	10,216	32,335	6,715	49,997	$1,958	139%
50 % Leak	1,165	1,625	2,595	382.3	4,219.9	4.7	0.781	10,884	37,541	7,121	56,278	$2,204	157%

Chicago	Hours Above 55 % RH	AC Runtime (h)	Htg Runtime (h)	Backup Heat Runtime (h)	AHU Fan Runtime (h)	AC COP (-)	AC SHR (-)	AC Energy (MJ)	Htg Energy (MJ)	AHU Fan Energy (MJ)	TOTAL ENERGY (MJ)	Total Costs	Relative Energy
0 % & No thermal	203	815	2,288	70.0	3,103.7	4.5	0.819	5,369	24,753	5,238	36,092	$1,283	71%
0 % Leak	190	943	2,639	187.4	3,582.0	4.5	0.839	6,217	32,197	6,045	45,190	$1,607	88%
10 % Leak	189	1,031	2,833	281.2	3,863.9	4.5	0.827	6,816	37,118	6,520	51,186	$1,820	100%
20 % Leak	192	1,119	3,007	394.4	4,125.5	4.6	0.818	7,410	42,561	6,962	57,664	$2,050	113%
30 % Leak	220	1,208	3,150	532.6	4,358.0	4.6	0.812	8,003	48,636	7,354	64,725	$2,301	126%
40 % Leak	310	1,296	3,285	697.0	4,581.3	4.7	0.806	8,591	55,589	7,731	72,642	$2,583	142%
50 % Leak	427	1,386	3,408	900.9	4,793.8	4.7	0.801	9,174	63,893	8,090	81,888	$2,912	160%

Minneapolis	Hours Above 55 % RH	AC Runtime (h)	Htg Runtime (h)	Backup Heat Runtime (h)	AHU Fan Runtime (h)	AC COP (-)	AC SHR (-)	AC Energy (MJ)	Htg Energy (MJ)	AHU Fan Energy (MJ)	TOTAL ENERGY (MJ)	Total Costs	Relative Energy
0 % & No thermal	15	711	2,902	216.9	3,613.5	4.5	0.838	4,670	36,410	6,098	47,909	$1,437	69%
0 % Leak	13	822	3,258	443.5	4,079.8	4.4	0.856	5,407	47,766	6,885	60,789	$1,824	88%
10 % Leak	13	897	3,432	612.5	4,328.9	4.5	0.846	5,912	55,105	7,305	69,053	$2,072	100%
20 % Leak	15	973	3,577	802.2	4,550.0	4.5	0.839	6,421	62,936	7,678	77,767	$2,333	113%
30 % Leak	27	1,050	3,698	1,009.5	4,748.5	4.6	0.833	6,937	71,179	8,013	86,861	$2,606	126%
40 % Leak	48	1,127	3,816	1,234.7	4,942.6	4.6	0.829	7,444	80,060	8,341	96,576	$2,897	140%
50 % Leak	89	1,207	3,946	1,483.7	5,152.5	4.7	0.825	7,964	89,955	8,695	107,345	$3,220	155%

Note: All simulation cases account for thermal losses along with leakage losses except the case denoted '0 % & No thermal'.

55

Table 5.10. Effect of duct leakage on annual energy use for a slab-on-grade house at lowered cooling set point by 1.1 °C (2.0 °F)

Houston	Hours Above 55 % RH	AC Runtime (h)	Htg Runtime (h)	Backup Heat Runtime (h)	AHU Fan Runtime (h)	AC COP (-)	AC SHR (-)	AC Energy (MJ)	Htg Energy (MJ)	AHU Fan Energy (MJ)	TOTAL ENERGY (MJ)	Total Costs	Relative Energy
0 % & No thermal	1,186	1,929	610	0.3	2,539.6	4.2	0.801	15,943	6,870	5,143	28,687	$677	79%
0 % Leak	988	2,220	710	2.1	2,930.4	4.2	0.822	18,386	8,042	5,934	33,093	$781	91%
10 % Leak	1,035	2,451	777	5.1	3,227.6	4.3	0.792	20,333	8,844	6,536	36,445	$861	100%
20 % Leak	1,213	2,663	845	9.5	3,508.7	4.4	0.772	22,105	9,724	7,105	39,666	$937	109%
30 % Leak	1,867	2,858	915	18.0	3,773.2	4.5	0.757	23,717	10,759	7,641	42,848	$1,012	118%
40 % Leak	2,851	3,051	989	36.0	4,040.3	4.5	0.746	25,288	12,191	8,182	46,392	$1,095	127%
50 % Leak	3,336	3,237	1,069	63.5	4,306.1	4.6	0.736	26,785	14,046	8,720	50,283	$1,187	138%

Las Vegas	Hours Above 55 % RH	AC Runtime (h)	Htg Runtime (h)	Backup Heat Runtime (h)	AHU Fan Runtime (h)	AC COP (-)	AC SHR (-)	AC Energy (MJ)	Htg Energy (MJ)	AHU Fan Energy (MJ)	TOTAL ENERGY (MJ)	Total Costs	Relative Energy
0 % & No thermal	-	1,788	684	0.3	2,472.5	3.7	1.000	18,346	8,965	5,840	33,883	$1,186	78%
0 % Leak	-	2,114	805	0.3	2,918.3	3.7	1.000	21,779	10,517	6,893	39,920	$1,397	92%
10 % Leak	-	2,280	884	0.3	3,164.2	3.7	0.999	23,494	11,496	7,474	43,196	$1,512	100%
20 % Leak	-	2,444	973	1.2	3,416.7	3.8	0.998	25,155	12,625	8,070	46,581	$1,630	108%
30 % Leak	-	2,603	1,079	3.7	3,681.6	3.8	0.997	26,742	14,031	8,696	50,201	$1,757	116%
40 % Leak	-	2,760	1,198	8.8	3,957.3	3.9	0.996	28,275	15,712	9,347	54,067	$1,892	125%
50 % Leak	-	2,917	1,323	22.6	4,239.9	3.9	0.995	29,786	17,787	10,015	58,319	$2,041	135%

Washington, DC	Hours Above 55 % RH	AC Runtime (h)	Htg Runtime (h)	Backup Heat Runtime (h)	AHU Fan Runtime (h)	AC COP (-)	AC SHR (-)	AC Energy (MJ)	Htg Energy (MJ)	AHU Fan Energy (MJ)	TOTAL ENERGY (MJ)	Total Costs	Relative Energy
0 % & No thermal	157	1,171	1,554	13.0	2,725.8	4.4	0.813	7,717	15,317	4,600	28,365	$1,111	74%
0 % Leak	65	1,364	1,831	54.2	3,195.0	4.4	0.835	9,008	19,345	5,392	34,477	$1,350	89%
10 % Leak	158	1,499	2,001	89.0	3,500.4	4.5	0.818	9,918	22,035	5,907	38,592	$1,512	100%
20 % Leak	301	1,632	2,170	134.5	3,802.2	4.5	0.806	10,802	25,092	6,416	43,042	$1,686	112%
30 % Leak	563	1,758	2,331	192.6	4,089.5	4.6	0.797	11,632	28,528	6,901	47,793	$1,872	124%
40 % Leak	1,015	1,883	2,500	270.1	4,383.0	4.6	0.791	12,442	32,734	7,396	53,304	$2,088	138%
50 % Leak	1,311	2,008	2,647	382.6	4,654.5	4.7	0.785	13,246	38,021	7,854	59,853	$2,344	155%

Chicago	Hours Above 55 % RH	AC Runtime (h)	Htg Runtime (h)	Backup Heat Runtime (h)	AHU Fan Runtime (h)	AC COP (-)	AC SHR (-)	AC Energy (MJ)	Htg Energy (MJ)	AHU Fan Energy (MJ)	TOTAL ENERGY (MJ)	Total Costs	Relative Energy
0 % & No thermal	182	1,002	2,303	69.9	3,304.9	4.4	0.828	6,521	24,884	5,577	37,714	$1,341	71%
0 % Leak	173	1,159	2,657	187.4	3,815.3	4.4	0.847	7,554	32,354	6,438	47,078	$1,674	88%
10 % Leak	176	1,267	2,849	281.2	4,115.8	4.5	0.833	8,277	37,266	6,945	53,220	$1,892	100%
20 % Leak	175	1,375	3,024	394.4	4,398.2	4.5	0.823	8,994	42,715	7,422	59,863	$2,128	112%
30 % Leak	246	1,483	3,169	533.5	4,651.8	4.6	0.815	9,705	48,830	7,850	67,117	$2,386	126%
40 % Leak	365	1,591	3,311	697.0	4,901.8	4.6	0.809	10,407	55,823	8,272	75,233	$2,675	141%
50 % Leak	498	1,699	3,438	901.3	5,136.4	4.7	0.803	11,098	64,171	8,668	84,668	$3,010	159%

Minneapolis	Hours Above 55 % RH	AC Runtime (h)	Htg Runtime (h)	Backup Heat Runtime (h)	AHU Fan Runtime (h)	AC COP (-)	AC SHR (-)	AC Energy (MJ)	Htg Energy (MJ)	AHU Fan Energy (MJ)	TOTAL ENERGY (MJ)	Total Costs	Relative Energy
0 % & No thermal	8	884	2,919	216.9	3,802.3	4.4	0.845	5,730	36,561	6,416	49,439	$1,483	70%
0 % Leak	4	1,021	3,276	443.2	4,297.0	4.4	0.864	6,627	47,932	7,251	62,541	$1,876	88%
10 % Leak	6	1,114	3,449	612.5	4,563.3	4.5	0.852	7,251	55,263	7,701	70,946	$2,128	100%
20 % Leak	7	1,209	3,598	802.2	4,807.8	4.5	0.843	7,883	63,128	8,113	79,855	$2,396	113%
30 % Leak	8	1,304	3,724	1,009.6	5,028.1	4.6	0.831	8,501	71,417	8,485	89,134	$2,674	126%
40 % Leak	48	1,399	3,845	1,234.7	5,244.2	4.6	0.831	9,116	80,330	8,850	99,027	$2,971	140%
50 % Leak	129	1,497	3,979	1,484.0	5,476.5	4.7	0.826	9,745	90,267	9,242	109,985	$3,300	155%

Figures 5.3 and 5.4 present the number of hours above 55 % relative humidity and relative energy use, respectively, for a slab-on-grade house in Houston with different duct leak rates at the three studied thermostat set point temperatures. The energy use is related to that of a house with 10 % leak rate (assumed as a representative of no-fault duct installation) at the default thermostat set point (Table 5.9). At a leak rate greater than 20 %, the heat pump was unable to lower the number of hours above 55 %

relative humidity although the amount of moisture in the air was lowered and a lower indoor air temperature improved indoor thermal comfort to some degree. For the house with a 40 % duct leakage, the energy use is predicted to be 47 % and 97 % higher than for the reference house if the set point temperature is lowered by 1.1 °C and 2.2 °C, respectively (Figure 5.4).

The results contained in Table 5.12 (derived from Tables 5.10 and 5.11) present a change in the annual energy use for the baseline houses due to lowering the cooling set point. For Las Vegas, Washington, Chicago, and Minneapolis, the change in energy use is the same for the slab-on-grade house and the house with a basement. The use of energy increased by the same percentage for a slab-on-grade house and a house with a basement located in the same climate. As expected, the effect of lowering the set point temperature was small on the total energy use in houses located in heating dominated climates.

Table 5.11. Effect of duct leakage on annual energy use for a slab-on-grade house in Houston at lowered cooling set point by 2.2 °C (4.0 °F)

Houston	Hours Above 55 % RH	AC Runtime (h)	Htg Runtime (h)	Backup Heat Runtime (h)	AHU Fan Runtime (h)	AC COP (-)	AC SHR (-)	AC Energy (MJ)	Htg Energy (MJ)	AHU Fan Energy (MJ)	TOTAL ENERGY (MJ)	Total Costs	Relative Energy
0 % & No thermal	536	2,759	995	0.3	3,511.5	4.3	0.841	22,498	11,221	7,602	42,053	$993	82%
0 % Leak	389	3,106	1,116	2.3	3,948.8	4.3	0.855	25,383	12,592	8,550	47,256	$1,116	93%
10 % Leak	435	3,376	1,193	5.3	4,276.4	4.4	0.825	27,602	13,468	9,253	51,054	$1,205	100%
20 % Leak	737	3,627	1,280	9.7	4,601.1	4.4	0.803	29,645	14,516	9,936	54,829	$1,295	107%
30 % Leak	1,889	3,842	1,352	18.0	4,895.4	4.5	0.786	31,384	15,547	10,519	58,182	$1,374	114%
40 % Leak	2,685	4,054	1,438	35.3	5,194.0	4.5	0.772	33,084	17,064	11,122	62,002	$1,464	121%
50 % Leak	3,197	4,250	1,517	61.9	5,475.9	4.6	0.760	34,637	18,858	11,677	65,904	$1,556	129%
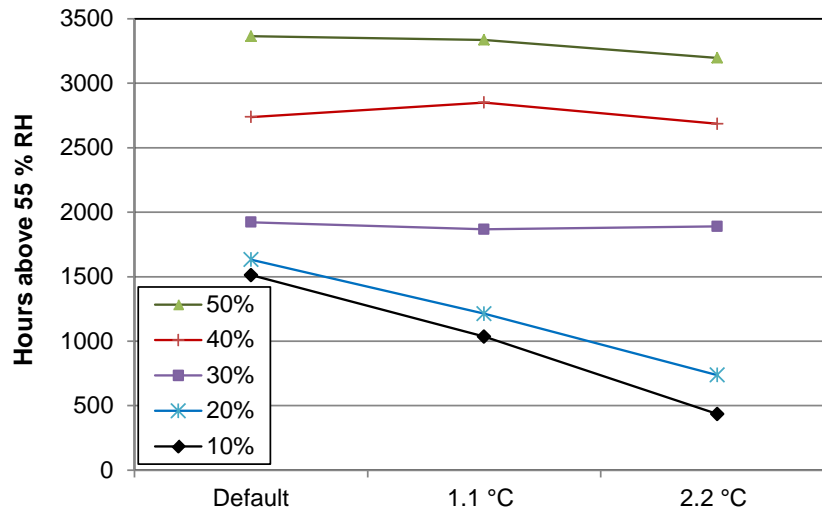
Figure 5.3. Number of hours above 55 % relative humidity for a slab-on-grade house in Houston with duct leak rates from 10 % to 50 % at three thermostat set point temperatures

57
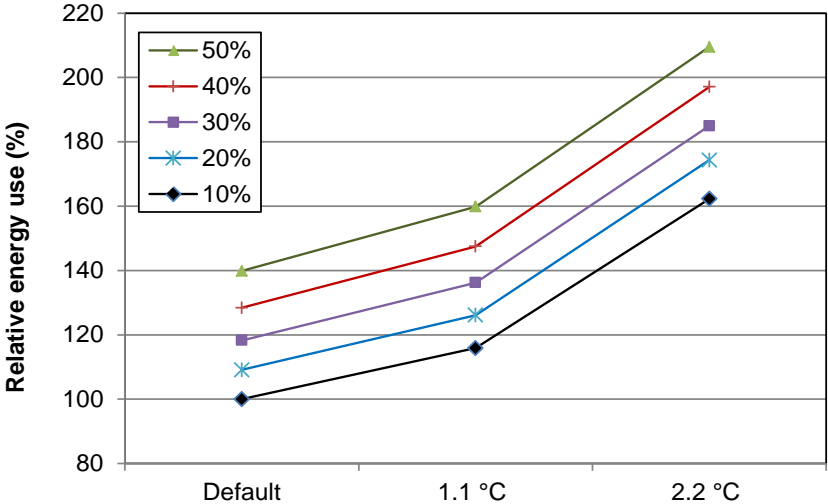
Figure 5.4. . Energy use for a slab-on-grade house in Houston with duct leak rates from 10 % to 50 % at three thermostat set point temperatures related to energy use for the house at the default set point and 10 % leak rate (shown in Table 5.9)

Table 5.12. Effect of lowering cooling set point by 1.1 °C (2.0 °F) on annual energy use of a baseline slab-on-grade house and a house with basement

Slab-on-grade house		Hours Above 55 % RH	Space Temp Max (C)	AC Runtime (h)	Htg Runtime (h)	Backup Heat Runtime (h)	AHU Fan Runtime (h)	AC COP (-)	AC SHR (-)	AC Energy (MJ)	Htg Energy (MJ)	AHU Fan Energy (MJ)	TOTAL ENERGY (MJ)	Total Costs	Relative Energy	Cooling Energy
Houston	Normal Set Pt	1,512	26.6	1,981	749	5.1	2,730.5	4.3	0.785	16,660	8,537	5,529	31,457	$743	100%	100%
	Lower Set Pt	1,035	26.1	2,451	777	5.1	3,227.6	4.3	0.792	20,333	8,844	6,536	36,445	$861	116%	122%
Las Vegas	Normal Set Pt	-	27.0	1,966	865	0.3	2,831.1	3.7	0.999	20,531	11,251	6,687	39,200	$1,372	100%	100%
	Lower Set Pt	-	26.6	2,280	884	0.3	3,164.2	3.7	0.999	23,494	11,496	7,474	43,196	$1,512	110%	114%
Washington, DC	Normal Set Pt	253	25.1	1,207	1,971	89.0	3,178.0	4.5	0.809	8,098	21,759	5,363	35,952	$1,408	100%	100%
	Lower Set Pt	158	24.4	1,499	2,001	89.0	3,500.4	4.5	0.818	9,918	22,035	5,907	38,592	$1,512	107%	122%
Chicago	Normal Set Pt	189	25.0	1,031	2,833	281.2	3,863.9	4.5	0.827	6,816	37,118	6,520	51,186	$1,820	100%	100%
	lower Set Pt	176	24.4	1,267	2,849	281.2	4,115.8	4.5	0.833	8,277	37,266	6,945	53,220	$1,892	104%	121%
Minneapolis	Normal Set Pt	13	25.2	897	3,432	612.5	4,328.9	4.5	0.846	5,912	55,105	7,305	69,053	$2,072	100%	100%
	lower Set Pt	6	24.5	1,114	3,449	612.5	4,563.3	4.5	0.852	7,251	55,263	7,701	70,946	$2,128	103%	123%

House with basement		Hours Above 55 % RH	Space Temp Max (C)	AC Runtime (h)	Htg Runtime (h)	Backup Heat Runtime (h)	AHU Fan Runtime (h)	AC COP (-)	AC SHR (-)	AC Energy (MJ)	Htg Energy (MJ)	AHU Fan Energy (MJ)	TOTAL ENERGY (MJ)	Total Costs	Relative Energy	Cooling Energy
Las Vegas	Normal Set Pt	-	25.3	1,552	718	0.3	2,269.9	3.7	1.000	16,107	9,407	5,362	31,607	$1,106	100%	100%
	Lower Set Pt	-	24.2	1,809	731	0.3	2,539.6	3.7	1.000	18,571	9,573	5,999	34,874	$1,221	110%	115%
Washington, DC	Normal Set Pt	654	24.0	742	1,907	27.0	2,649.5	4.4	0.775	5,008	19,120	4,471	29,330	$1,149	100%	100%
	Lower Set Pt	306	23.0	976	1,925	27.0	2,900.5	4.4	0.793	6,484	19,284	4,895	31,394	$1,230	107%	129%
Chicago	Normal Set Pt	289	24.0	631	2,785	129.8	3,416.1	4.4	0.797	4,198	31,565	5,765	42,259	$1,503	100%	100%
	lower Set Pt	160	23.0	826	2,796	129.7	3,621.3	4.4	0.810	5,419	31,661	6,111	43,923	$1,562	104%	129%
Minneapolis	Normal Set Pt	61	24.0	515	3,424	354.2	3,939.8	4.4	0.810	3,428	46,239	6,648	57,048	$1,711	100%	100%
	lower Set Pt	43	23.0	689	3,434	354.2	4,123.5	4.4	0.824	4,520	46,328	6,958	58,538	$1,756	103%	132%

5.2.4 Effect of Indoor Coil Airflow

This fault covers the case where a heat pump properly sized for the building load operates with improperly sized ductwork. As a result, the indoor coil airflow is not nominal. The effect of improper airflow in the cooling mode was determined using the baseline performance maps for the air conditioner used in a past study because they were shown to be very close to the correlations derived from NIST lab testing (Section 3.2.1). The impact of indoor airflow on heat pump performance in the heating mode was not considered in the heat pump baseline performance maps, therefore, the NIST correlations were used to determine this impact. The simulated indoor airflows, ranging from -36 % to +28 % of the nominal flow corresponded to external static pressures of (177, 171, 168, 165, and 149) Pa ((0.71, 0.69, 0.67, 0.66, 0.60) inch H_2O), respectively.

Reduced airflow results in an increase in energy consumption, and this effect is similar for all houses in all climates studied (Tables 5.13 and 5.14). Figure 5.5, generated for slab-on-grade houses, also provides a good representation of simulation results for houses with a basement. For the lowest airflow, 36 % below the nominal value, the energy use increased from 11 % to 14 %.
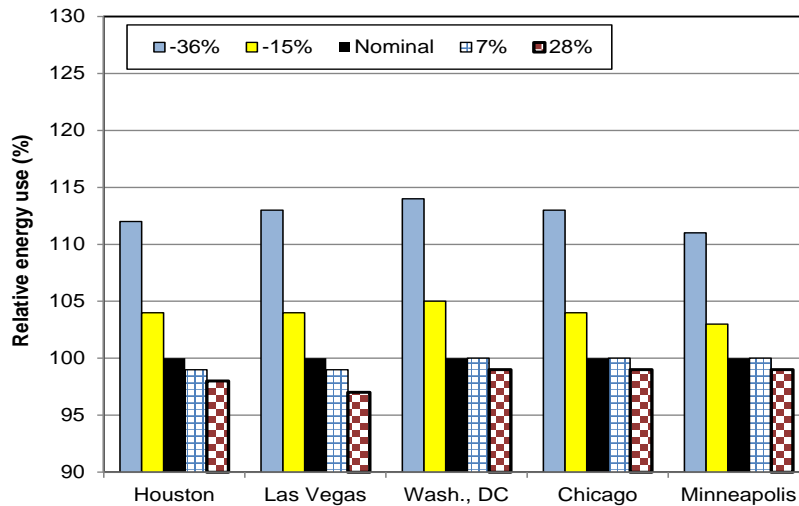
Figure 5.5. Annual energy use for slab-on-grade houses for different indoor coil airflows relative to energy use for the house in the same location with nominal airflow rate

In the cooling mode, reducing the airflow below the nominal value of 181.1 $m^3 \cdot h^{-1} \cdot kW^{-1}$ (375 cfm/ton) causes a decrease in the indoor coil temperature and provides better humidity control, but results in higher energy use because the sensible capacity is reduced and running time increased. Conversely, providing more airflow hurts humidity control in the house but decreases energy use. The efficiency of the system goes up, and more importantly, the latent removal decreases so energy use decreases. To account for a possible scenario where the homeowner lowers the temperature setting on the thermostat in an effort to make the indoor environment more comfortable, Tables 5.15 and 5.16 provide simulation results for both houses for cases where the thermostat set point is reduced 1.1 °C (2.0 °F) below the 'default' values shown in Table 4.8.

Tables 5.13 and 5.15 show the energy usage penalties associated with lowering the airflow and reducing the thermostat set point to aid in humidity control. In Table 5.13 for Houston, a hot and humid climate, the slab-on-grade house spends 1183 hours above 55 % RH even with the airflow reduced by 36 %, resulting in a 12 % increase in annual energy usage (The total energy draw was 35334 MJ). Keeping the airflow at the nominal value but lowering the thermostat set point by 1.1 °C (2.0 °F), as shown in table 5.15, reduces the number of hours above 55 % RH to a comparable number of hours of 1035 while increasing the energy

Table 5.13. Effect of indoor coil airflow on annual energy use for a slab-on-grade house when operating at the default cooling set point

Houston	Hours Above 55 % RH	AC Runtime (h)	Htg Runtime (h)	Backup Heat Runtime (h)	AHU Fan Runtime (h)	AC COP (-)	AC SHR (-)	AC Energy (MJ)	Htg Energy (MJ)	AHU Fan Energy (MJ)	TOTAL ENERGY (MJ)	Total Costs	Relative Energy
-36 % flow	1,183	2,272	853	9.7	3,125.5	3.9	0.770	18,783	10,982	4,838	35,334	$834	112%
-15 % flow	1,364	2,074	785	6.6	2,858.7	4.2	0.780	17,332	9,405	5,331	32,800	$774	104%
nominal flow	1,512	1,981	749	5.1	2,730.5	4.3	0.785	16,660	8,537	5,529	31,457	$743	100%
7 % flow	1,617	1,951	743	4.9	2,693.9	4.4	0.787	16,455	8,465	5,609	31,262	$738	99%
28 % flow	2,026	1,878	726	4.7	2,603.3	4.5	0.793	16,080	8,259	5,727	30,798	$727	98%

Las Vegas	Hours Above 55 % RH	AC Runtime (h)	Htg Runtime (h)	Backup Heat Runtime (h)	AHU Fan Runtime (h)	AC COP (-)	AC SHR (-)	AC Energy (MJ)	Htg Energy (MJ)	AHU Fan Energy (MJ)	TOTAL ENERGY (MJ)	Total Costs	Relative Energy
-36 % flow	-	2,268	1,000	1.3	3,268.2	3.3	0.992	23,192	14,547	5,902	44,373	$1,553	113%
-15 % flow	-	2,057	910	0.6	2,966.6	3.6	0.998	21,369	12,396	6,454	40,951	$1,433	104%
nominal flow	-	1,966	865	0.3	2,831.1	3.7	0.999	20,531	11,251	6,687	39,200	$1,372	100%
7 % flow	-	1,933	856	0.4	2,789.0	3.8	1.000	20,232	11,126	6,775	38,865	$1,360	99%
28 % flow	-	1,866	837	0.3	2,702.4	3.9	1.000	19,667	10,875	6,936	38,211	$1,337	97%

Washington, DC	Hours Above 55 % RH	AC Runtime (h)	Htg Runtime (h)	Backup Heat Runtime (h)	AHU Fan Runtime (h)	AC COP (-)	AC SHR (-)	AC Energy (MJ)	Htg Energy (MJ)	AHU Fan Energy (MJ)	TOTAL ENERGY (MJ)	Total Costs	Relative Energy
-36 % flow	26	1,409	2,175	119.1	3,583.9	4.0	0.786	9,295	26,391	4,623	41,041	$1,607	114%
-15 % flow	153	1,271	2,042	98.0	3,312.6	4.3	0.801	8,476	23,334	5,148	37,689	$1,476	105%
nominal flow	253	1,207	1,971	89.0	3,178.0	4.5	0.809	8,098	21,759	5,363	35,952	$1,408	100%
7 % flow	305	1,184	1,959	87.0	3,143.5	4.5	0.812	7,974	21,618	5,455	35,778	$1,401	100%
28 % flow	520	1,132	1,931	83.7	3,063.8	4.6	0.821	7,738	21,376	5,617	35,463	$1,389	99%

Chicago	Hours Above 55 % RH	AC Runtime (h)	Htg Runtime (h)	Backup Heat Runtime (h)	AHU Fan Runtime (h)	AC COP (-)	AC SHR (-)	AC Energy (MJ)	Htg Energy (MJ)	AHU Fan Energy (MJ)	TOTAL ENERGY (MJ)	Total Costs	Relative Energy
-36 % flow	160	1,217	3,046	350.6	4,263.5	4.1	0.798	7,920	43,548	5,500	57,699	$2,052	113%
-15 % flow	183	1,089	2,909	301.3	3,997.4	4.4	0.816	7,159	39,221	6,212	53,323	$1,896	104%
nominal flow	189	1,031	2,833	281.2	3,863.9	4.5	0.827	6,816	37,118	6,520	51,186	$1,820	100%
7 % flow	190	1,009	2,817	277.3	3,826.5	4.6	0.831	6,695	36,913	6,640	50,980	$1,813	100%
28 % flow	216	960	2,781	270.0	3,740.4	4.6	0.844	6,462	36,577	6,858	50,628	$1,800	99%

Minneapolis	Hours Above 55 % RH	AC Runtime (h)	Htg Runtime (h)	Backup Heat Runtime (h)	AHU Fan Runtime (h)	AC COP (-)	AC SHR (-)	AC Energy (MJ)	Htg Energy (MJ)	AHU Fan Energy (MJ)	TOTAL ENERGY (MJ)	Total Costs	Relative Energy
-36 % flow	3	1,066	3,613	727.2	4,679.7	4.1	0.813	6,917	62,805	6,037	76,491	$2,295	111%
-15 % flow	9	950	3,496	646.3	4,446.1	4.4	0.834	6,225	57,542	6,909	71,408	$2,142	103%
nominal flow	13	897	3,432	612.5	4,328.9	4.5	0.846	5,912	55,105	7,305	69,053	$2,072	100%
7 % flow	15	878	3,418	606.3	4,295.6	4.6	0.851	5,803	54,874	7,454	68,863	$2,066	100%
28 % flow	27	832	3,387	592.6	4,218.8	4.6	0.866	5,581	54,499	7,735	68,546	$2,056	99%

use by 16 % (36445 MJ compared to 31457 MJ). Reduced airflow or lowered cooling set point in other climates - in which the number of hours above 55 % was small - resulted in significant energy use penalties and a small reduction of high RH hours.

Table 5.14. Effect of indoor coil airflow on annual energy use for a house with basement when operating at the default cooling set point

Las Vegas	Hours Above 55 % RH	AC Runtime (h)	Htg Runtime (h)	Backup Heat Runtime (h)	AHU Fan Runtime (h)	AC COP (-)	AC SHR (-)	AC Energy (MJ)	Htg Energy (MJ)	AHU Fan Energy (MJ)	TOTAL ENERGY (MJ)	Total Costs	Relative Energy
-36 % flow	-	1,765	805	0.3	2,569.9	3.3	0.994	18,011	11,795	4,641	35,178	$1,231	111%
-15 % flow	-	1,616	750	0.3	2,366.2	3.5	1.000	16,707	10,302	5,148	32,889	$1,151	104%
nominal flow	-	1,552	718	0.3	2,269.9	3.7	1.000	16,107	9,407	5,362	31,607	$1,106	100%
7 % flow	-	1,529	713	0.3	2,241.9	3.7	1.000	15,890	9,341	5,446	31,409	$1,099	99%
28 % flow	-	1,478	698	0.3	2,175.8	3.8	1.000	15,443	9,145	5,585	30,905	$1,082	98%

Washington, DC	Hours Above 55 % RH	AC Runtime (h)	Htg Runtime (h)	Backup Heat Runtime (h)	AHU Fan Runtime (h)	AC COP (-)	AC SHR (-)	AC Energy (MJ)	Htg Energy (MJ)	AHU Fan Energy (MJ)	TOTAL ENERGY (MJ)	Total Costs	Relative Energy
-36 % flow	245	851	2,091	39.7	2,941.7	4.0	0.746	5,661	22,995	3,795	33,183	$1,300	113%
-15 % flow	463	777	1,974	30.8	2,751.8	4.3	0.765	5,217	20,502	4,276	30,727	$1,203	105%
nominal flow	653	742	1,907	27.0	2,649.5	4.4	0.775	5,007	19,120	4,471	29,330	$1,149	100%
7 % flow	743	729	1,895	25.7	2,624.5	4.4	0.779	4,933	18,999	4,554	29,218	$1,144	100%
28 % flow	1,030	699	1,861	22.7	2,560.1	4.5	0.791	4,790	18,680	4,694	28,895	$1,132	99%

Chicago	Hours Above 55 % RH	AC Runtime (h)	Htg Runtime (h)	Backup Heat Runtime (h)	AHU Fan Runtime (h)	AC COP (-)	AC SHR (-)	AC Energy (MJ)	Htg Energy (MJ)	AHU Fan Energy (MJ)	TOTAL ENERGY (MJ)	Total Costs	Relative Energy
-36 % flow	218	729	2,992	170.2	3,721.0	4.0	0.761	4,784	37,000	4,800	47,316	$1,682	112%
-15 % flow	250	663	2,862	142.6	3,524.9	4.3	0.784	4,388	33,460	5,478	44,058	$1,567	104%
nominal flow	289	631	2,785	129.8	3,416.1	4.4	0.797	4,198	31,565	5,765	42,259	$1,503	100%
7 % flow	299	620	2,768	126.9	3,387.0	4.5	0.802	4,131	31,369	5,877	42,108	$1,497	100%
28 % flow	377	590	2,727	118.4	3,317.3	4.6	0.818	3,992	30,921	6,082	41,726	$1,484	99%

Minneapolis	Hours Above 55 % RH	AC Runtime (h)	Htg Runtime (h)	Backup Heat Runtime (h)	AHU Fan Runtime (h)	AC COP (-)	AC SHR (-)	AC Energy (MJ)	Htg Energy (MJ)	AHU Fan Energy (MJ)	TOTAL ENERGY (MJ)	Total Costs	Relative Energy
-36 % flow	49	597	3,615	428.4	4,211.9	4.0	0.770	3,921	52,744	5,433	62,829	$1,885	110%
-15 % flow	55	542	3,497	377.7	4,039.3	4.3	0.796	3,589	48,444	6,277	59,042	$1,771	103%
nominal flow	61	515	3,424	354.2	3,939.8	4.4	0.810	3,428	46,239	6,648	57,048	$1,711	100%
7 % flow	68	506	3,410	348.1	3,915.8	4.5	0.816	3,372	46,004	6,795	56,902	$1,707	100%
28 % flow	78	482	3,373	330.3	3,854.6	4.5	0.834	3,255	45,391	7,067	56,445	$1,693	99%

Table 5.15. Effect of indoor coil airflow on annual energy use for a slab-on-grade house when operating at a cooling set point that is 1.1 °C (2.0 °F) lower than the default value

Houston	Hours Above 55 % RH	AC Runtime (h)	Htg Runtime (h)	Backup Heat Runtime (h)	AHU Fan Runtime (h)	AC COP (-)	AC SHR (-)	AC Energy (MJ)	Htg Energy (MJ)	AHU Fan Energy (MJ)	TOTAL ENERGY (MJ)	Total Costs	Relative Energy
-36 % flow	572	2,789	884	9.8	3,672.5	3.9	0.779	22,733	11,373	5,685	40,522	$957	111%
-15 % flow	846	2,556	813	6.6	3,369.4	4.2	0.788	21,082	9,739	6,283	37,836	$893	104%
nominal flow	1,035	2,451	777	5.1	3,227.6	4.3	0.792	20,333	8,844	6,536	36,445	$861	100%
7 % flow	1,139	2,413	770	4.9	3,183.6	4.4	0.794	20,083	8,766	6,629	36,209	$855	99%
28 % flow	1,628	2,326	752	4.7	3,078.5	4.5	0.799	19,631	8,556	6,773	35,692	$843	98%

Las Vegas	Hours Above 55 % RH	AC Runtime (h)	Htg Runtime (h)	Backup Heat Runtime (h)	AHU Fan Runtime (h)	AC COP (-)	AC SHR (-)	AC Energy (MJ)	Htg Energy (MJ)	AHU Fan Energy (MJ)	TOTAL ENERGY (MJ)	Total Costs	Relative Energy
-36 % flow	-	2,613	1,022	1.3	3,635.2	3.4	0.991	26,339	14,874	6,565	48,509	$1,698	112%
-15 % flow	-	2,382	931	0.6	3,312.5	3.6	0.998	24,409	12,684	7,207	45,031	$1,576	104%
nominal flow	-	2,280	884	0.3	3,164.2	3.7	0.999	23,494	11,496	7,474	43,196	$1,512	100%
7 % flow	-	2,242	874	0.4	3,116.5	3.8	0.999	23,156	11,360	7,571	42,818	$1,499	99%
28 % flow	-	2,166	855	0.3	3,021.1	3.9	1.000	22,516	11,112	7,754	42,114	$1,474	97%

Washington, DC	Hours Above 55 % RH	AC Runtime (h)	Htg Runtime (h)	Backup Heat Runtime (h)	AHU Fan Runtime (h)	AC COP (-)	AC SHR (-)	AC Energy (MJ)	Htg Energy (MJ)	AHU Fan Energy (MJ)	TOTAL ENERGY (MJ)	Total Costs	Relative Energy
-36 % flow	4	1,742	2,212	119.1	3,953.8	4.0	0.798	11,319	26,773	5,100	43,923	$1,720	114%
-15 % flow	58	1,576	2,075	97.8	3,650.9	4.3	0.811	10,365	23,644	5,674	40,415	$1,583	105%
nominal flow	158	1,499	2,001	89.0	3,500.4	4.5	0.818	9,918	22,035	5,907	38,592	$1,512	100%
7 % flow	203	1,473	1,989	87.4	3,461.8	4.5	0.820	9,777	21,902	6,007	38,418	$1,505	100%
28 % flow	461	1,410	1,960	83.6	3,369.8	4.6	0.828	9,487	21,640	6,178	38,036	$1,490	99%

Chicago	Hours Above 55 % RH	AC Runtime (h)	Htg Runtime (h)	Backup Heat Runtime (h)	AHU Fan Runtime (h)	AC COP (-)	AC SHR (-)	AC Energy (MJ)	Htg Energy (MJ)	AHU Fan Energy (MJ)	TOTAL ENERGY (MJ)	Total Costs	Relative Energy
-36 % flow	131	1,490	3,067	350.6	4,556.5	4.1	0.808	9,571	43,759	5,878	59,939	$2,131	113%
-15 % flow	160	1,336	2,927	301.3	4,263.4	4.3	0.824	8,683	39,398	6,625	55,439	$1,971	104%
nominal flow	176	1,267	2,849	281.2	4,115.8	4.5	0.833	8,277	37,266	6,945	53,220	$1,892	100%
7 % flow	176	1,240	2,833	277.4	4,073.6	4.5	0.837	8,131	37,061	7,068	52,992	$1,884	100%
28 % flow	199	1,183	2,799	270.0	3,981.5	4.6	0.848	7,859	36,740	7,300	52,631	$1,871	99%

Minneapolis	Hours Above 55 % RH	AC Runtime (h)	Htg Runtime (h)	Backup Heat Runtime (h)	AHU Fan Runtime (h)	AC COP (-)	AC SHR (-)	AC Energy (MJ)	Htg Energy (MJ)	AHU Fan Energy (MJ)	TOTAL ENERGY (MJ)	Total Costs	Relative Energy
-36 % flow	-	1,318	3,636	727.0	4,954.4	4.0	0.822	8,438	63,034	6,391	78,595	$2,358	111%
-15 % flow	1	1,178	3,515	646.2	4,693.4	4.3	0.841	7,628	57,722	7,294	73,375	$2,201	103%
nominal flow	6	1,114	3,449	612.5	4,563.3	4.5	0.852	7,251	55,263	7,701	70,946	$2,128	100%
7 % flow	6	1,091	3,436	606.3	4,526.0	4.5	0.856	7,118	55,039	7,854	70,742	$2,122	100%
28 % flow	13	1,036	3,404	592.6	4,440.5	4.6	0.869	6,853	54,661	8,141	70,387	$2,112	99%

Note: Although the relative energy use shown in this table is equal or less than the values shown in Table 5.13 (baseline), the total energy use for cases presented in Table 5.15 is higher than those presented in Table 5.13.

63

Table 5.16. Effect of indoor coil airflow on annual energy use for a house with basement when operating at cooling set point that is 1.1 °C (2.0 °F) lower than the default value

Las Vegas	Hours Above 55 % RH	AC Runtime (h)	Htg Runtime (h)	Backup Heat Runtime (h)	AHU Fan Runtime (h)	AC COP (-)	AC SHR (-)	AC Energy (MJ)	Htg Energy (MJ)	AHU Fan Energy (MJ)	TOTAL ENERGY (MJ)	Total Costs	Relative Energy
-36 % flow	-	1,765	805	0.3	2,569.9	3.3	0.994	18,011	11,795	4,641	35,178	$1,231	111%
-15 % flow	-	1,616	750	0.3	2,366.2	3.5	1.000	16,707	10,302	5,148	32,889	$1,151	104%
nominal flow	-	1,552	718	0.3	2,269.9	3.7	1.000	16,107	9,407	5,362	31,607	$1,106	100%
7 % flow	-	1,529	713	0.3	2,241.9	3.7	1.000	15,890	9,341	5,446	31,409	$1,099	99%
28 % flow	-	1,478	698	0.3	2,175.8	3.8	1.000	15,443	9,145	5,585	30,905	$1,082	98%

Washington, DC	Hours Above 55 % RH	AC Runtime (h)	Htg Runtime (h)	Backup Heat Runtime (h)	AHU Fan Runtime (h)	AC COP (-)	AC SHR (-)	AC Energy (MJ)	Htg Energy (MJ)	AHU Fan Energy (MJ)	TOTAL ENERGY (MJ)	Total Costs	Relative Energy
-36 % flow	67	1,118	2,111	39.9	3,229.1	3.9	0.767	7,332	23,207	4,165	35,435	$1,388	113%
-15 % flow	184	1,021	1,993	30.8	3,013.7	4.2	0.784	6,755	20,680	4,683	32,850	$1,287	105%
nominal flow	306	976	1,925	27.0	2,900.5	4.4	0.793	6,484	19,284	4,895	31,394	$1,230	100%
7 % flow	378	959	1,913	25.7	2,871.9	4.4	0.797	6,387	19,164	4,983	31,266	$1,225	100%
28 % flow	666	918	1,878	22.7	2,796.0	4.5	0.808	6,191	18,831	5,126	30,880	$1,209	98%

Chicago	Hours Above 55 % RH	AC Runtime (h)	Htg Runtime (h)	Backup Heat Runtime (h)	AHU Fan Runtime (h)	AC COP (-)	AC SHR (-)	AC Energy (MJ)	Htg Energy (MJ)	AHU Fan Energy (MJ)	TOTAL ENERGY (MJ)	Total Costs	Relative Energy
-36 % flow	111	952	3,004	170.2	3,956.5	4.0	0.777	6,166	37,130	5,104	49,132	$1,747	112%
-15 % flow	142	867	2,872	142.6	3,738.2	4.3	0.798	5,663	33,556	5,809	45,759	$1,627	104%
nominal flow	160	826	2,796	129.7	3,621.3	4.4	0.810	5,419	31,661	6,111	43,923	$1,562	100%
7 % flow	165	811	2,777	127.2	3,588.5	4.5	0.815	5,337	31,467	6,227	43,762	$1,556	100%
28 % flow	193	774	2,738	118.5	3,511.6	4.5	0.829	5,153	31,024	6,438	43,346	$1,541	99%

Minneapolis	Hours Above 55 % RH	AC Runtime (h)	Htg Runtime (h)	Backup Heat Runtime (h)	AHU Fan Runtime (h)	AC COP (-)	AC SHR (-)	AC Energy (MJ)	Htg Energy (MJ)	AHU Fan Energy (MJ)	TOTAL ENERGY (MJ)	Total Costs	Relative Energy
-36 % flow	17	799	3,627	428.5	4,425.4	4.0	0.788	5,165	52,870	5,709	64,475	$1,934	110%
-15 % flow	31	726	3,508	377.7	4,233.4	4.2	0.811	4,735	48,549	6,579	60,595	$1,818	104%
nominal flow	43	689	3,434	354.2	4,123.5	4.4	0.824	4,520	46,328	6,958	58,538	$1,756	100%
7 % flow	46	677	3,421	347.9	4,097.9	4.4	0.829	4,448	46,096	7,111	58,386	$1,752	100%
28 % flow	54	644	3,383	330.3	4,027.2	4.5	0.845	4,285	45,481	7,383	57,881	$1,736	99%

Note: Although the relative energy use shown in this table is equal or less than the values shown in Table 5.14 (baseline), the total energy use for cases presented in Table 5.16 is higher than those presented in Table 5.14.

5.2.5 Effect of Refrigerant Undercharge

When the amount of refrigerant charge in the TXV-controlled system is below the nominal value, the performance of the unit is degraded. Tables 5.17 and 5.18 show the results for the slab-on-grade house and the basement house, respectively. Figure 5.6 shows the relative energy use for the slab-on-grade house, which provides a good representation of the energy use in the house with a basement as well. The figure indicates that the energy use increases exponentially with increasing refrigerant undercharge. For the 30 % refrigerant undercharge level the energy use increases by as much as (17 ~ 23) %. The moisture removal capacity of the unit is also degraded when the unit is undercharged.

Table 5.17. Effect of refrigerant undercharge on annual energy use for a slab-on-grade house

	Under Charge	Hours Above 55 % RH	AC Runtime (h)	Htg Runtime (h)	Backup Heat Runtime (h)	AHU Fan Runtime (h)	AC COP (-)	AC SHR (-)	AC Energy (MJ)	Htg Energy (MJ)	AHU Fan Energy (MJ)	TOTAL ENERGY (MJ)	Total Costs	Relative Energy
Houston	0 %	1,512	1,981	749	5.1	2,730.5	4.3	0.785	16,660	8,537	5,529	31,457	$743	100%
	-10 %	1,581	2,052	778	5.8	2,830.4	4.2	0.787	17,098	8,787	5,731	32,348	$764	103%
	-20 %	1,676	2,176	855	8.5	3,031.2	4.0	0.789	17,901	9,562	6,138	34,333	$811	109%
	-30 %	1,811	2,366	1,000	20.2	3,366.3	3.8	0.792	19,131	11,284	6,817	37,963	$896	121%
Las Vegas	0 %	-	1,966	865	0.3	2,831.1	3.7	0.999	20,531	11,251	6,687	39,200	$1,372	100%
	-10 %	-	2,044	900	0.4	2,944.4	3.6	1.000	21,109	11,573	6,955	40,369	$1,413	103%
	-20 %	-	2,177	1,000	1.0	3,176.8	3.5	1.000	22,133	12,652	7,504	43,021	$1,506	110%
	-30 %	-	2,379	1,199	3.7	3,578.0	3.2	1.000	23,671	14,919	8,451	47,773	$1,672	122%
Washington, DC	0 %	253	1,207	1,971	89.0	3,178.0	4.5	0.809	8,098	21,759	5,363	35,952	$1,408	100%
	-10 %	281	1,246	2,020	91.5	3,266.2	4.4	0.811	8,304	22,133	5,512	36,680	$1,437	102%
	-20 %	312	1,317	2,168	109.9	3,485.6	4.2	0.815	8,690	23,868	5,882	39,172	$1,534	109%
	-30 %	382	1,433	2,450	154.3	3,882.8	3.9	0.819	9,319	27,533	6,552	44,135	$1,729	123%
Chicago	0 %	189	1,031	2,833	281.2	3,863.9	4.5	0.827	6,816	37,118	6,520	51,186	$1,820	100%
	-10 %	189	1,063	2,886	286.2	3,948.6	4.4	0.830	6,984	37,586	6,663	51,964	$1,848	102%
	-20 %	193	1,123	3,035	327.6	4,158.4	4.2	0.834	7,311	40,065	7,017	55,125	$1,960	108%
	-30 %	188	1,221	3,281	433.9	4,502.1	3.9	0.841	7,842	45,504	7,597	61,674	$2,193	120%
Minneapolis	0 %	13	897	3,432	612.5	4,328.9	4.5	0.846	5,912	55,105	7,305	69,053	$2,072	100%
	-10 %	15	925	3,475	621.3	4,400.0	4.4	0.850	6,056	55,608	7,425	69,821	$2,095	101%
	-20 %	15	977	3,604	687.0	4,581.0	4.2	0.855	6,342	58,734	7,730	73,538	$2,206	106%
	-30 %	15	1,062	3,804	839.1	4,866.2	3.9	0.862	6,802	65,356	8,212	81,101	$2,433	117%

Table 5.18. Effect of refrigerant undercharge on annual energy use for a house with basement

|	Under Charge	Hours Above 55 % RH	AC Runtime (h)	Htg Runtime (h)	Backup Heat Runtime (h)	AHU Fan Runtime (h)	AC COP (-)	AC SHR (-)	AC Energy (MJ)	Htg Energy (MJ)	AHU Fan Energy (MJ)	TOTAL ENERGY (MJ)	Total Costs	Relative Energy
Las Vegas	0 %	-	1,552	718	0.3	2,269.9	3.7	1.000	16,107	9,407	5,362	31,607	$1,106	100%
	-10 %	-	1,606	745	0.3	2,350.5	3.6	1.000	16,512	9,651	5,552	32,448	$1,136	103%
	-20 %	-	1,703	817	0.3	2,520.0	3.4	1.000	17,302	10,405	5,952	34,391	$1,204	109%
	-30 %	-	1,861	966	0.3	2,827.1	3.2	1.000	18,620	12,013	6,678	38,042	$1,331	120%
Washington, DC	0 %	654	742	1,907	27.0	2,649.5	4.4	0.775	5,008	19,120	4,471	29,330	$1,149	100%
	-10 %	694	762	1,954	27.5	2,715.9	4.3	0.777	5,111	19,412	4,583	29,838	$1,169	102%
	-20 %	755	800	2,099	35.1	2,898.9	4.1	0.780	5,321	20,749	4,892	31,693	$1,241	108%
	-30 %	851	863	2,384	55.2	3,246.7	3.8	0.785	5,673	23,624	5,479	35,508	$1,391	121%
Chicago	0 %	289	631	2,785	129.8	3,416.1	4.4	0.797	4,198	31,565	5,765	42,259	$1,503	100%
	-10 %	294	647	2,838	131.2	3,485.1	4.3	0.800	4,283	31,904	5,881	42,800	$1,522	101%
	-20 %	295	679	2,995	156.3	3,673.9	4.2	0.804	4,453	33,893	6,200	45,277	$1,610	107%
	-30 %	304	732	3,282	221.2	4,014.3	3.9	0.810	4,749	38,240	6,774	50,495	$1,795	119%
Minneapolis	0 %	61	515	3,424	354.2	3,939.8	4.4	0.810	3,428	46,239	6,648	57,048	$1,711	100%
	-10 %	65	529	3,472	357.3	4,001.0	4.3	0.813	3,497	46,578	6,752	57,559	$1,727	101%
	-20 %	68	554	3,616	403.2	4,169.8	4.1	0.818	3,636	49,132	7,036	60,536	$1,816	106%
	-30 %	69	597	3,861	518.1	4,457.6	3.9	0.825	3,871	54,824	7,522	66,950	$2,008	117%
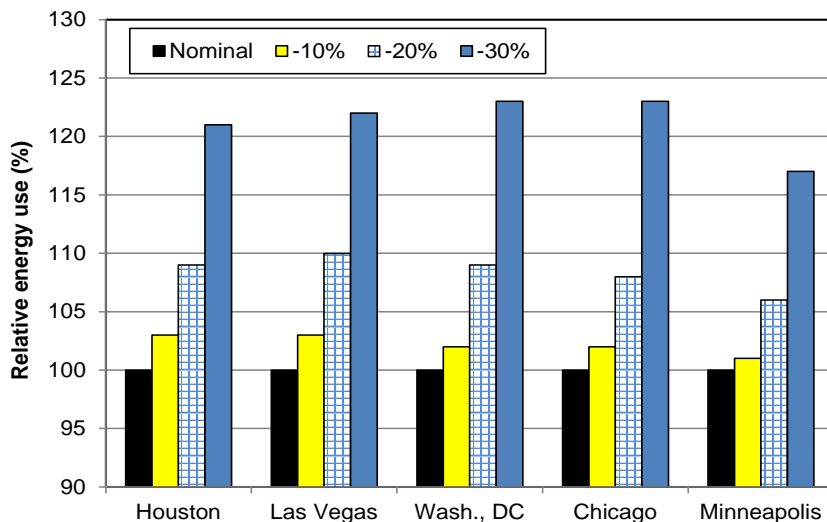
Figure 5.6. Annual energy use for slab-on-grade houses at different levels of refrigerant undercharge relative to the annual energy use for the house in the same location when the heat pump operates with the nominal refrigerant charge

65

5.2.6 Effect of Refrigerant Overcharge

When the amount of refrigerant charge in the system is above the correct (nominal) value, the performance of the unit is degraded. Table 5.19 and 5.20 show the results for the slab-on-grade house and for the basement house, respectively. The heat pump uses (10 ~ 16) % more energy when overcharged by 30 %, with somewhat higher increases in energy use occurring in localities with a significant heating season (i.e., Chicago, Washington, DC, and Minneapolis). Figure 5.7 shows the relative energy use for the slab-on-grade house, which provides a good representation of the energy use in the house with a basement as well. The moisture removal capability of the unit is not affected by the overcharge fault.

Table 5.19. Effect of refrigerant overcharge on annual energy use for a slab-on-grade house

	Over Charge	Hours Above 55 % RH	AC Runtime (h)	Htg Runtime (h)	Backup Heat Runtime (h)	AHU Fan Runtime (h)	AC COP (-)	AC SHR (-)	AC Energy (MJ)	Htg Energy (MJ)	AHU Fan Energy (MJ)	TOTAL ENERGY (MJ)	Total Costs	Relative Energy
Houston	0 %	1,512	1,981	749	5.1	2,730.5	4.3	0.785	16,660	8,537	5,529	31,457	$743	100%
	10 %	1,553	1,955	764	5.8	2,718.5	4.3	0.786	16,743	8,912	5,505	31,891	$753	101%
	20 %	1,572	1,937	778	6.5	2,714.9	4.2	0.787	17,006	9,616	5,498	32,851	$776	104%
	30 %	1,547	1,932	796	7.3	2,728.4	4.1	0.786	17,486	10,736	5,525	34,478	$814	110%
Las Vegas	0 %	-	1,966	865	0.3	2,831.1	3.7	0.999	20,531	11,251	6,687	39,200	$1,372	100%
	10 %	-	1,945	884	0.4	2,828.3	3.7	0.999	20,689	11,742	6,681	39,843	$1,394	102%
	20 %	-	1,929	904	0.6	2,833.4	3.6	0.999	21,042	12,711	6,693	41,178	$1,441	105%
	30 %	-	1,919	925	0.7	2,843.8	3.5	0.999	21,577	14,180	6,717	43,206	$1,512	110%
Washington, DC	0 %	253	1,207	1,971	89.0	3,178.0	4.5	0.809	8,098	21,759	5,363	35,952	$1,408	100%
	10 %	277	1,191	2,004	94.3	3,194.7	4.4	0.810	8,144	22,476	5,391	36,744	$1,439	102%
	20 %	281	1,183	2,037	100.6	3,220.6	4.3	0.811	8,296	23,977	5,435	38,439	$1,506	107%
	30 %	264	1,181	2,074	106.4	3,255.3	4.2	0.809	8,544	26,260	5,493	41,029	$1,607	114%
Chicago	0 %	189	1,031	2,833	281.2	3,863.9	4.5	0.827	6,520	37,118	6,520	51,186	$1,820	100%
	10 %	190	1,016	2,871	293.4	3,887.7	4.5	0.828	6,849	38,136	6,561	52,277	$1,859	102%
	20 %	191	1,009	2,904	308.1	3,913.7	4.4	0.829	6,976	40,241	6,604	54,552	$1,940	107%
	30 %	189	1,008	2,945	321.4	3,953.0	4.3	0.827	7,188	43,466	6,671	58,056	$2,064	113%
Minneapolis	0 %	13	897	3,432	612.5	4,328.9	4.5	0.846	5,912	55,105	7,305	69,053	$2,072	100%
	10 %	15	885	3,465	633.6	4,350.4	4.5	0.848	5,945	56,322	7,341	70,339	$2,110	102%
	20 %	15	879	3,494	656.0	4,372.9	4.4	0.848	6,053	58,820	7,379	72,984	$2,190	106%
	30 %	13	878	3,528	678.6	4,405.8	4.3	0.847	6,236	62,694	7,435	77,096	$2,313	112%

Table 5.20. Effect of refrigerant overcharge on annual energy use for a house with basement

|	Over Charge	Hours Above 55 % RH	AC Runtime (h)	Htg Runtime (h)	Backup Heat Runtime (h)	AHU Fan Runtime (h)	AC COP (-)	AC SHR (-)	AC Energy (MJ)	Htg Energy (MJ)	AHU Fan Energy (MJ)	TOTAL ENERGY (MJ)	Total Costs	Relative Energy
Las Vegas	0 %	-	1,552	718	0.3	2,269.9	3.7	1.000	16,107	9,407	5,362	31,607	$1,106	100%
	10 %	-	1,538	733	0.3	2,270.4	3.6	1.000	16,261	9,814	5,363	32,170	$1,126	102%
	20 %	-	1,527	747	0.3	2,274.2	3.6	1.000	16,565	10,587	5,372	33,256	$1,164	105%
	30 %	-	1,521	763	0.3	2,283.8	3.5	1.000	17,021	11,782	5,394	34,929	$1,223	111%
Washington, DC	0 %	654	742	1,907	27.0	2,649.5	4.4	0.775	5,008	19,120	4,471	29,330	$1,149	100%
	10 %	695	734	1,940	28.9	2,674.8	4.3	0.776	5,050	19,735	4,514	30,031	$1,176	102%
	20 %	695	730	1,972	32.5	2,702.7	4.3	0.776	5,154	21,110	4,561	31,557	$1,236	108%
	30 %	658	730	2,009	35.0	2,739.6	4.1	0.775	5,317	23,264	4,623	33,936	$1,329	116%
Chicago	0 %	289	631	2,785	129.8	3,416.1	4.4	0.797	4,198	31,565	5,765	42,259	$1,503	100%
	10 %	295	624	2,823	138.0	3,447.7	4.4	0.799	4,234	32,451	5,818	43,234	$1,537	102%
	20 %	294	621	2,862	146.8	3,482.6	4.3	0.798	4,319	34,408	5,877	45,335	$1,612	107%
	30 %	285	621	2,902	156.0	3,523.1	4.2	0.797	4,457	37,502	5,945	48,636	$1,729	115%
Minneapolis	0 %	61	515	3,424	354.2	3,939.8	4.4	0.810	3,428	46,239	6,648	57,048	$1,711	100%
	10 %	65	510	3,462	369.4	3,971.6	4.4	0.812	3,456	47,300	6,702	58,190	$1,746	102%
	20 %	65	507	3,497	385.6	4,004.3	4.3	0.812	3,528	49,673	6,757	60,690	$1,821	106%
	30 %	62	507	3,534	402.7	4,040.4	4.2	0.810	3,640	53,431	6,818	64,621	$1,939	113%
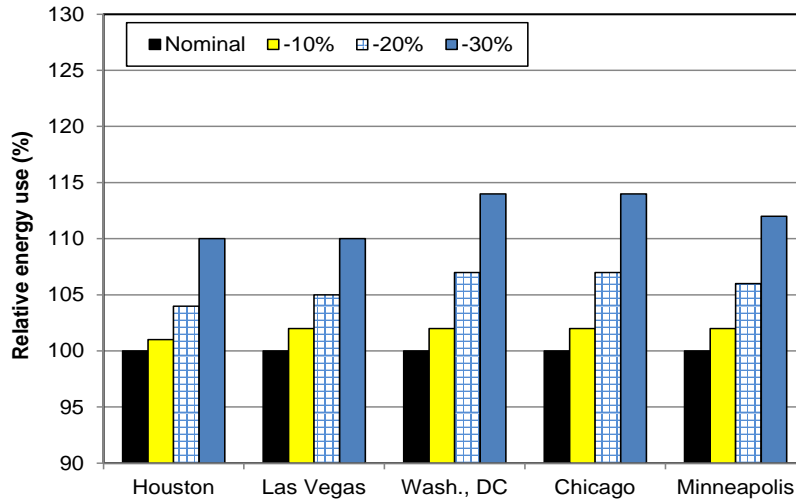
Figure 5.7. Annual energy use for slab-on-grade houses at different levels of refrigerant overcharge relative to the annual energy use for the house in the same location when the heat pump operates with the nominal refrigerant charge

5.2.7 Effect of Excessive Refrigerant Subcooling

The level of this fault was determined by an increase of refrigerant subcooling at the TXV inlet at the operating condition defined by the AHRI Standard 210/240 test-A (AHRI, 2008). Refrigerant subcooling is indicative of refrigerant charge in a TXV-equipped system, and excessive subcooling is equivalent to the fault of refrigerant overcharge. When the amount of subcooling at the TXV inlet is increased the cooling system performance is degraded. Table 5.21 shows the results for the slab-on-grade house, and Table 5.22 shows the results for the basement house. Figure 5.8 shows the relative energy use for the slab-on-grade house, which provides a good representation of the energy use in the house with a basement as well. In general, increasing subcooling increases the capacity of the unit but degrades its efficiency. Both the cooling and heating energy use increased by about 20 % at the maximum fault level (200 %, i.e., an increase of subcooling from 4.4 °C (8.0 °F) to 13.2 °C (24.0 °F)). We may note that a 100 % increase in subcooling corresponds approximately to the 20 % overcharge fault discussed in Section 5.2.6.

Table 5.21. Effect of excessive refrigerant subcooling on annual energy use for a slab-on-grade house

	Excessive Sub-Cooling	Hours Above 55 % RH	AC Runtime (h)	Htg Runtime (h)	Backup Heat Runtime (h)	AHU Fan Runtime (h)	AC COP (-)	AC SHR (-)	AC Energy (MJ)	Htg Energy (MJ)	AHU Fan Energy (MJ)	TOTAL ENERGY (MJ)	Total Costs	Relative Energy
Houston	0 %	1,512	1,981	749	5.1	2,730.5	4.3	0.785	16,660	8,537	5,529	31,457	$743	100%
	100 %	1,432	1,964	735	4.9	2,699.3	4.1	0.782	17,560	9,496	5,466	33,253	$785	106%
	200 %	1,483	1,976	710	4.5	2,686.0	3.5	0.786	20,480	10,377	5,439	37,028	$874	118%
Las Vegas	0 %	-	1,966	865	0.3	2,831.1	3.7	0.999	20,531	11,251	6,687	39,200	$1,372	100%
	100 %	-	1,950	848	0.4	2,797.3	3.6	0.998	21,599	12,522	6,607	41,460	$1,451	106%
	200 %	-	1,971	818	0.3	2,789.5	3.0	1.000	25,241	13,716	6,589	46,277	$1,620	118%
Washington, DC	0 %	253	1,207	1,971	89.0	3,178.0	4.5	0.809	8,098	21,759	5,363	35,952	$1,408	100%
	100 %	194	1,199	1,954	90.1	3,153.1	4.3	0.803	8,565	24,299	5,321	38,916	$1,524	108%
	200 %	223	1,208	1,912	88.8	3,119.5	3.6	0.807	10,023	26,696	5,264	42,714	$1,673	119%
Chicago	0 %	189	1,031	2,833	281.2	3,863.9	4.5	0.827	6,816	37,118	6,520	51,186	$1,820	100%
	100 %	180	1,024	2,812	286.4	3,836.3	4.3	0.820	7,217	41,052	6,474	55,475	$1,972	108%
	200 %	183	1,031	2,769	282.3	3,799.9	3.7	0.824	8,446	44,775	6,412	60,365	$2,146	118%
Minneapolis	0 %	13	897	3,432	612.5	4,328.9	4.5	0.846	5,912	55,105	7,305	69,053	$2,072	100%
	100 %	11	892	3,416	620.7	4,308.1	4.3	0.839	6,266	60,185	7,270	74,453	$2,234	108%
	200 %	12	898	3,375	614.9	4,272.7	3.6	0.843	7,332	64,959	7,210	80,233	$2,407	116%

Note: Subcooling of 4.4 °C (8.0 °F) was used as a no-fault condition.

Table 5.22. Effect of excessive refrigerant subcooling on annual energy use for a house with basement

	Excessive Sub-Cooling	Hours Above 55 % RH	AC Runtime (h)	Htg Runtime (h)	Backup Heat Runtime (h)	AHU Fan Runtime (h)	AC COP (-)	AC SHR (-)	AC Energy (MJ)	Htg Energy (MJ)	AHU Fan Energy (MJ)	TOTAL ENERGY (MJ)	Total Costs	Relative Energy
Las Vegas	0 %	-	1,552	718	0.3	2,269.9	3.7	1.000	16,107	9,407	5,362	31,607	$1,106	100%
	100 %	-	1,533	705	0.3	2,237.5	3.5	0.999	16,878	10,496	5,285	33,391	$1,169	106%
	200 %	-	1,554	682	0.3	2,236.6	3.0	1.000	19,787	11,530	5,283	37,332	$1,307	118%
Washington, DC	0 %	654	742	1,907	27.0	2,649.5	4.4	0.775	5,008	19,120	4,471	29,330	$1,149	100%
	100 %	532	737	1,891	28.0	2,628.0	4.2	0.770	5,293	21,594	4,435	32,054	$1,255	109%
	200 %	620	741	1,850	27.6	2,591.2	3.6	0.774	6,182	23,960	4,373	35,246	$1,380	120%
Chicago	0 %	289	631	2,785	129.8	3,416.1	4.4	0.797	4,198	31,565	5,765	42,259	$1,503	100%
	100 %	260	628	2,767	134.2	3,395.2	4.2	0.791	4,450	35,482	5,729	46,393	$1,650	110%
	200 %	278	631	2,721	133.7	3,352.8	3.6	0.794	5,197	39,277	5,658	50,863	$1,808	120%
Minneapolis	0 %	61	515	3,424	354.2	3,939.8	4.4	0.810	3,428	46,239	6,648	57,048	$1,711	100%
	100 %	57	513	3,410	362.3	3,922.9	4.2	0.803	3,633	51,396	6,620	62,380	$1,871	109%
	200 %	60	516	3,372	359.6	3,887.3	3.6	0.808	4,244	56,387	6,560	67,922	$2,038	119%

Note: Subcooling of 4.4 °C (8.0 °F) was used as a no-fault condition.
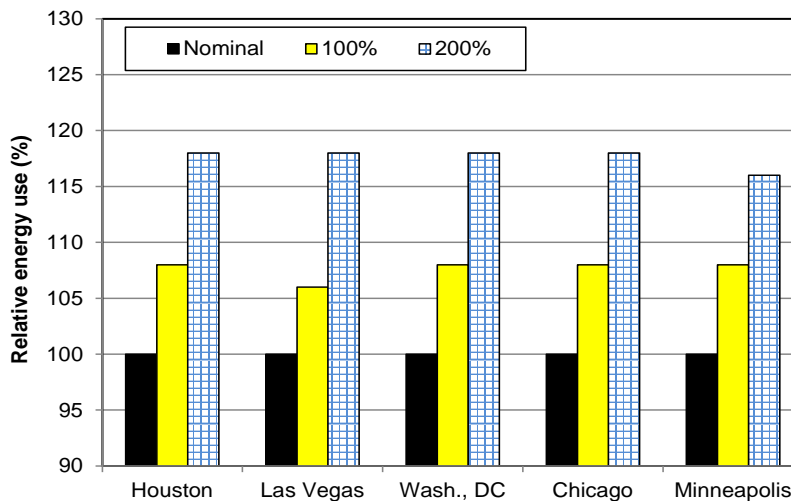
Figure 5.8. Annual energy use for slab-on-grade houses at different level of refrigerant subcooling relative to the annual energy use for the house in the same location with the heat pump operating with the nominal refrigerant charge and subcooling

5.2.8 Effect of Non-Condensable Gases

If the refrigerant system gets non-condensable gases (e.g., air) mixed in with the refrigerant, the performance of the unit is degraded. Table 5.23 shows the results for the slab-on-grade house, and Table 5.24 shows the results for the basement house. The overall results show a (1 ~ 2) % energy use increase in climates with a significant heating season and a 4 % increase in the warmer climates. The moisture removal capability of the unit is only minimally affected by the non-condensable gases in the system.

Table 5.23.   Effect of non-condensable gases on annual energy use for a slab-on-grade house

	Non Condensibles	Hours Above 55 % RH	AC Runtime (h)	Htg Runtime (h)	Backup Heat Runtime (h)	AHU Fan Runtime (h)	AC COP (-)	AC SHR (-)	AC Energy (MJ)	Htg Energy (MJ)	AHU Fan Energy (MJ)	TOTAL ENERGY (MJ)	Total Costs	Relative Energy
Houston	0 %	1,512	1,981	749	5.1	2,730.5	4.3	0.785	16,660	8,537	5,529	31,457	$743	100%
	10 %	1,527	2,006	735	4.9	2,740.9	4.2	0.785	17,359	8,579	5,550	32,220	$761	102%
	20 %	1,579	1,985	713	4.3	2,697.7	4.0	0.787	17,947	8,598	5,463	32,739	$773	104%
Las Vegas	0 %	-	1,966	865	0.3	2,831.1	3.7	0.999	20,531	11,251	6,687	39,200	$1,372	100%
	10 %	-	1,976	848	0.3	2,823.9	3.6	0.999	21,368	11,295	6,670	40,065	$1,402	102%
	20 %	-	1,949	821	0.3	2,769.7	3.5	1.000	22,127	11,328	6,542	40,730	$1,426	104%
Washington, DC	0 %	253	1,207	1,971	89.0	3,178.0	4.5	0.809	8,098	21,759	5,363	35,952	$1,408	100%
	10 %	255	1,234	1,947	86.0	3,180.8	4.3	0.809	8,468	21,875	5,368	36,442	$1,427	101%
	20 %	277	1,233	1,901	81.1	3,133.9	4.1	0.810	8,793	21,906	5,289	36,719	$1,438	102%
Chicago	0 %	189	1,031	2,833	281.2	3,863.9	4.5	0.827	6,816	37,118	6,520	51,186	$1,820	100%
	10 %	186	1,055	2,802	275.8	3,856.9	4.3	0.827	7,126	37,276	6,508	51,642	$1,836	101%
	20 %	188	1,055	2,754	264.2	3,808.7	4.2	0.829	7,395	37,352	6,427	51,905	$1,846	101%
Minneapolis	0 %	13	897	3,432	612.5	4,328.9	4.5	0.846	5,912	55,105	7,305	69,053	$2,072	100%
	10 %	13	918	3,406	603.0	4,324.7	4.3	0.847	6,182	55,304	7,298	69,515	$2,085	101%
	20 %	14	919	3,366	582.3	4,284.4	4.1	0.848	6,416	55,348	7,230	69,726	$2,092	101%

Table 5.24.   Effect of non-condensable gases on annual energy use for a house with basement

	Non Condensibles	Hours Above 55 % RH	AC Runtime (h)	Htg Runtime (h)	Backup Heat Runtime (h)	AHU Fan Runtime (h)	AC COP (-)	AC SHR (-)	AC Energy (MJ)	Htg Energy (MJ)	AHU Fan Energy (MJ)	TOTAL ENERGY (MJ)	Total Costs	Relative Energy
Las Vegas	0 %	-	1,552	718	0.3	2,269.9	3.7	1.000	16,107	9,407	5,362	31,607	$1,106	100%
	10 %	-	1,565	705	0.3	2,270.4	3.5	1.000	16,771	9,474	5,363	32,339	$1,132	102%
	20 %	-	1,550	685	0.3	2,235.4	3.4	1.000	17,390	9,540	5,280	32,941	$1,153	104%
Washington, DC	0 %	654	742	1,907	27.0	2,649.5	4.4	0.775	5,008	19,120	4,471	29,330	$1,149	100%
	10 %	649	760	1,882	26.0	2,641.7	4.2	0.775	5,236	19,279	4,458	29,704	$1,163	101%
	20 %	677	761	1,841	23.2	2,602.0	4.0	0.776	5,438	19,434	4,391	29,995	$1,175	102%
Chicago	0 %	289	631	2,785	129.8	3,416.1	4.4	0.797	4,198	31,565	5,765	42,259	$1,503	100%
	10 %	288	647	2,753	127.3	3,400.0	4.2	0.797	4,387	31,817	5,737	42,674	$1,517	101%
	20 %	287	649	2,706	119.9	3,354.6	4.1	0.799	4,560	32,046	5,661	42,999	$1,529	102%
Minneapolis	0 %	61	515	3,424	354.2	3,939.8	4.4	0.810	3,428	46,239	6,648	57,048	$1,711	100%
	10 %	61	528	3,399	347.5	3,927.5	4.2	0.810	3,584	46,560	6,628	57,503	$1,725	101%
	20 %	64	530	3,354	333.6	3,884.3	4.1	0.812	3,726	46,815	6,555	57,828	$1,735	101%

5.2.9 Effect of Voltage

When input voltage to the unit is changed from the nominal value, the performance of the unit is degraded. Tables 5.25 and 5.26 show the results for the slab-on-grade house and the basement house, respectively. The condition of 25 % overvoltage results in a (9 ~10) % increase in annual energy consumption. This effect on the energy use does not include an adjustment for indoor fan power change with voltage. The undervoltage of 8 % resulted in an insignificant (within 1 %) change in the energy use. Higher levels of undervoltage were not studied because of a possible heat pump catastrophic failure.

Table 5.25. Effect of voltage on annual energy use for a slab-on-grade house

	Voltage	Hours Above 55 % RH	AC Runtime (h)	Htg Runtime (h)	Backup Heat Runtime (h)	AHU Fan Runtime (h)	AC COP (-)	AC SHR (-)	AC Energy (MJ)	Htg Energy (MJ)	AHU Fan Energy (MJ)	TOTAL ENERGY (MJ)	Total Costs	Relative Energy
Houston	-8 %	1,508	1,992	748	5.0	2,740.1	4.3	0.785	16,677	8,464	5,549	31,421	$742	100%
	0 %	1,512	1,981	749	5.1	2,730.5	4.3	0.785	16,660	8,537	5,529	31,457	$743	100%
	8 %	1,519	1,974	752	5.3	2,725.8	4.3	0.785	16,970	8,733	5,520	31,954	$754	102%
	25 %	1,547	1,966	767	5.9	2,733.2	3.9	0.786	18,676	9,616	5,535	34,559	$816	110%
Las Vegas	-8 %	-	1,977	863	0.3	2,840.0	3.7	0.999	20,715	11,143	6,708	39,299	$1,375	100%
	0 %	-	1,966	865	0.3	2,831.1	3.7	0.999	20,531	11,251	6,687	39,200	$1,372	100%
	8 %	-	1,958	870	0.3	2,827.2	3.7	0.999	20,741	11,523	6,678	39,674	$1,389	101%
	25 %	-	1,947	888	0.4	2,835.3	3.4	0.999	22,465	12,694	6,697	42,587	$1,491	109%
Washington, DC	-8 %	252	1,213	1,969	88.6	3,181.3	4.5	0.809	8,062	21,594	5,368	35,756	$1,400	99%
	0 %	253	1,207	1,971	89.0	3,178.0	4.5	0.809	8,098	21,759	5,363	35,952	$1,408	100%
	8 %	256	1,202	1,979	89.7	3,181.8	4.4	0.809	8,289	22,211	5,369	36,601	$1,434	102%
	25 %	274	1,197	2,010	94.8	3,207.7	3.9	0.810	9,211	24,175	5,413	39,530	$1,548	110%
Chicago	-8 %	188	1,035	2,830	280.3	3,865.2	4.5	0.827	6,770	36,879	6,522	50,904	$1,810	99%
	0 %	189	1,031	2,833	281.2	3,863.9	4.5	0.827	6,816	37,118	6,520	51,186	$1,820	100%
	8 %	189	1,027	2,842	283.5	3,868.8	4.4	0.827	6,988	37,781	6,529	52,030	$1,850	102%
	25 %	189	1,022	2,879	294.2	3,901.4	3.9	0.828	7,786	40,678	6,584	55,779	$1,983	109%
Minneapolis	-8 %	13	901	3,430	611.0	4,331.0	4.5	0.846	5,871	54,824	7,309	68,736	$2,062	100%
	0 %	13	897	3,432	612.5	4,328.9	4.5	0.846	5,912	55,105	7,305	69,053	$2,072	100%
	8 %	14	894	3,440	616.2	4,334.1	4.4	0.846	6,064	55,920	7,314	70,029	$2,101	101%
	25 %	14	890	3,470	635.5	4,360.3	3.9	0.848	6,764	59,502	7,358	74,356	$2,231	108%

Table 5.26. Effect of voltage on annual energy use for a house with basement

|	Voltage	Hours Above 55 % RH	AC Runtime (h)	Htg Runtime (h)	Backup Heat Runtime (h)	AHU Fan Runtime (h)	AC COP (-)	AC SHR (-)	AC Energy (MJ)	Htg Energy (MJ)	AHU Fan Energy (MJ)	TOTAL ENERGY (MJ)	Total Costs	Relative Energy
Las Vegas	-8 %	-	1,561	716	0.3	2,277.2	3.6	1.000	16,243	9,319	5,379	31,672	$1,109	100%
	0 %	-	1,552	718	0.3	2,269.9	3.7	1.000	16,107	9,407	5,362	31,607	$1,106	100%
	8 %	-	1,545	721	0.3	2,266.0	3.6	1.000	16,275	9,635	5,352	31,994	$1,120	101%
	25 %	-	1,536	736	0.3	2,272.1	3.4	1.000	17,649	10,604	5,367	34,351	$1,202	109%
Washington, DC	-8 %	656	746	1,905	26.8	2,650.9	4.4	0.775	4,987	18,969	4,473	29,161	$1,142	99%
	0 %	654	742	1,907	27.0	2,649.5	4.4	0.775	5,008	19,120	4,471	29,330	$1,149	100%
	8 %	657	740	1,916	27.1	2,655.0	4.3	0.775	5,125	19,545	4,481	29,883	$1,170	102%
	25 %	674	736	1,945	29.6	2,681.6	3.9	0.775	5,687	21,380	4,525	32,324	$1,266	110%
Chicago	-8 %	286	634	2,782	129.7	3,415.8	4.5	0.797	4,175	31,353	5,764	42,023	$1,494	99%
	0 %	289	631	2,785	129.8	3,416.1	4.4	0.797	4,198	31,565	5,765	42,259	$1,503	100%
	8 %	289	629	2,793	131.8	3,422.0	4.3	0.797	4,302	32,212	5,775	43,020	$1,530	102%
	25 %	295	627	2,829	138.4	3,455.6	3.9	0.798	4,792	34,940	5,831	46,295	$1,646	110%
Minneapolis	-8 %	61	518	3,421	353.6	3,938.8	4.4	0.810	3,408	45,973	6,647	56,759	$1,703	99%
	0 %	61	515	3,424	354.2	3,939.8	4.4	0.810	3,428	46,239	6,648	57,048	$1,711	100%
	8 %	61	514	3,432	357.0	3,946.0	4.3	0.810	3,514	47,027	6,659	57,931	$1,738	102%
	25 %	63	511	3,469	369.9	3,980.7	3.9	0.811	3,911	50,497	6,717	61,857	$1,856	108%
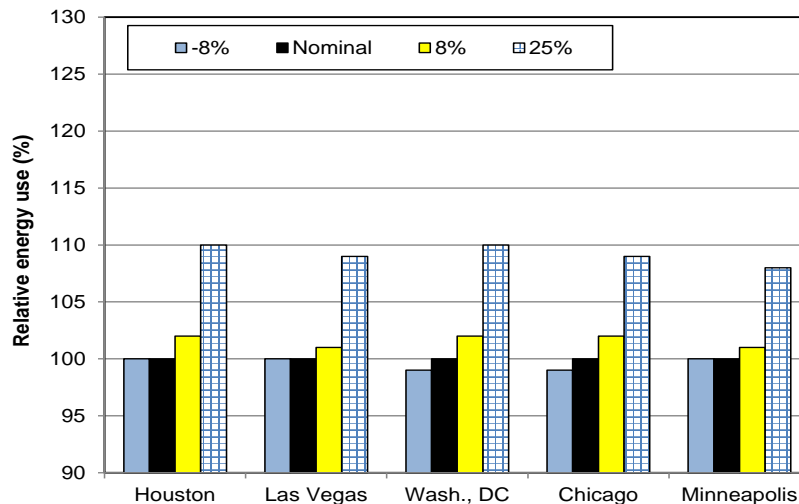
Figure 5.9. Annual energy use for slab-on-grade houses at different levels of input voltages relative to the energy use for the house in the same location when the heat pump operates with nominal voltage

5.2.10 Effect of TXV Sizing

Only undersizing of the TXV in the cooling mode is considered in this study. When the size of the TXV does not match the compressor size, the performance of the system is degraded. Table 5.27 shows the results for the slab-on-grade houses and Table 5.28 shows the results for the basement houses. Generally, the impact is modest at 20 % undersizing in any climate and remains relatively small for Minneapolis at even higher fault levels. However, the impact becomes significant at 40 % undersizing, particularly in hot climates where the energy use increases by (10 ~ 14) %. Moisture removal is only modestly affected.

Table 5.27. Effect of TXV sizing on annual energy use for a slab-on-grade house

	Undersized TXV	Hours Above 55 % RH	AC Runtime (h)	Htg Runtime (h)	Backup Heat Runtime (h)	AHU Fan Runtime (h)	AC COP (-)	AC SHR (-)	AC Energy (MJ)	Htg Energy (MJ)	AHU Fan Energy (MJ)	TOTAL ENERGY (MJ)	Total Costs	Relative Energy
Houston	0 %	1,512	1,981	749	5.1	2,730.5	4.3	0.785	16,660	8,537	5,529	31,457	$743	100%
	20 %	1,516	2,000	749	5.1	2,748.6	4.3	0.785	16,855	8,536	5,566	31,688	$748	101%
	40 %	1,534	2,312	749	5.1	3,060.6	3.6	0.784	20,357	8,533	6,198	35,819	$846	114%
	60 %	1,575	2,767	749	5.1	3,515.9	2.8	0.780	25,508	8,531	7,120	41,890	$989	133%
Las Vegas	0 %	-	1,966	865	0.3	2,831.1	3.7	0.999	20,531	11,251	6,687	39,200	$1,372	100%
	20 %	-	1,973	865	0.3	2,837.4	3.7	0.999	20,623	11,242	6,702	39,298	$1,375	100%
	40 %	-	2,210	865	0.3	3,074.8	3.3	1.000	23,723	11,242	7,263	42,959	$1,504	110%
	60 %	-	2,647	864	0.3	3,511.2	2.6	1.000	29,509	11,235	8,294	49,770	$1,742	127%
Washington, DC	0 %	253	1,207	1,971	89.0	3,178.0	4.5	0.809	8,098	21,759	5,363	35,952	$1,408	100%
	20 %	257	1,234	1,971	89.0	3,204.0	4.3	0.809	8,341	21,754	5,407	36,233	$1,419	101%
	40 %	260	1,449	1,971	89.0	3,420.1	3.6	0.810	10,317	21,758	5,771	38,577	$1,511	107%
	60 %	258	1,751	1,970	88.9	3,720.8	2.8	0.810	13,097	21,748	6,279	41,855	$1,639	116%
Chicago	0 %	189	1,031	2,833	281.2	3,863.9	4.5	0.827	6,816	37,118	6,520	51,186	$1,820	100%
	20 %	188	1,058	2,833	281.2	3,890.7	4.4	0.827	7,064	37,117	6,566	51,478	$1,830	101%
	40 %	188	1,246	2,833	281.2	4,079.1	3.6	0.830	8,792	37,116	6,884	53,523	$1,903	105%
	60 %	182	1,512	2,833	281.2	4,344.2	2.8	0.834	11,229	37,113	7,331	56,405	$2,006	110%
Minneapolis	0 %	13	897	3,432	612.5	4,328.9	4.5	0.846	5,912	55,105	7,305	69,053	$2,072	100%
	20 %	13	922	3,432	612.5	4,354.1	4.3	0.847	6,139	55,106	7,348	69,324	$2,080	100%
	40 %	13	1,087	3,431	612.5	4,518.4	3.5	0.851	7,649	55,099	7,625	71,104	$2,133	103%
	60 %	11	1,321	3,431	612.5	4,751.9	2.8	0.856	9,787	55,097	8,019	73,634	$2,209	107%

Table 5.28. Effect of TXV sizing on annual energy use for a house with basement

|	Undersized TXV	Hours Above 55 % RH	AC Runtime (h)	Htg Runtime (h)	Backup Heat Runtime (h)	AHU Fan Runtime (h)	AC COP (-)	AC SHR (-)	AC Energy (MJ)	Htg Energy (MJ)	AHU Fan Energy (MJ)	TOTAL ENERGY (MJ)	Total Costs	Relative Energy
Las Vegas	0 %	-	1,552	718	0.3	2,269.9	3.7	1.000	16,107	9,407	5,362	31,607	$1,106	100%
	20 %	-	1,558	718	0.3	2,276.2	3.7	1.000	16,187	9,408	5,376	31,704	$1,110	100%
	40 %	-	1,738	718	0.3	2,455.9	3.2	1.000	18,575	9,408	5,801	34,516	$1,208	109%
	60 %	-	2,117	717	0.3	2,834.1	2.5	1.000	23,631	9,403	6,694	40,460	$1,416	128%
Washington, DC	0 %	654	742	1,907	27.0	2,649.5	4.4	0.775	5,008	19,120	4,471	29,330	$1,149	100%
	20 %	653	756	1,907	27.0	2,663.0	4.3	0.775	5,132	19,120	4,494	29,477	$1,155	101%
	40 %	649	877	1,907	27.0	2,784.1	3.5	0.778	6,269	19,121	4,698	30,819	$1,207	105%
	60 %	635	1,066	1,907	27.0	2,972.8	2.8	0.782	8,022	19,120	5,017	32,890	$1,288	112%
Chicago	0 %	289	631	2,785	129.8	3,416.1	4.4	0.797	4,198	31,565	5,765	42,259	$1,503	100%
	20 %	283	645	2,785	129.8	3,430.6	4.3	0.797	4,327	31,569	5,789	42,418	$1,508	100%
	40 %	284	750	2,785	129.8	3,534.9	3.5	0.801	5,312	31,564	5,965	43,573	$1,549	103%
	60 %	282	908	2,785	129.7	3,692.9	2.7	0.808	6,779	31,559	6,232	45,302	$1,611	107%
Minneapolis	0 %	61	515	3,424	354.2	3,939.8	4.4	0.810	3,428	46,239	6,648	57,048	$1,711	100%
	20 %	61	527	3,424	354.2	3,950.5	4.3	0.811	3,531	46,236	6,667	57,165	$1,715	100%
	40 %	59	611	3,424	354.2	4,035.1	3.5	0.815	4,326	46,235	6,809	58,102	$1,743	102%
	60 %	56	739	3,424	354.2	4,163.3	2.7	0.822	5,516	46,235	7,026	59,507	$1,785	104%
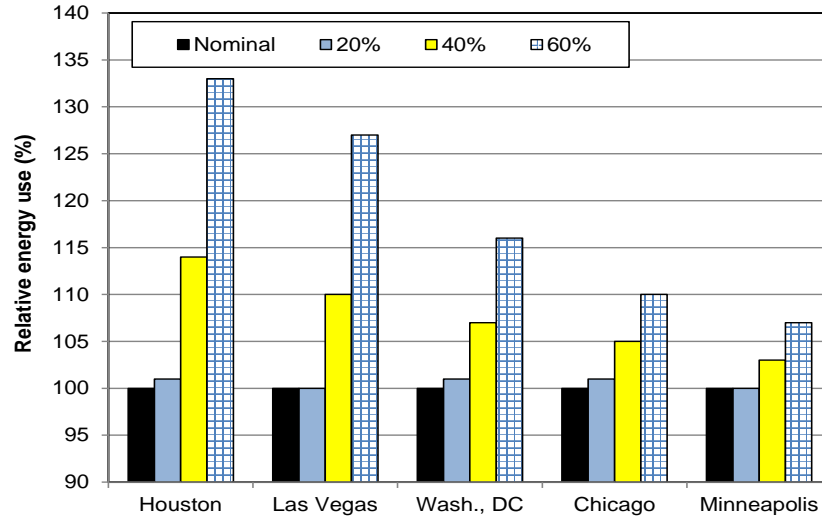
Figure 5.10. Annual energy use for slab-on-grade houses at different levels of TXV undersizing relative to the annual energy use for the house when the heat pump operates with a properly sized TXV

5.2.11 Discussion of the Effects of Single Faults

Figure 5.11 shows examples of annual energy used by a heat pump installed with different installation faults in a slab-on-grade house. The levels of individual faults were selected to reflect, to some degree, the installation condition which might not be noticed by a poorly trained technician. (The authors recognize the speculative aspect of this selection.)
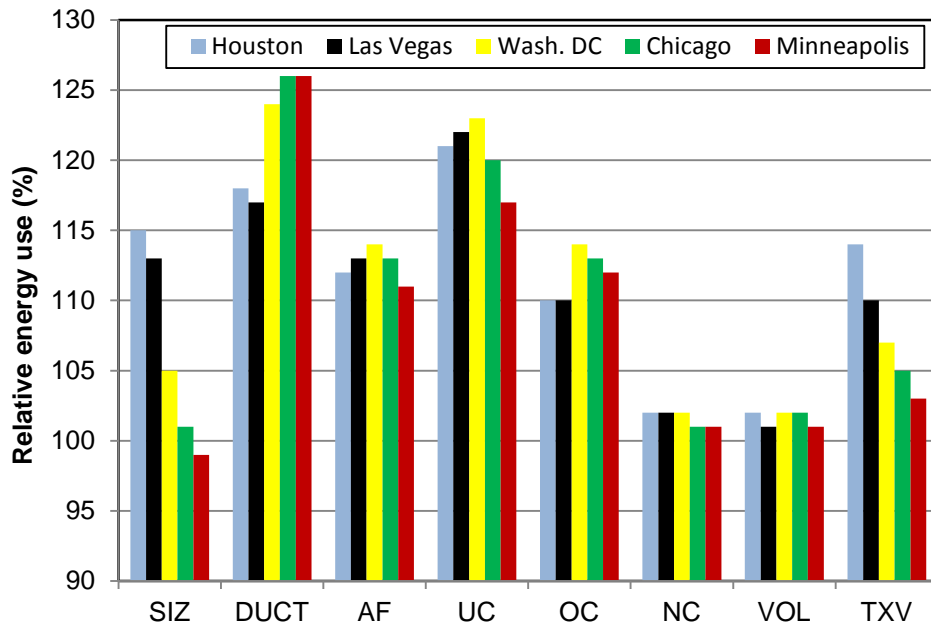
Figure 5.11. Annual energy use by a heat pump in a slab-on-grade house resulting from a single-fault installation, referenced to a fault-free installation. (Table 5.29 shows the selected fault levels)

72

Table 5.29 Levels of individual faults used in Figure 5.11

Fault Type	Fault Level (%)
Heat Pump Sizing (SIZ)[a]	+ 50
Duct Leakage (DUCT)	30
Indoor Coil Airflow (AF)	- 36
Refrigerant Undercharge (UC)	- 30
Refrigerant Overcharge (OC)	+ 30
Non-Condensable Gases (NC)	10
Electric Voltage (VOL)	+ 8
TXV Undersizing (TXV)	- 40

(a) Oversize scenario (2) described in Section 5.2.2.

Simulation results show no drastic differences in the effect of installation faults on energy use in a slab-on-grade house and a basement house, except for the duct leakage fault. For the slab-on-grade house, this fault has the potential to result in a higher increase in energy use that any other fault. The impact of this fault is higher for the heating dominated climate (Chicago and Minneapolis, 26 %) than for the cooling dominated climate (Houston, 18 %). Obviously, duct leakage will also result in some increase of energy use for the basement house; however, the model we used would not discern this effect.

The second most influential fault is refrigerant undercharge. For the 30 % undercharge fault level, the energy use increase is of the order of 20 % irrespective of the climate and building type. Refrigerant overcharge can also result in a significant increase in energy use, (10 ~16) % at the 30 % overcharge fault level. Improper indoor airflow can affect similar performance degradation.

Equipping a house with an oversized heat pump has a small effect if the air duct is oversized accordingly (which may be the case with a new construction). However, if the air duct is too restrictive and the nominal indoor airflow is maintained by adjusting the fan speed (scenario (2)), a 15 % increase in energy use for the house in Houston is predicted.

The cooling TXV undersized fault has also the potential to significantly increase the energy use. The effect of this fault will be most pronounced in localities with a high number of cooling mode operating hours. The cooling mode TXV undersized by 40 % results in (9 ~ 14) % more energy used in Houston as compared to a (3 ~ 5) % in Chicago.

The impact of the remaining faults – non-condensables and improper voltage – is under 4 %. The non-condensables and improper voltage faults, however, represent a substantial risk for durability of equipment and are very important to be diagnosed during a heat pump installation.

5.3 Simulations with Dual Faults
5.3.1 Studied Fault Combinations
The analysis in this section considers the combination of two faults, A and B. Each set of faults was considered in four combinations (Table 5.30).

Table 5.30. Combinations of studied faults

Fault combination case	Level of fault A	Level of fault B
A	moderate	moderate
B	moderate	worst
C	worst	moderate
D	worst	worst

The moderate level will be the value at the middle of the range, while the worst level will be the highest (or lowest) probable level of the fault value. Table 5.31 defines the set or combinations of dual faults simulated for cases where heating and cooling were considered together. Table 5.32 defines the sets of faults that apply for the cooling-only case. The most right-hand column in both tables shows an approximate effect of the studied fault sets on the energy use: the faults effects may be additive (A+B), less than additive (<A+B), or greater the additive (>A+B).

Table 5.31. Dual fault sets considered in simulations (heating and cooling) and their approximate collective effect on annual energy use

Fault set #	Fault A (moderate & worst level)[a]	Fault B (moderate & worst level)	Effect on energy use
1	Duct leakage (20 %, 40 %)	Oversize[b] (25 %, 50 %)	A+B
2	Duct leakage (20 %, 40 %)	Indoor coil airflow (-15 %, -36 %)	< A+B
3	Duct leakage (20 %, 40 %)	Refrigerant undercharge (-15 %, -30 %)	A+B or > A+B
4	Duct leakage (20 %, 40 %)	Refrigerant overcharge (15 %, 30 %)	A+B
5	Duct leakage (20 %, 40 %)	Non-condensables (10 %, 20 %)	A+B
6	Oversize[b] (25 %, 50 %)	Refrigerant undercharge (-15 %, -30 %)	A+B
7	Oversize[b] (25 %, 50 %)	Refrigerant overcharge (15 %, 30 %)	A+B
8	Oversize[b] (25 %, 50 %)	Non-condensables (10 %, 20 %)	A+B
9	Indoor coil airflow (-15 %, -36 %)	Refrigerant undercharge (-15 %, -30 %)	< A+B
10	Indoor coil airflow (-15 %, -36 %)	Refrigerant overcharge (15 %, 30 %)	< A+B
11	Indoor coil airflow (-15 %, -36 %)	Non-condensables (10 %, 20 %)	< A+B

(a) moderate = mid-level value,   worst = lowest/highest level value
(b) Oversize scenario (2) was selected because it covers the prevalent field bias (undersized ducts)

Table 5.32. Dual fault sets considered in simulations (heating and cooling) and their approximate collective effect on annul energy use; TXV fault existing in cooling only [(a)]

Fault set #	Fault A (moderate & worst level)[(b)]	Fault B (moderate & worst level)	Effect on energy use
12	Duct leakage (20 %, 40 %)	Cooling TXV undersizing (-20 %, -60 %)	A+B
13	Oversize[(c)] (25 %, 50 %)	Cooling TXV undersizing (-20 %, -60 %))	A+B
14	Indoor coil airflow (-15 %, -36 %)	Cooling TXV undersizing (-20 %, -60 %)	< A+B

(a) Faults listed as Faults A exist in cooling and heating
(b) moderate = mid-level value,   worst = lowest/highest level value
(c) Oversize scenario (2) was selected because it covers the prevalent field bias (undersized ducts)

5.3.2. Effects of Dual Faults

Simulations were performed for 14 dual fault sets, with 4 runs per set, in the 9 house/climate combinations for a total of 504 runs. Because of similarity between the obtained results, the tables below are limited to representative cases, which include the slab-on-grade house for Houston, Washington, DC, and Minneapolis, and the house with a basement for Washington, DC. For the Houston house, Table 5.33 shows results for dual fault sets 1 through 5, which represent all studied dual faults involving duct leakage; Table 5.34 shows results for dual fault sets 6 through 8, which represent all studied dual faults involving the oversized heat pump, except the case with duct leakage presented in Table 5.33; and Table 5.35 presents the remaining three studied cases with dual faults present in both cooling and heating.   Table 5.36 presents the effect on annual energy use of the undersized cooling TXV with either duct leakage, oversized heat pump, or low airflow rate faults, which occur in both cooling and heating mode. Tables 5.37 through 5.47 present simulation results for the remaining cases. For nine out of fourteen sets studied, the effect of dual faults was approximately additive (Table 5.31). For the remaining five sets – all involving indoor coil airflow – the effect was less than additive. A few results that are not immediately intuitive are discussed at the end of this section.

Table 5.33. Relative energy use for dual fault sets 1 to 5 for the slab-on-grade house in Houston

Duct leakage with oversized heat pump, low airflow rate, undercharged, overcharged, and non-condensable gases faults

Dual Fault Set: 1		20% Duct Leakage	40% Duct Leakage	Dual Fault Set: 2		20% Duct Leakage	40% Duct Leakage
	100%	109%	128%		100%	109%	128%
25% Oversized	109%	121%	148%	-15% Airflow	104%	110%	129%
50% Oversized	115%	128%	159%	-36% Airflow	112%	114%	130%

Dual Fault Set: 3		20% Duct Leakage	40% Duct Leakage	Dual Fault Set: 4		20% Duct Leakage	40% Duct Leakage
	100%	109%	128%		100%	109%	128%
15% Undercharged	105%	115%	136%	15% Overcharged	103%	112%	132%
30% Undercharged	121%	132%	156%	30% Overcharged	110%	119%	141%

Dual Fault Set: 5		20% Duct Leakage	40% Duct Leakage
	100%	109%	128%
10% Non-Condensibles	102%	112%	131%
20% Non-Condensibles	104%	113%	133%

Table 5.34. Relative energy use for dual fault sets 6 to 8 for the slab-on-grade house in Houston

Oversized heat pump with undercharged, overcharged, and non-condensable gases faults

Dual Fault Set: 6		25% Oversized	50% Oversized	Dual Fault Set: 7		25% Oversized	50% Oversized
	100%	109%	115%		100%	109%	115%
15% Undercharged	105%	115%	121%	15% Overcharged	103%	112%	118%
30% Undercharged	121%	133%	140%	30% Overcharged	110%	119%	125%

Dual Fault Set: 8		25% Oversized	50% Oversized
	100%	109%	115%
10% Non-Condensibles	102%	112%	118%
20% Non-Condensibles	104%	113%	120%

Table 5.35. Relative energy use for dual fault sets 9 to 11 for the slab-on-grade house in Houston

Low airflow rate with undercharged, overcharged, and non-condensable gases faults

Dual Fault Set: 9		-15% Airflow	-36% Airflow	Dual Fault Set: 10		-15% Airflow	-36% Airflow
	100%	104%	112%		100%	104%	112%
15% Undercharged	105%	107%	111%	15% Overcharged	103%	105%	109%
30% Undercharged	121%	123%	127%	30% Overcharged	110%	112%	116%

Dual Fault Set: 11		-15% Airflow	-36% Airflow
	100%	104%	112%
10% Non-Condensibles	102%	104%	109%
20% Non-Condensibles	104%	106%	111%

Table 5.36. Relative energy use for dual fault sets 12 to 14 involving cooling mode TXV for the slab-on-grade house in Houston

Undersized TXV with duct leakage, oversized heat pump, and low airflow rate faults

Dual Fault Set: 12		20% Duct Leakage	40% Duct Leakage	Dual Fault Set: 13		25% Oversized	50% Oversized
	100%	109%	128%		100%	109%	115%
20% TXV Undersizing	101%	110%	129%	20% TXV Undersizing	101%	110%	116%
60% TXV Undersizing	133%	143%	163%	60% TXV Undersizing	133%	150%	161%

Dual Fault Set: 14		-15% Airflow	-36% Airflow
	100%	104%	112%
20% TXV Undersizing	101%	103%	107%
60% TXV Undersizing	133%	135%	139%

Table 5.37. Relative energy use for dual fault sets 1 to 5 for the slab-on-grade house in Washington, DC

Duct leakage with oversized heat pump , low airflow rate, undercharged, overcharged, and non-condensable gases faults

Dual Fault Set: 1		20% Duct Leakage	40% Duct Leakage
	100%	112%	139%
25% Oversized	103%	117%	152%
50% Oversized	105%	119%	156%

Dual Fault Set: 2		20% Duct Leakage	40% Duct Leakage
	100%	112%	139%
-15% Airflow	105%	112%	137%
-36% Airflow	114%	114%	137%

Dual Fault Set: 3		20% Duct Leakage	40% Duct Leakage
	100%	112%	139%
15% Undercharged	105%	117%	146%
30% Undercharged	123%	137%	172%

Dual Fault Set: 4		20% Duct Leakage	40% Duct Leakage
	100%	112%	139%
15% Overcharged	104%	116%	145%
30% Overcharged	114%	127%	157%

Dual Fault Set: 5		20% Duct Leakage	40% Duct Leakage
	100%	112%	139%
10% Non-Condensibles	101%	113%	140%
20% Non-Condensibles	102%	114%	141%

Table 5.38. Relative energy use for dual fault sets 6 to 8 for the slab-on-grade house in Washington, DC

Oversized heat pump with undercharged, overcharged, and non-condensable gases faults

Dual Fault Set: 6		25% Oversized	50% Oversized
	100%	103%	105%
15% Undercharged	105%	108%	110%
30% Undercharged	123%	127%	129%

Dual Fault Set: 7		25% Oversized	50% Oversized
	100%	103%	105%
15% Overcharged	104%	107%	109%
30% Overcharged	114%	118%	119%

Dual Fault Set: 8		25% Oversized	50% Oversized
	100%	103%	105%
10% Non-Condensibles	101%	105%	107%
20% Non-Condensibles	102%	106%	108%

Table 5.39. Relative energy use for dual fault sets 9 to 11 for the slab-on-grade house in Washington, DC

Low airflow rate with undercharged, overcharged, and non-condensable gases faults

Dual Fault Set: 9		-15% Airflow	-36% Airflow
	100%	105%	114%
15% Undercharged	105%	106%	109%
30% Undercharged	123%	124%	127%

Dual Fault Set: 10		-15% Airflow	-36% Airflow
	100%	105%	114%
15% Overcharged	104%	106%	109%
30% Overcharged	114%	116%	119%

Dual Fault Set: 11		-15% Airflow	-36% Airflow
	100%	105%	114%
10% Non-Condensibles	101%	103%	106%
20% Non-Condensibles	102%	104%	107%

Table 5.40.   Relative energy use for dual fault sets 12 to 14 involving the cooling mode TXV for the slab-on-grade house in Washington, DC

Undersized TXV with duct leakage, oversized heat pump, and low airflow rate faults

Dual Fault Set: 12		20% Duct Leakage	40% Duct Leakage
	100%	112%	139%
20% TXV Undersizing	101%	113%	140%
60% TXV Undersizing	116%	129%	157%

Dual Fault Set: 13		25% Oversized	50% Oversized
	100%	103%	105%
20% TXV Undersizing	101%	104%	106%
60% TXV Undersizing	116%	123%	127%

Dual Fault Set: 14		-15% Airflow	-36% Airflow
	100%	105%	114%
20% TXV Undersizing	101%	102%	105%
60% TXV Undersizing	116%	118%	121%

Table 5.41. Relative energy use for dual fault sets 1 to 5 for the slab-on-grade house in Minneapolis

Duct leakage with oversized heat pump , low airflow rate, undercharged, overcharged, and non-condensable gases faults

Dual Fault Set: 1		20% Duct Leakage	40% Duct Leakage
	100%	113%	140%
25% Oversized	100%	114%	148%
50% Oversized	99%	114%	149%

Dual Fault Set: 2		20% Duct Leakage	40% Duct Leakage
	100%	113%	140%
-15% Airflow	103%	113%	138%
-36% Airflow	111%	113%	137%

Dual Fault Set: 3		20% Duct Leakage	40% Duct Leakage
	100%	113%	140%
15% Undercharged	103%	116%	144%
30% Undercharged	117%	132%	162%

Dual Fault Set: 4		20% Duct Leakage	40% Duct Leakage
	100%	113%	140%
15% Overcharged	104%	116%	144%
30% Overcharged	112%	125%	153%

Dual Fault Set: 5		20% Duct Leakage	40% Duct Leakage
	100%	113%	140%
10% Non-Condensibles	101%	113%	140%
20% Non-Condensibles	101%	113%	140%

Table 5.42. Relative energy use for dual fault sets 6 to 8 for the slab-on-grade house in Minneapolis

Oversized heat pump with undercharged, overcharged, and non-condensable gases faults

Dual Fault Set: 6		25% Oversized	50% Oversized
	100%	100%	99%
15% Undercharged	103%	103%	103%
30% Undercharged	117%	118%	117%

Dual Fault Set: 7		25% Oversized	50% Oversized
	100%	100%	99%
15% Overcharged	104%	103%	103%
30% Overcharged	112%	112%	112%

Dual Fault Set: 8		25% Oversized	50% Oversized
	100%	100%	99%
10% Non-Condensibles	101%	101%	101%
20% Non-Condensibles	101%	101%	101%

Table 5.43. Relative energy use for dual fault sets 9 to 11 for the slab-on-grade house in Minneapolis

Low airflow rate with undercharged, overcharged, and non-condensable gases faults

Dual Fault Set: 9		-15% Airflow	-36% Airflow
	100%	103%	111%
15% Undercharged	103%	104%	106%
30% Undercharged	117%	118%	121%

Dual Fault Set: 10		-15% Airflow	-36% Airflow
	100%	103%	111%
15% Overcharged	104%	104%	107%
30% Overcharged	112%	112%	115%

Dual Fault Set: 11		-15% Airflow	-36% Airflow
	100%	103%	111%
10% Non-Condensibles	101%	102%	104%
20% Non-Condensibles	101%	102%	104%

Table 5.44. Relative energy use for dual fault sets 12 to 14 involving the cooling mode TXV for the slab-on-grade house in Minneapolis

Undersized TXV with duct leakage, oversized heat pump, and low airflow rate faults

Dual Fault Set: 12		20% Duct Leakage	40% Duct Leakage
	100%	113%	140%
20% TXV Undersizing	100%	113%	140%
60% TXV Undersizing	107%	120%	147%

Dual Fault Set: 13		25% Oversized	50% Oversized
	100%	100%	99%
20% TXV Undersizing	100%	100%	100%
60% TXV Undersizing	107%	108%	108%

Dual Fault Set: 14		-15% Airflow	-36% Airflow
	100%	103%	111%
20% TXV Undersizing	100%	101%	103%
60% TXV Undersizing	107%	108%	110%

Table 5.45. Relative energy use for dual fault sets 6 to 8 for the basement house in Washington, DC

Oversized heat pump with undercharged, overcharged, and non-condensable gases faults

Dual Fault Set: 6		25% Oversized	50% Oversized
	100%	104%	108%
15% Undercharged	104%	109%	112%
30% Undercharged	121%	126%	129%

Dual Fault Set: 7		25% Oversized	50% Oversized
	100%	104%	108%
15% Overcharged	105%	109%	112%
30% Overcharged	116%	120%	124%

Dual Fault Set: 8		25% Oversized	50% Oversized
	100%	104%	108%
10% Non-Condensibles	101%	106%	109%
20% Non-Condensibles	102%	107%	111%

Table 5.46.   Relative energy use for dual fault sets 9 to 11 for the basement house in Washington, DC

Low airflow rate with undercharged, overcharged, and non-condensable gases faults

Dual Fault Set: 9		-15% Airflow	-36% Airflow
	100%	105%	113%
15% Undercharged	104%	105%	106%
30% Undercharged	121%	122%	124%

Dual Fault Set: 10		-15% Airflow	-36% Airflow
	100%	105%	113%
15% Overcharged	105%	106%	107%
30% Overcharged	116%	117%	118%

Dual Fault Set: 11		-15% Airflow	-36% Airflow
	100%	105%	113%
10% Non-Condensibles	101%	102%	103%
20% Non-Condensibles	102%	103%	105%

Table 5.47.   Relative energy use for dual fault sets 13 to 14 involving the cooling mode TXV for the basement house in Washington, DC

Undersized TXV with duct leakage, oversized heat pump, and low airflow rate faults

Dual Fault Set: 13		25% Oversized	50% Oversized
	100%	104%	108%
20% TXV Undersizing	101%	105%	108%
60% TXV Undersizing	112%	118%	123%

Dual Fault Set: 14		-15% Airflow	-36% Airflow
	100%	105%	113%
20% TXV Undersizing	101%	101%	103%
60% TXV Undersizing	112%	113%	115%

While reviewing the above results, a reader may be surprised to see that in a few cases the energy use with two simultaneous faults is as at a similar level as that for the more influential single fault. The most confounding are perhaps the results obtained for the dual fault set # 2 involving air duct leakage and reduced indoor coil airflow (Table 5.37). In this case, for the 40 % duct leakage existing alone the energy use increases by 39 %, and for the 36 % reduction in the airflow the energy use increases by 14 %; however, when these two faults exist simultaneously the combined effect is an increase of energy use by 37 %, which is less than that when the duct leakage fault exists alone. This result can be explained by the fact that at a lowered airflow the heat pump satisfies the load using less air (it produces a larger temperature spread between the return and supply air). Hence, in absolute numbers, the amount of energy lost due duct leakage is smaller because the leaked air is a percentage of the total airflow. Simply, duct leakage is a dominating fault, and a reduction of the effect of this fault more than compensates for the losses associated with the reduced airflow (decreased air-side heat transfer coefficient and increased compressor power due to increased temperature lift).

Also interesting results for the low indoor airflow combined with either the refrigerant overcharge (dual set fault # 10) or non-condensable gases (dual set fault # 11) can be reviewed in Table 5.39. If the low airflow fault exists alone, the energy use increases by 14 % for the 36 % airflow reduction. This fault demonstrates itself in a lower temperature of the evaporator, which results in a somewhat lower sensible capacity and increased latent capacity of the air conditioner. Since in performed simulations the air conditioner had to satisfy the thermostat (i.e., the same sensitive load) and the rate of moisture removal increased, the energy use increased. Now, refrigerant overcharge fault or non-condensables fault causes the condenser pressure to increase. This pulls up the pressure (and temperature) of the evaporator, which reduces the latent load the air conditioner handles. At moderate levels of the overcharge and non-condensables faults, the energetic benefit of the lowered latent load is greater than that of a modest COP penalty associate with

80

these faults. Consequently, moderate levels of refrigerant overcharge and non-condensables faults caused a reduction of energy used by the unit with 36 % reduced air flow. Greater levels of these faults reverse this energy use trend. (Note that the above explanation discusses the first order effects of a rather complicated reaction of the systems to these faults, e.g., a lower air-side heat transfer coefficient, lower indoor fan power, and the effect on performance in the heating mode).

Relatively less perplexing is the interaction between the low airflow fault and undersized TXV fault (Table 5.40, dual fault set # 14). In this case, a 20 % undersized cooling-mode TXV improved the performance of the system operated with a reduced indoor coil airflow. Since a reduced airflow reduces the system capacity, a TVX that was 20 % undersized for the rated capacity showed to be a better match for the 'reduced capacity' system than the TXV properly sized for the rated capacity.

It should be noted that airflow reduction lowers equipment capacity and may compromise occupant's comfort when approaching design conditions. Additionally, in extreme cases or in combination with other faults, it may lead to indoor coil frosting during cooling operation and equipment tripping or failure.

5.3.3. Discussion of the Effects of Dual Faults
As expected, the collective impact of two simultaneous faults on the energy consumption varies and depends on the faults considered. In most cases the collective effect can be described as being additive; however, the effect can exceed or be markedly below this additive value, including being approximately equal to the individual effect of one of the faults involved, as noted in Tables 5.31 and 5.32. The above characterization applies to all house/climate combinations. The relative impact on energy use also is similar for all cases studied (Figures 5.12, and 5.13).
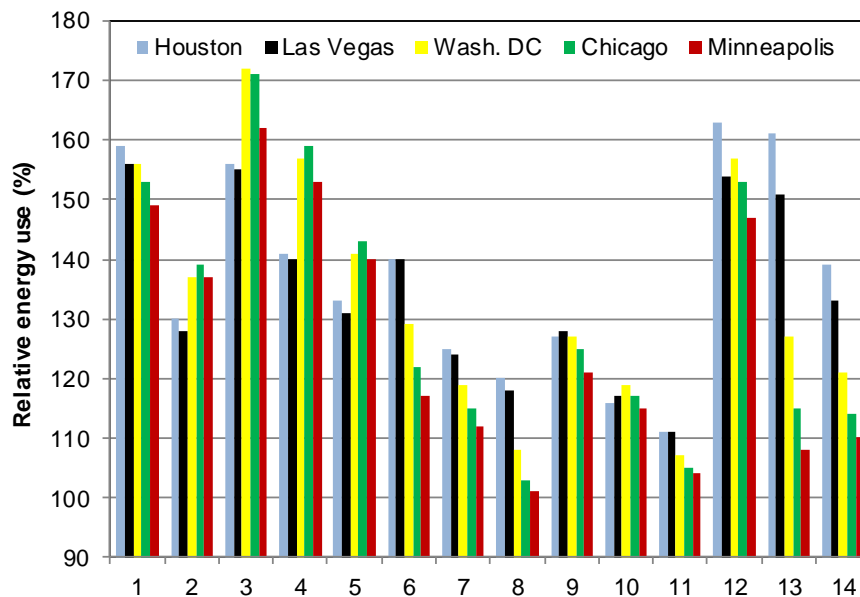
Figure 5.12. Annual energy use for slab-on-grade houses with 14 dual-faults relative to the energy use for the houses with fault-free installations
(Faults defined in Tables 5.31 and 5.32; Table 5.30 case d, worst level for both faults)
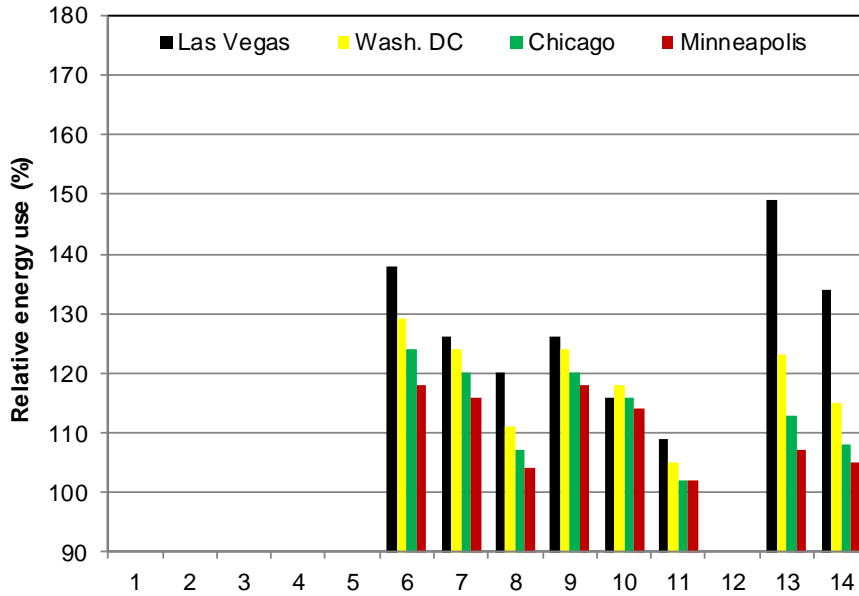
Figure 5.13. Annual energy use for houses with basement with 8 dual-fault installations referenced to the energy use for the houses with fault-free installations
(Faults defined in Tables 5.31 and 5.32, Table 5.30 case d; worst level for both faults; the omitted dual faults involve duct leakage, which was not considered in houses with basement)

5.4 Effects of Triple Faults

Triple faults were not simulated in this study because the open literature does not provide sufficient data on effects of multiple faults to allow for their characterization and use in annual simulations of building/heat pump systems. Nevertheless, the occurrence of three simultaneous faults is plausible, particularly for the most common faults such as refrigerant undercharge, improper indoor airflow, or duct leakage. It is reasonable to assume that the effect of a triple fault will be as least as high as that of any of the possible three fault pairs considered individually; however, the effect of the third fault can increase the effect of the other two faults in an additive manner. As an example of a triple fault, SCE (2012) reported almost 70 % degradation in capacity for a split air conditioner operating under highly restricted airflow of the condenser, 40 % refrigerant undercharge, and 56 % reduction in the indoor airflow.

6. CONCLUDING REMARKS

Extensive simulations of house/heat pump systems in five climatic zones lead to the following conclusions:

- o   Effect of different installation faults on annual energy use is similar for a slab-on-grade house (ducts located in the unconditioned attic) and a basement house (ducts located in the semi-conditioned basement), except the duct leakage fault.
- o   Effect of different installation faults is similar in different climates except for the following cases:
  - Duct leakage: significant increase in the indoor RH for an installation in a hot & humid climate
  - Heat pump oversizing with undersized air ducts: in heating-dominated climates, heat pump oversizing reduces the use of backup heat, which compensates for the increased indoor fan energy use associated with overcoming the higher external static pressure
- o   Undersized cooling mode TXV: little effect in heating-dominated climates, while a significant increase of energy use is possible in cooling-dominated climates.

The effect of simultaneous faults can be additive (e.g., duct leakage and non-condensable gases), little changed relative to the single fault condition (e.g., low indoor airflow and refrigerant undercharge), or well-beyond additive (duct leakage and refrigerant undercharge).

The study found duct leakage, refrigerant undercharge, oversized heat pump with non-oversized ductwork, low indoor airflow due to undersized ductwork, and refrigerant overcharge to have the most potential for causing significant performance degradation and increased annual energy consumption. Increases of energy use by 30 % due to improper installation practices seem to be plausible. A well-designed and documented survey of heat pump installations would be helpful in establishing the prevalence of different installation faults and effective practices for their elimination.

A significant increase in annual energy use can be caused by lowering the thermostat in the cooling mode to improve indoor comfort in cases of excessive indoor humidity levels. For Houston, TX, lowering the thermostat setting by 1.1 °C (2.0 °F) increased the annual energy use by 20 %, and the energy use increase rate is even higher due to further lowering the setting (the effect is not linear).

The authors contend that the laboratory and modeling results from this analysis using a 2.5 ton heat pump are representative of all unitary equipment including commercial split-systems and single package units (e.g., roof top units).

The goal of this study was to assess the impacts that HVAC system installation faults had on equipment electricity consumption. The effect of the installation faults on occupant comfort was not the main focus of the study, and this research did not seek to quantify any impacts on indoor air quality, or noise generation (e.g., airflow noise from air moving through restricted ducts). Additionally, the study does not address the effects that installation faults have on equipment reliability/robustness (number of starts/stops, etc.), maintainability (e.g., access issues), or costs of initial installation and ongoing maintenance.

7. NOMENCLATURE

A = area [m^2, (ft^2)]
ACH50 = air changes per hour at 50 pascal pressure differential
AF = improper indoor airflow rate fault
AHU = air handling unit
a = coefficient of multivariate polynomial
C = capacitance term: air mass in space multiplied by a multiplication factor in Eq. (4.1)
C_D = heat pump cyclic degradation coefficient
CF = improper outdoor airflow rate (condenser fouling) fault
COP = coefficient of performance
c_p = specific heat of air [$J \cdot g^{-1} \cdot °C^{-1}$, ($Btu \cdot lb^{-1} \cdot °F^{-1}$)]
cfm = volumetric flow rate of air in I-P units ($ft^3 \cdot min^{-1}$)
DUCT = duct leakage fault
EER = energy efficiency ratio [$Btu \cdot h^{-1} \cdot W^{-1}$]
FDD = fault detection and diagnosis
ELA = equivalent leakage area [m^2, (ft^2)]
FSE = fit standard error; equal to the square root of the sum of the squared errors divided by the degrees of freedom
F = fault level [% or dimensionless (fraction)]
F_R = fraction of total return airflow (m_R) from zone 2
F_S = fraction of total supply airflow (m_S) into zone 2
Gross capacity = total capacity (sensible and latent for evaporator) provided by the coil (does not include indoor fan heat)
Gross COP = gross coil capacity divided by outdoor unit power. Outdoor unit power does not include indoor fan power
HP = heat pump
HSPF = heating seasonal performance factor
HVAC = heating, ventilating, air conditioning
Htg = heating
h_i = convective coefficient for exterior of duct [$W \cdot m^{-2} \cdot °C^{-1}$, ($Btu \cdot h^{-1} \cdot ft^{-2} \cdot °F^{-1}$)]
Latent capacity = portion of the cooling capacity that removes moisture (latent) energy (reduces the moisture content (humidity ratio) of the air stream)
LL = liquid line restriction fault
m = number of coefficients or mass flow rate [$kg \cdot s^{-1}$, ($lb \cdot s^{-1}$); or $kg \cdot h^{-1}$, ($lb \cdot h^{-1}$)]
m_R = return airflow to AHU [$kg \cdot s^{-1}$, ($lb \cdot s^{-1}$)]
m'_R = airflow into return duct after accounting for leakage [$kg \cdot s^{-1}$, ($lb \cdot s^{-1}$)], i.e., $m'_R = m_R \cdot (1 - F_R)$
m_S = supply airflow from air-handling unit [$kg \cdot s^{-1}$, ($lb \cdot s^{-1}$)]
N = number of data points
NC = presence of non-condensable gases fault
OC = refrigerant overcharge fault, % (or fraction) departure from the correct value
P = pressure [Pa, (mm H_2O)]
Q = capacity or heat loss or heat gain [W, ($Btu \cdot h^{-1}$)]
$Q_{internal}$ = internal moisture gains [W, ($Btu \cdot h^{-1}$)]
$Q_{AC,latent}$ = moisture removal by air conditioner [W, ($Btu \cdot h^{-1}$)]
R = thermal resistance in I-P system of units [($h \cdot ft^2 \cdot °F \cdot Btu^{-1}$)]
R(SI) = thermal resistance in SI system of units [$K \cdot m^2 \cdot W^{-1}$]
RH = relative humidity [%]

SC = refrigerant subcooling at the liquid line service valve [°C, (°F)] or excessive refrigerant subcooling fault, % (or fraction) departure from the correct value
SEER = seasonal energy efficiency ratio [(Btu·W^{-1}·h^{-1})]
Sensible capacity = portion of cooling capacity that removes sensible energy (decreases the temperature of the air stream)
SHGC = solar heat gain coefficient
SHR = sensible heat ratio (sensible capacity divided by total capacity)
SIZ = heat pump sizing fault, % (or fraction) above or below the correct capacity
T = temperature [°C, (°F)]
T_{ID} = indoor dry-bulb temperature [°C, (°F)]
T_{IDP} = indoor dew-point temperature [°C, (°F)]
T_{OD} = outdoor dry-bulb temperature [°C, (°F)]
TMY3 = data set 3 with typical meteorological year weather data
TXV = thermostatic expansion valve or TXV undersizing fault in cooling
T_{ACout} = average temperature of air leaving AHU [°C]
T^{dep} = outdoor temperature at which a cooling mode TXV opens fully, as calculated by Eq. (3.2) [(°C)]
t = time [s, (s)]
U = overall heat transfer coefficient [W·m^{-2}·K^{-1}, (Btu·h^{-1}·ft^{-2}·F^{-1})]
UC = refrigerant undercharge fault, % (or fraction) departure from the correct value
V = volumetric flow rate [m^3·h^{-1}, (ft^3·min^{-1})]
VOL = electric line voltage fault
W = power [W, (W)]
W_{ODU} = power of outdoor unit; includes compressor, outdoor fan and control powers [W, (W)]
W_{tot} = total power; includes W_{ODU} and indoor fan power [W, (W)]
w = humidity ratio [g·g^{-1}, (lb·lb^{-1})]
w_{ACout} = average humidity ratio of air leaving AHU [g·g^{-1}, (lb·lb^{-1})]
X = measured performance parameter
Y = normalized performance parameter

Greek Symbol
Δ = difference

Subscripts
AR = air in the return duct
AS = air in the supply duct
i = indoor or feature index
in = incoming or inside
inf = infiltration
o = outdoor
out = outcoming or outside
R = return duct or refrigerant
r = reduced
S = supply duct
sat = saturation
tot = total
z1 = zone 1
z2 = zone 2

8. REFERENCES

ACCA, 2009. ANSI/ACCA Standard 9 QIVP-2009, HVAC Quality Installation Verification Protocols. Air Conditioning Contractors of America, Arlington, VA., http://www.acca.org/

ACCA, 2010. ANSI/ACCA Standard 5 QI-2010, HVAC Quality Installation Specification. Air Conditioning Contractors of America, Arlington, VA., http://www.acca.org/quality

ACCA, 2011a. ANSI/ACCA 2 Manual J – 2011, Residential Load Calculation 8th Edition. Air Conditioning Contractors of America, Arlington, VA., http://www.acca.org/

ACCA, 2011b. ANSI/ACCA Standard 9 QIVP - 2011, HVAC Quality Installation Verification Protocols, Air Conditioning Contractors of America, Arlington, VA., http://www.acca.org/quality

ACCA, 2012. ANSI/ACCA 11 Manual Zr – 2012, Residential HVAC System Zoning, Air Conditioning Contractors of America, Arlington, VA., http://www.acca.org/

ACCA, 2013. ANSI/ACCA 4 QM – 2013, Residential Maintenance. Air Conditioning Contractors of America, Arlington, VA., http://www.acca.org/quality.

ASHRAE, 2004. ANSI/ASHRAE Standard 152-2004, Method of Test for Determining the Design and Seasonal Efficiencies of Residential Thermal Distribution Systems. American Society of Heating, Refrigerating, and Air-Conditioning Engineers, Atlanta, GA. http://www.ashrae.org

AHRI, 2008. ANSI/AHRI Standard 210/240, Performance Rating of Unitary Air Conditioning and Air-Source Heat Pump Equipment, Standard 210/240. Air-Conditioning, Heating, and Refrigeration Institute, Arlington, VA., http://www.ahrinet.org

ASHRAE, 2009a. ASHRAE Handbook of Fundamentals. Chapter 17, Residential Cooling and Heating Load Calculations. American Society of Heating, Refrigerating, and Air-Conditioning Engineers, Atlanta, GA. http://www.ashrae.org

ASHRAE, 2009b. ANSI/ASHRAE Standard 160-2009, Criteria for Moisture-Control Design Analysis in Buildings, American Society of Heating. Refrigerating, and Air-Conditioning Engineers, Atlanta, GA. http://www.ashrae.org

ASHRAE, 2010. ANSI/ASHRAE Standard 116-2010, Methods of Testing for Rating Seasonal Efficiency of Unitary Air Conditioners and Heat Pumps. American Society of Heating, Refrigerating, and Air-Conditioning Engineers, Atlanta, GA. http://www.ashrae.org

ASHRAE, 2013. ANSI/ASHRAE Standard 62.2-2013, Ventilation and Acceptable Indoor Air Quality in Low-Rise Residential Buildings. American Society of Heating, Refrigerating, and Air-Conditioning Engineers, Atlanta, GA. http://www.ashrae.org

Andrews, J.W., 1997. Error Analysis for Duct Leakage Tests in ASHRAE Standard 152P. Brookhaven National Laboratory Report 64679.

Arasteh, D., Kohler, C., Griffith., B., 2009. Modeling Windows in Energy Plus with Simple Performance Indices.
http://windows.lbl.gov/win_prop/ModelingWindowsInEnergyPlusWithSimplePerformanceIndices.pdf

Barnaby, C.S., Spitler, J.D., 2004. Updating the ASHRAE/ACCA Residential Heating and Cooling Load Calculation Procedures and Data. ASHRAE 1199-RP, American Society of Heating, Refrigerating, and Air-Conditioning Engineers, Atlanta, GA. http://www.ashrae.org

California Energy Commission, 2008. Strategic Plan to Reduce the Energy Impact of Air Conditioners, CEC-400-2008-010, California Energy Commission, CA. http://www.energy.ca.gov/2008publications/CEC-400-2008-010/CEC-400-2008-010.pdf

CDH Energy Corp., 2010. TRN-RESDH5: TRNSYS Residential AC/Dehumidifier Model – SHORT TIMESTEP. A Tool for Evaluating Hybrid Configurations and Control Options in Single-Zone Building Applications, Operating and Reference Manual. Cazenovia, NY.

Chen, B., Braun, J.E., 2001. Simple rule-based methods for fault detection and diagnostics applied to packaged air conditioners. ASHRAE Transactions 87(2). http://www.ashrae.org

Cho, S. H., Hong, Y., Kim, W., Zaheer-uddin, M., 2005. Multi-fault detection and diagnosis of HVAC systems: an experimental study. International Journal of Energy Research, 29, 471-483.

Cummings, J. B., Tooley, J. J., 1989. Infiltration and Pressure Differences Induced by Forced Air Systems in Florida Residences. ASHRAE Transactions, 95(2). http://www.ashrae.org

Comstock, M.C., Braun, J.E., and Groll, E.A., 2001. The Sensitivity of Chiller Performance to Common Faults. HVAC&R Research, 7(3), 263-279.

Davis, B., Robins, D., 2008. Field Monitoring of High Efficiency Residential heat Pumps, 2008 ACEEE Summer Study on Energy Efficiency in Buildings, American Council for an Energy Efficient Economy, Washington, DC. http://www.aceee.org

DOE, 2011. Buildings Energy Data Book, Residential Sector Energy Consumption. U.S. Department of Energy, http://buildingsdatabook.eren.doe.gov/docs/xls_pdf/2.1.6.pdf

Dougherty, B. P., 2003. New Defaults for Cyclic Degradation Coefficient Used in Rated Air Conditioners and Heat Pumps. Seminar 40, Annual Meeting, American Society of Heating, Refrigerating, and Air-Conditioning Engineers, Atlanta, GA. http://www.ashrae.org

Downey, T., Proctor, J., 2002. What Can 13,000 Air Conditioner's Tell Us? 2002 ACEEE Summer Study on Energy Efficiency in Buildings, American Council for an Energy Efficient Economy, Washington, DC. http://www.aceee.org

Du, Z. and Jin, X., 2008. Multiple faults diagnosis for sensors in air handling unit using Fisher discriminant analysis. Energy Conversion and Management, 49(12), 3654-3665.

EIA, 2012. Form 826 data for local utility in 2010 for residential sector. U.S. Energy Information Agency, http://www.eia.gov/cneaf/electricity/page/eia826.html

EPA, 2001. Indoor Humidity Assessment Tool, Reference Manual. U.S. Environmental Agency, www.epa.gov/iaq/schooldesign/saves.html

Farzad, M. and O'Neal, D., 1991, System performance characteristics of an air conditioner over a range of charging conditions, International Journal of Refrigeration 14(6), 321-328.

Federal Register 1979. Test Procedures for Central Air Conditioners Including Heat Pumps. Federal Register 44 (249): 76700–76723. Nov. 19.

Foster, R., South, M., Neme, C., Edgar, G., Murphy, P., 2002. Residential HVAC Quality Installation: New Partnership Opportunities and Approaches. ACEEE 2002 Summer Study on Energy Efficiency in Buildings, American Council for an Energy Efficient Economy, Washington, DC.

Francisco, P.W., Palmiter, L., 2000. Field Validation of Standard 152P. ASHRAE Transactions, 106(2), 771–783. http://www.ashrae.org

Fugler, D. 1999. Conclusions from Ten Years of Canadian Attic Research. ASHRAE Transactions, 105(1). http://www.ashrae.org

Henderson, H.I., 1992. Simulating Combined Thermostat, Air Conditioner and Building Performance in a House. ASHRAE Transactions, 98(1). http://www.ashrae.org

Henderson, H., Rengarajan, K., 1996. A Model to Predict the Latent Capacity of Air Conditioners and Heat Pumps at Part Load Conditions with the Constant Fan Mode. ASHRAE Transactions 102(1). http://www.ashrae.org

Henderson, H.I., Sand, J., 2003. An Hourly Building Simulation Tool to Evaluate Hybrid Desiccant System Configuration Options. ASHRAE Transactions, 109(2). http://www.ashrae.org

Henderson, H., Shirey, D., Raustad,R., 2007. Closing the Gap: Getting Full Performance from Residential Central Air Conditioners. Task 4 - Develop New Climate-Sensitive Air Conditioner, Simulation Results and Cost Benefit Analysis'. Final Report FSEC-CR-1716-07. Florida Solar Energy Center, Cocoa, FL. http://www.fsec.ucf.edu/en

Henderson, H.I., 1990. An Experimental Investigation of the Effects of Wet and Dry Coil Conditions on Cyclic Performance in the SEER Procedure. Int. Refrigeration Conference at Purdue University, West Lafayette, IN.

Hendron, R. 2008. Building America Research Benchmark Definition. Technical Report, NREL/TP-550-44816, Updated December 19, 2008, National Renewable Energy Laboratory, Golden, CO.

Hunt, M., Heinemeier K., Hoeschele, M., Weitzel, E., 2010. HVAC Energy Efficiency Maintenance Study. Davis Energy Group, Inc., Davis, CA. http://www.calmac.org/publications/HVAC_EE_Maintenance_Final.pdf

Karg, R., Krigger, J., 2000. Specification of Energy-Efficient Installations and Maintenance Practices for Residential HVAC Systems. White Paper, Consortium for Energy Efficiency, Boston, MA, USA. http://www.cee1.org/resid/rs-ac/reshvacspec.pdf

Kim, M., Payne, W. V., Domanski, P. A., Yoon, S. H., Hermes, C.J.L., 2009. Performance of a Residential Heat Pump Operating in the Cooling Mode with Single Faults Imposed. Applied Thermal Engineering 29(4), 770-778.

Kim, M., Payne, W.V., Hermes, C.J.L., Domanski, P. A., 2006. Performance of a Residential Heat Pump Operating in the Cooling Mode with Single Faults Imposed, NISTIR 7350, National Institute of Standards and Technology, Gaithersburg, MD. http://www.bfrl.nist.gov/863/HVAC/pubs/2006%20Building%20Publications%20-%20NISTIR_7350.htm

Kim, M., Yoon, S. H., Payne, W. V., Domanski, P. A., 2008a. Cooling Mode Fault Detection and Diagnosis Method for a Residential Heat Pump. NIST special Publication 1087, National Institute of Standards and Technology, Gaithersburg, MD. http://www.bfrl.nist.gov/863/HVAC/pubs/index.htm

Kim, M., Yoon, S. H., Domanski, P. A., and Payne, W. V., 2008b. Design of a steady-state detector for fault detection and diagnosis of a residential air conditioner. International Journal of Refrigeration 31(5), 790-799.

Klein, S.A., Beckman, W.A., Mitchell, J.W., Duffie, J.A., Duffie, N.A., Freeman, T.L., Mitchell, J.C., Braun, J.E., Evans, B.L., Kummer, J.P., Urban, R.E., Fiksel, A., Thornton, J.W., Blair, N.J., Williams, P.M., Bradley, D.E., McDowell, T.P., Kummert, M. 2007. TRNSYS 16 – A Transient System Simulation Program. University of Wisconsin-Madison Solar Energy Laboratory, Madison, WI, USA.

Li, H. and Braun, J.E., 2007. Decoupling features and virtual sensors for diagnosis of faults in vapor compression air conditioners, International Journal of Refrigeration, 30(3), 546-564.

Modera, M.P., 1989. Residential Duct System Leakage: Magnitude, Impacts, and Potential for Reduction, ASHRAE Transactions 95(2), 561-569. http://www.ashrae.org

Mowris, R.J., Blankenship, A., Jones, E., 2004. Field Measurements of Air Conditioners with and without TXVs. ACEEE 2004 Summer study on Energy Efficiency in Buildings, American Council for an Energy Efficient Economy, Washington, DC. http://www.aceee.org

Navarro-Esbri J, Torrella E, Cabello R., 2006, A vapour compression chiller fault detection technique based on adaptive algorithms. Application to on-line refrigerant leakage detection, International Journal of Refrigeration, 29(5), 716-723.

Neal, C. L., 1998. Field Adjusted SEER [SEERFA], Residential Buildings: Technologies, Design, and Performance Analysis. 1998 ACEEE Summer study on Energy Efficiency in Buildings, American Council for an Energy Efficient Economy, Washington, DC. http://www.aceee.org

O'Neal, D. and Katipamula, S., 1991. Performance Degradation During On-Off Cycling of Single Speed Air Conditioners and Heat Pumps: Model Development and Analysis. ASHRAE Transactions, 97(2), 316-323.

Neme, C., Proctor, J., Nadel, S., 1999. Energy Savings Potential from Addressing Residential Air Conditioners and Heat Pump Installation Problems. Report Number A992, American Council for an Energy Efficient Economy, Washington, DC. http://www.aceee.org

Palmiter, L., Bond, T., 1991. Interaction of Mechanical Systems and Natural Infiltration. 12th AIVC Conference on Air Movement and Ventilation Control within Buildings, Air Infiltration and Ventilation Centre, Coventry, Great Britain.

Parken, W.H., Didion, D.A., Wojciechowski, P.H., and Chern, L. 1985. Field Performance of Three Residential Heat Pumps in the Cooling Mode. NBSIR 85-3107, National Bureau of Standards, Gaithersburg, MD.

Parken, W.H., Beausoliel, R.W., Kelly, G.E. 1977. Factors Affecting the Performance of a Residential Air-to-Air Heat Pump. ASHRAE Transactions. 83(1), 839-849. http://www.ashrae.org

Parker, D.S., P.A. Broman, J.B. Grant, L. Gu, M.T. Anello, R.K. Vieira, H.I. Henderson. 1999. ENERGYGAUGE USA: A Residential Building Energy Simulation Design Tool. Proceedings of Building Simulation 99(1), 73-79.

Parker, D.S., Sherwin, J.R., Raustad, R.A., Shirey, D.B. III., 1997. Impact of Evaporator Coil Airflow in Residential Air-Conditioning Systems. ASHRAE Transactions, 103(2), 395-405. http://www.ashrae.org

Payne, W. V., Domanski, P.A., Yoon, S.H., 2009. Heating Mode Performance of a Residential Heat Pump With Single Faults Imposed, NIST TN 1648, National Institute of Standards and Technology, Gaithersburg, MD. http://www.nist.gov/customcf/get_pdf.cfm?pub_id=903554

Payne, W. V., Kwon, (2014). Empirical correlations for residential heat pump thermostatic expansion valve undersizing in the cooling mode. (technical paper in preparation).

Proctor, J.P., 1997. Field Measurements of New Residential Air Conditioners in Phoenix, Arizona. ASHRAE Transactions, 103(2), 406-415. http://www.ashrae.org

Proctor, J., 2004, Residential and Small Commercial Central Air Conditioning; Rated Efficiency isn't Automatic. Presentation at the Public Session. ASHRAE Winter Meeting, Anaheim, CA. http://www.ashrae.org

RESNET, 2006. Home Energy Rating System (HERS), Residential Energy Services Network http://www.resnet.us

Rossi, T.M., 2004, Unitary Air Conditioner Field Performance. International Refrigeration and Air Conditioning Conference at Purdue, Paper No. R146, West Lafayette, IN.

Rudd, A., Henderson, H., Bergey, D., Shire, D., 2013. ASHRAE RP-1449: Energy Efficiency and Cost Assessment of Humidity Control Options for Residential Buildings. Final Report submitted to the American Society of Heating, Refrigerating, and Air Conditioning Engineers. Atlanta, GA. http://www.ashrae.org

Sachs, H., Henderson, H., Shirey, D., De Forest, W., 2009. A Robust Feature Set for Residential Air Conditioners. ACEEE Report Number A081 2009, American Council of an Energy Efficient Economy, Washington, DC. http://aceee.org

Sherman, M.H. 1992. Superposition in infiltration modeling. Indoor Air 1:101-14.

Shirey, D.B., Henderson, H.I., Raustad, R., 2006. Understanding the Dehumidification Performance of Air-Conditioning Equipment at Part-Load Conditions. Final Report FSEC-CR-1537-0. DOE/NETL Project No. DE-FC26-01NT41253. Florida Solar Energy Center, Cocoa, FL. http://www.fsec.ucf.edu/en

Siegel, J.A., McWilliams, J.A., and Walker, I.S. 2003. Comparison Between Predicted Duct Effectiveness from Proposed ASHRAE Standard 152P and Measured Field Data for Residential Forced Air Cooling Systems. ASHRAE Transactions 109(1). http://www.ashrae.org

Sonne, J. K., Parker, D.S., Shirey III, D.B., 2006. Measured Impacts of Proper Air Conditioner Sizing in Four Florida Case Study Homes. Report FSEC-CR-1641-06. Florida Solar Energy Center, Cocoa, FL. http://www.fsec.ucf.edu/en

Southern California Edison, Design and Engineering Services Customer Service Business Unit, SCE 2012. Evaluating the Effects of Common Faults on a Residential Split System. HT.11.SCE.007 Report. http://www.etcc-ca.com/sites/default/files/reports/HT.11.SCE_.007%20Faults%20on%20a%20Residential%20Split%20System_Final.pdf

Sterling, E.M., Arundel, A., Sterling., T.D., 1985. Criteria for Human Exposure to Humidity in Occupied Buildings, ASHRAE Transactions 91(1). http://www.ashrae.org

Taylor, J., Hourahan, G., 2006. Evaluation of Market Transformation Strategies for Verifying a Quality Installation Specification. 2006 ACEEE Summer Study on Energy Efficiency in Buildings, American Council for an Energy Efficient Economy, Washington, DC. http://www.aceee.org

Taylor, J., Hourahan, G., Parlapiano, W., 2004. Improving residential HVAC Installation Practices by Transforming National Markets. 2004 ACEEE Summer Study on Energy Efficiency in Buildings, American Council for an Energy Efficient Economy, Washington, DC. http://www.aceee.org

Walker, I., Wilson, D. 1998. Field Validation of Algebraic Equations for Stack and Wind Driven Air Infiltration Calculations. International Journal of HVAC&R Research (now ASHRAE HVAC&R Research Journal), 4(2). http://aceee.org

Walton, G., Dols, W. S., 2010. CONTAM User Guide and Program Documentation. NISTIR 7251. National Institute of Standards and Technology, Gaithersburg, MD 20899-8633 October, 2005; last revision December 14, 2010.

Wang, S., Zhou, Q., Xiao, F., 2010. A system-level fault detection and diagnosis strategy for HVAC involving sensor faults. Energy and Buildings, 42(4), 477-490.

Winkelmann, F., 1998. Underground Surfaces: How to Get a Better Underground Surface Heat Transfer Calculation in DOE-2.1E. Building Energy Simulation User News 19(1).

Wilcox, S., Marion, W., 2008. Users Manual for TMY3 Data Sets, Technical Report NREL/TP-581-43156, http://www.nrel.gov/docs/fy08osti/43156.pdf

ACKNOWLEDGEMENT

APPENDIX A: DUCT LOSSES

Duct losses − leakage and thermal − have been widely evaluated and studied in the field (Cummings and Tooley, 1989; Modera, 1989; Andrews, 1997; Siegel et al., 2003). The impacts of duct leakage and losses are especially significant in homes in the southern and western U.S. where ductwork is often installed outside the conditioned space (e.g., in the attic). Duct losses are complex phenomena where heat is lost to an unconditioned zone (typically the attic) and then in some cases 'regained' by reduced heat transfer between the conditioned and unconditioned zones (i.e., heat lost from attic ducts in the winter, tends to warm the attic and reduce heat loss through the ceiling). ASHRAE Standard 152 (ASHRAE 2004) has been developed to characterize the overall impact of thermal conduction and leak losses by determining the overall distribution efficiency (DE) for a system.

We used the leakage model developed for a prior TRNSYS-based simulation study of dehumidification systems (Henderson et al., 2007), as well as a study to evaluate the efficacy of a robust or 'fault tolerant' AC unit (Sachs et al., 2009). The model assumes all air leakage and conductions losses are from the ductwork to Zone 2 (the attic), as shown schematically in Figure A1. The following is the calculation scheme for the return duct and supply duct.
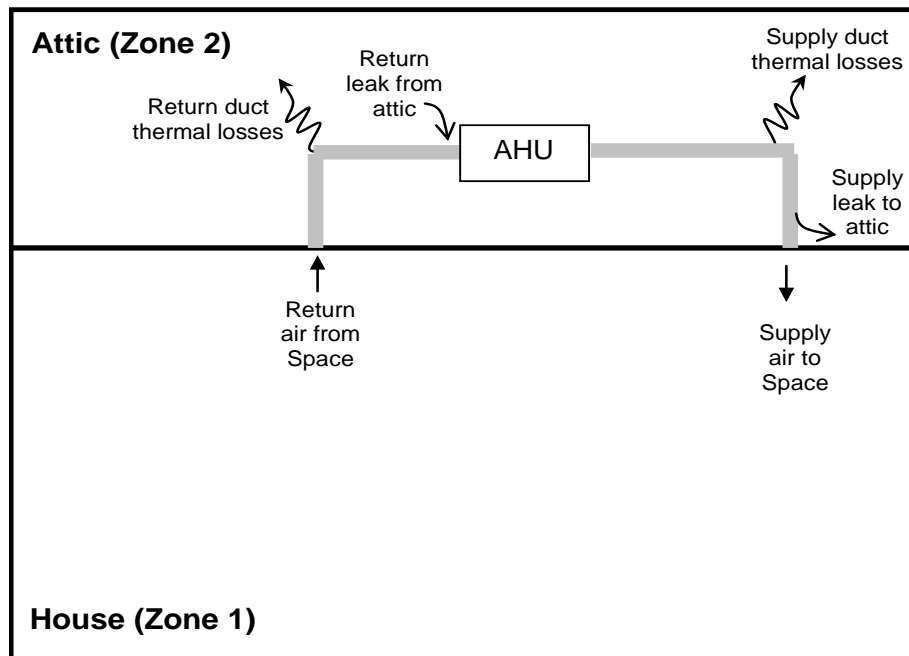

Figure A1. Schematic representation of duct leakage in a home with attic ducts

Return Duct
Air from the house zone (Zone 1) enters the return duct. According to evaluations of ASHRAE Standard 152 by Francisco and Palmiter (2000), the temperature change of air in a duct that passes through an unconditioned space at a uniform temperate (T_o) is defined as:

$$\frac{(T_{out} - T_o)}{(T_{in} - T_o)} = e^{-UA/m \cdot c_p} \tag{A1}$$

Applying Eq. (A1) to our case, the parameters of air arriving at the air handing unit (AHU) are given by:

$$T_{AR} = T_{z2} + (T_{z1} - T_{z2})e^{-A_R / \left[m'_R \cdot Cp \cdot (R_{duct} + 1/h_i) \right]} \tag{A2}$$

$$w_{AR} = w_{z1} \tag{A3}$$

Then the air parameters at the end of the return duct after the thermal losses are:

$$T_{AR}' = T_{AR} \cdot (1 - F_R) + T_{z2} \cdot F_R \tag{A4}$$

$$w_{AR}' = w_{AR} \cdot (1 - F_R) + w_{z2} \cdot F_R \tag{A5}$$

The heat gain to Zone 2 from thermal conduction is the same as the heat loss of the return air as it travels through the duct, which is defined as

$$Q_R = m_R \cdot (1 - F_R) \cdot c_p \cdot (T_{z1} - T_{AR}) \tag{A6}$$

Supply Duct
Supply air from the AHU unit (i.e., the average for the time step) enters the supply duct. The impact of thermal conduction losses are given by:

$$T_{AS} = T_{z2} + (T_{ACout} - T_{z2})e^{-A_S / m_S \cdot Cp \cdot R_{duct}} \tag{A7}$$

$$w_{AS} = w_{ACout} \tag{A6}$$

A portion of the supply airflow goes to the space (zone 1), while the balance goes into the attic (zone 2)

To Space (Zone 1): $\quad m_{S\text{-space}} = m_S \cdot (1 - F_S)$ $\qquad$ (A8)

To Zone 2: $\quad m_{S\text{-z2}} = m_S \cdot F_S$ $\qquad$ (A9)

The heat gain to Zone 2 from thermal conduction is the same as the heat loss of the supply air as it travel through the duct, which is defined as

$$Q_S = m_S \cdot c_p \cdot (T_{ACout} - T_{AS}) \tag{A10}$$

Zone 2 has two impacts from the duct losses:
- supply air (airflow of $m_{S\text{-z2}}$ at T_{AS} and w_{AS}) enters the zone to condition it,
- conduction losses from the return duct (Q_R) and the supply duct (Q_S) are added to the zone as a thermal gain.